Cardiff University

CONFIDENTIAL

CFR PEEK Monobloc with Screw Hole Fixation Acetabular Prosthesis

By

Marc Elliott

A thesis submitted in partial fulfilment for

the degree of Doctor of Philosophy

School of Engineering

2018

Acknowledgements

The completion of this project has relied on the input from not only me but from many colleagues and friends.

Firstly, I would like to thanks my boss at the time and good friend Dr Robert Bigsby who had chosen me for the project and has supported me for the last several years in my Biomet career; I have learned so much from him. Also Dr Imran Khan for his continued support and guidance not only for this project but for my time spent in Trauma and Hip Development role, Seth Nash who has continued to support me in my role within Biomet and for me to complete this. I share the same mind-set that my peers do that hard work will always pay off. Its genuinely felt a big thank you to my supervisors and sponsors as without these the project could not have taken place. My supervisors Professor Sam Evans and Dr Rhys Pullin have helped throughout the project offering guidance and advice and Biomet who have given me opportunities

I love orthopaedics and everyone I have mentioned has made this a fantastic opportunity and journey for me.

Finally I would like to express my gratitude for the support from my friends and family especially, my partner Louise, son Harry, Jacob and daughter Sophia Rose

Contents

1 Introduction 1
1.1 Aims and Objectives 2
1.2 Thesis Structure 3
2 Literature Review 5
2.1 History of total hip arthroplasty 5
2.2 Metal on Metal implants 8
2.3 Ceramic on Ceramic implants 12
2.4 PEEK and CFR PEEK 14
2.5 Mechanical Properties of PEEK and CFR PEEK 17
2.6 Biological properties of PEEK and CFR PEEK 18
2.7 CFR PEEK as an Implant – Femoral Stem 19
2.8 CFR PEEK as an Implant – Acetabular bearing 20
2.8.1 ABG II 20
2.8.2 Mitch PCR Cup™ 25
2.9 Wear Properties of CFR PEEK 27
2.10 Tribology in Orthopaedics 29
2.11 Mixed fluid regime 30
2.12 Boundary regime 31
2.13 Fluid film regime 31
2.14 Cadaveric Experiments 32
2.15 Finite Element Analysis 33
2.16 Dynamic Fatigue Testing 34
3 Design Evolution of Prosthesis 35
3.1 Introduction 35
3.2 Design Specification 35
3.3 Design Evolutions 36
3.3.1 Design Version One 36
3.3.2 Design Version Two 37
3.3.3 Design Version Three 37
3.3.4 Design Version Four 38

3.4 Thread and screw design 38
3.4.1 Thread design 38
3.5 Frangible Elements 41
4 Tribology Testing 42
4.1 Introduction 42
4.2 Methods 42
4.2.1 Radial clearances 42
4.2.2 Experimental procedure at Durham Facility 43
4.2.3 Experimental procedure at Bradford University 45
4.2.4 Kinetics and Kinematics 48
4.2.5 Stribeck Analysis 49
4.2.6 Theoretical calculations 50
4.3 Components for Tribology Testing 53
4.3.1 Stage 1 53
4.3.2 Stage 2 & Stage 3 54
4.3.3 Stage 4 54
4.3.4 Stage 5 55
4.4 Results and Discussion 56
4.4.1 Stage 1 60
4.4.2 Stage 2 63
4.4.3 Stage 3 65
4.4.4 Stage 4 66
4.4.5 Stage 5 67
4.5 Conclusion 76
5 Cadaveric Testing 78
5.1 Introduction 78
5.2 Cadaveric Experiment One 78
5.2.1 Experimental Procedure 78
5.2.2 Results and Discussion 82
5.2.3 Conclusion 85
5.3 Cadaveric Testing Experiment Two 86
5.3.1 Experimental Procedure 86
5.3.2 Results and Discussion 88

5.3.3 Conclusion 90
5.4 Cadaveric Testing Experiment Three 91
5.4.1 Experimental Procedure 91
5.4.2 Results and Discussion 92
5.4.3 Conclusion 109
5.5 Cadaveric Testing Experiment Four 109
5.5.1 Experimental Procedure 109
5.5.2 Results and Discussion 111
5.5.3 Conclusion 116
5.6 Chapter Conclusions 116
6 Finite Element Analysis of the CFR PEEK Monobloc Cup 117
6.1 Introduction 117
6.2 Experimental Procedure 118
6.3 Results and Discussion 120
6.4 Conclusion 127
7 Dynamic Fatigue Testing 128
7.1 Introduction 128
7.2 Experimental Procedure 128
7.3 Results and Discussion 132
7.4 Conclusion 134
8 Discussion 135
9 Conclusions and Future Work 137
9.1 Conclusions 137
9.2 Further work 137
10 References 139

1. Introduction

Osteoarthritis, rheumatoid arthritis and osteonecrosis, as well as bone tumours, fractures or injuries are common causes of hip joint damage. In addition to hip pain further symptoms or experiences of these conditions include depression and anxiety, stiffness, decreased range of motion, mobility issues, weight gain and sleeplessness due to pain. If severe damage occurs a hip prosthesis may be necessary, and this can occur at any age; this could involve replacing just the surface of the femoral head (hip resurfacing), the femoral surface and the acetabulum (total hip resurfacing, THR) or the entire joint including the proximal part of the femur (total hip arthroplasty, THA). The benefits of hip arthroplasty to the patent include:

- Improved quality of life;
- Improve mobility and range of motion;
- Pain relief;
- Return to sporting activities.

The author can directly relate to the symptoms and benefits of hip arthroplasty. His mother has suffered from osteoarthritis in her thirties with a bilateral hip arthroplasty at forty, and twenty years on the original hip implants remain. The benefits are instant, as seen by author in his teens, with improved mobility occurring overnight. Even today, many years later, failures of these constructs occur. Common factors that can cause fractures or loosening include poor material combinations, small head diameters, excessive wear and fixation failures. A further personal experience of failure is observing his mother's hip joints failing due to dislocation.

This project focuses on the development of a new hip arthroplasty technology for Zimmer-Biomet where the author works as a design and research engineer. The thesis was completed part-time over a five-year period in conjunction with the company's own development work. The author coordinated, completed and analysed all aspects of the project except where otherwise specified.

1.1 Aims and Objectives

The primary aim of this thesis was to design and develop an alternative to the widely used Metal on Metal (MoM) implants, an example of which is shown in Figure 1.1. Key aspects, identified by the author, were to ensure that large femoral heads were retained, a new method of fixation was required and alternative bearing materials should be explored. The aim is that this will ultimately benefit the patient, improving wellbeing and standard of living through extended implant life and reduced risk of failure.

Figure 1.1: MoM THA & THR (CapeRay, 2013)

To achieve these three primary aims, the work focused on several aspects of the final design, as identified by the author:

- Stress and strain in the implant and acetabulum, and hence strength and fatigue life;
- Outside geometry, which is important for fixation;
- Surface finish, which is critical to wear performance;
- Radial clearance, which determines the lubrication regime and contact pressures;
- The use of screw holes in the bearing surface as a novel fixation method;
- Design of the screw holes and the screws that engage in them.

Early in the development the author identified Carbon Fibre Reinforced PolyEtherEtherKetone (CFR PEEK) as an alternative acetabular bearing material, sliding against transition toughened platelet alumina composite (TTPA). Historically cobalt- chromium- molybdenum (CoCrMo) alloys have been used for acetabular components implants articulating with femoral heads of the same material; this design has been used extensively in THA and THR. Three main questions arise in using CFR

PEEK: deformation of the acetabular component on impaction to the acetabulum, deformation under loading and friction and wear between the femoral head and the acetabular cup. Deformation is particularly important when using CFR PEEK because it has a much lower stiffness than CoCrMo (30 GPa vs 240 GPa), and when using a large femoral head there is no room for a thick, rigid acetabular cup. Polymeric bearing materials are typically used with an outer metal shell, which provides rigidity; with a large diameter head this is not possible due to lack of space and the acetabular cup must be a single component (monobloc).

1.2 Thesis Structure

The thesis is broken down into the following chapters. A literature review on hip arthroplasty, tribology, cadaveric testing, finite element analysis and fatigue testing is presented in Chapter 2. Chapter 3 presents a design specification developed by the author and agreed by Zimmer Biomet.

A fundamental experiment when developing a novel orthopaedic implant is to ascertain the optimum mechanics, and performance of the implant, this is presented in Chapter 4. Cadaveric studies undertaken by the author are presented in Chapter 5. The installation of the implant was completed by a surgeon under the supervision and direction of the author. As part of the study the amount of deformation under impaction of the implant with different reaming parameters was identified by the author. This ultimately determined the geometry of the implant.

Chapter 6 details a Finite Element Analysis (FEA) to assess the effect of varying implant design parameters and also to compare how different materials perform against CFR PEEK. The FEA was completed by Continuum Blue Ltd, an external contractor of Zimmer Biomet. The author detailed all fundamentals of the model including loading, geometry and boundary conditions. The results of the study were analysed by the author and are presented. The results provided an insight into how the implant will perform in-vivo.

Chapter 7 describes a necessary experiment to evaluate the fatigue properties of the implant and to replicate in-vivo conditions; to the author's knowledge this is a novel experiment. Chapter 8 summarises the design evolution of the CFR PEEK Monobloc Shell and how tribology, FEA and cadaveric experiments determined the final design of the implant.

Finally, Chapter 8 discusses the novelty of this work. This includes locking screw holes in the bearing surface, optimised radial clearance and a surface finish to produce optimised friction and wear factors.

2 Literature Review

2.1 History of total hip arthroplasty

Hip replacement surgery has been undertaken since the late 1800's, with the first recorded procedure undertaken by Professor Themistocles Gluck (Gomez and Morcuende 2005) using an ivory ball and socket joint secured to the bone with nickel-plated screws. Several other surgeons followed this including Sir Robert Jones who used a gold strip to cover reconstructed femoral heads; this at the time had the longest follow up report of 21 years (Gomez and Morcuende 2005). Norwegian-born American surgeon Marius Smith-Peterson (Gomez and Morcuende 2005) experimented with glass, celluloid, Bakelite, Pyrex and Vitallium® with various levels of success. Vitallium® is a trademark name for cobalt-chromium-molybdenum alloy (CoCrMo) and was developed in 1923; this material will be spoken about further but has been used several times since its first introduction.

17 years on from the introduction of CoCrMo, Fredrick Roeck Thompson developed a monobloc stem with Austin Moore implanting the first in 1940 (Gomez and Morcuende 2005). Harold Bohlman and Austin Moore further developed the prosthesis as shown in Figure 2.1.

Figure 2.1: Austin Moore hip prosthesis

This prosthesis is still used today to treat elderly patients who have either no or limited mobility. This implant replaces the femoral head leaving it to articulate against the cartilage in the acetabulum; this is referred to as a hemi arthroplasty as shown in Figure 2.2.

Figure 2.2: Hemiarthroplasty (Orthopaedics 2015)

In the early 1950's total hip arthroplasty started to be developed (Tansey 2006) again using CoCrMo. Edward J Haboush cemented in place a femoral and an acetabular component using acrylic. In that same year Kenneth McKee (Tansey 2006) failed using the same concept but using stainless steel, this was changed to CoCrMo when results improved. At the same time the pioneer of total hip arthroplasty, Sir John Charnley, was developing implants. In the 1960s he began to use Ultra High Molecular Weight Polyethylene (UHMWPE) for the acetabular cup, instead of PTFE which he had previously used with poor results. His aim was to minimise friction in the joint and therefore to reduce the load transferred to the bone and improve fixation.

The basic Charnley design, (Figure 2.3) using a UHMWPE acetabular cup and acrylic cement fixation, remains one of the most common in use today. Many other designs have developed this basic concept, including the widely used Exeter hip which uses a tapered, polished stem to improve fixation.

Modern hip replacement generally achieves excellent results. The major cause of failure and revision is aseptic loosening which is attributed to the effects of wear debris, as shown in Table 2.1. Periprosthetic osteolysis is damage to the bone around a prosthesis caused by polyethylene wear debris generated during the life-span of a joint replacement, this causes subsequent loss of implant fixation (Gonzalez Della Valle, Su et al. 2004, Bichara, Malchau et al. 2014). It has been demonstrated that it is not the wear volume that determines the biological response to

the debris, but the concentration of the wear volume that is within the critical size range (0.2–0.8 μm) for macrophage activation (Ingham and Fisher 2000). Particles in this size range cause inflammation leading to osteolysis.

Table 2.1: Aseptic Loosening (NJR 2015)

Year of first revision in the NJR	Single Stage		First documented stage of two-stage	
	Primary not in the NJR [%]	Primary in the NJR [%]	Primary not in the NJR [%]	Primary in the NJR [%]
2003	65.4	10.5	52.2	0 of 5
2004	70.7	13.3	41.8	20.7
2005	71.6	21.5	26.0	22.8
2006	69.4	33.1	19.6	14.9
2007	66.5	32.5	20.5	9.7
2008	67.2	21.4	27.3	10.4
2009	64.1	29.0	18.2	14.0
2010	60.1	28.6	18.0	10.0
2011	57.0	25.6	12.6	7.8
2012	56.4	24.2	13.3	8.5
2013	53.6	24.8	11.5	8.9
2014	55.2	25.7	12.5	7.7
Total	**62.0**	**26.4**	**19.7**	**10.2**

Figure 2.3: Charnley total hip replacement (Images 2002)

In an attempt to reduce the problem of wear debris, UHMWPE has evolved since its first use with the introduction of harder Highly Cross-Linked Polyethylene (HXLPE). This has further developed with the recent introduction of vitamin E infused polyethylene's (Kurtz, Gawel et al. 2011). With polyethylene wear presenting issues, hard bearings were developed which included Ceramic on Ceramic (CoC) and Metal on Metal (MoM) bearings. These hard bearing implants show significantly less wear when compared with polyethylene bearings (Lieberman, Kay et al. 1996, Essner, Sutton et al. 2005, Shimmin, Beaule et al. 2008, Williams, Leslie et al. 2008, Wang, Wu et al. 2012).

2.2 Metal on Metal implants

MoM implants were first developed in the 1930 – 50's which included the McMinn, Wiles and McKee – Farrar prosthesis shown in Figure 2.4. These however were discarded for the following reasons: high frictional torque, equatorial binding, carcinogenesis concerns, metal sensitivity concerns, high infection rates, increased strain in the periprosthetic trabecular bone and Charnley's introduction of polyethylene in the 1960s (Steven M. Kurtz and and Richard Underwood 2011).

Figure 2.4: McKee – Farrar prosthesis (Steven M. Kurtz and and Richard Underwood 2011)

Second generation MoM components were introduced into the market in the 1990s as an alternative to Total Hip Arthroplasty (THA) to meet the demands of the younger active patient. These differed from first generation implants as they were a total hip construct as opposed to a hemi arthroplasty. This concept had several theoretical benefits; return to high level impact sports, preservation of femoral and acetabular bone stock, lack of instability, preservation of articular proprioception, maintenance of coxofemoral biomechanics, maintenance of lower limb length and facilitation of future revision surgery (Daniel, Pynsent et al. 2004, Fisher, Isaac et al. 2007, Shimmin, Beaule et al. 2008, Lons, Arnould et al. 2015). They also exhibited lower volumetric wear rates in comparison to conventional metal-on-polyethylene bearings (AAOS 2012). In vitro testing has shown a 500 fold wear reduction over standard polyethylene with CoC (Essner, Sutton et al. 2005).

It is estimated that since 1996 1.5 million MoM hip implants have been implanted as shown in Figure 2.5 (AAOS 2012, Siddiqui, Sabah et al. 2013) with recalls beginning to start in the year 2008 (FDA 2008). It is estimated that one million total hip replacements are performed worldwide every year and with an ageing population this number is likely to increase (Holzwarth and Cotogno 2012).

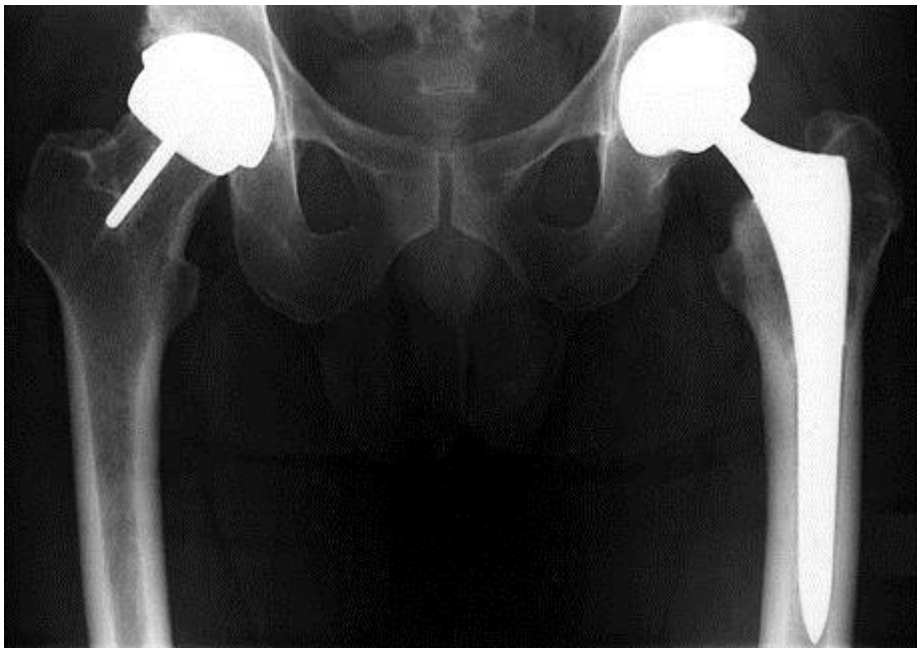

Figure 2.5: Hip resurfacing on the left and total hip on the right (Institute 2014)

The recall of these types of implants was seen to be one of the most significant developments in modern hip arthroplasty. The failures were attributed to several factors which included the material used, the design and mal positioning of the implant. Even though it has been demonstrated that MoM presents very low wear, the cobalt and chromium particles have been shown to cause solid or cystic periprosthetic soft-tissue lesions, termed pseudotumors which are often associated with pain, loss of function and muscle necrosis (Delaunay, Petit et al. 2010, Langton, Jameson et al. 2010, Siddiqui, Sabah et al. 2013, Madl, Kovochich et al. 2015, Oliveira, Candelária et al. 2015). The accumulation of the metal debris in the soft tissue is termed metallosis with an example shown in Figure 2.6 and 2.7.

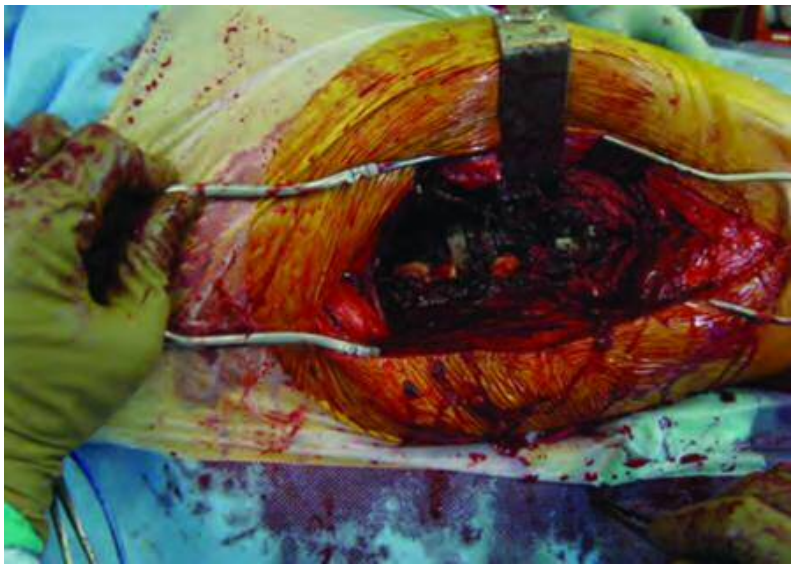

Figure 2.6: Visible metallosis at revision surgery (Myburgh, Snyckers et al. 2012)

Figure 2.7: Black fluid from patient with metallosis (Oliveira, Candelária et al. 2015)

MoM implants rely on hydrodynamic lubrication by the synovial fluid; this is critically influenced by the radial clearance which affects the friction, lubrication mode and the potential for squeaking joints (Goldsmith, Dowson et al. 2001, Langton, Jameson et al. 2010). The mal positioning of the implant further increases the wear. There are two current explanations; a loss of entrainment of synovial fluid resulting in the interruption of the lubrication, this can be caused by radial clearances as previously mentioned and cup deformation. Edge loading due to incorrect cup positioning results in a large local increase in contact pressure and consequent film thickness reduction at the cup rim

which in turn causes increased wear (Underwood, Zografos et al. 2012, Jim W. Pierrepont, PhD3. et al. 2014).

2.3 Ceramic on Ceramic implants

CoC bearings were first developed in the early 1970s to address to demands of younger more active patients and minimise wear debris associated with polyethylene (Toni, Terzi et al. 2000, Chevalier and Gremillard 2009, D'Antonio and Sutton 2009). The first CoC hip replacement was implanted by Pierre Boutin in 1970 in the form of an all-alumina ceramic cup and alumina ceramic head (Walter, Lusty et al. 2006). CoC components have a similar traits to those of MoM, they allow for large head bearings which is an advantage in preventing dislocations (Burroughs, Hallstrom et al. 2005, Matsushita, Nakashima et al. 2009, Stroh, Issa et al. 2013). Dislocations are shown to be fourth reason for revision surgery as shown in Table 2.2.

Table 2.2: Reason for revision (NJR 2015)

Year of first revision in the NJR	Type of revision procedure		
	Single stage (n=69,655) [%]	Stage one of two-stage (n=4,664) [%]	Stage two of two-stage (n=5,540) [%]
Aseptic loosening	52.0	14.3	13.6
Pain	23.6	16.1	10.7
Lysis	15.8	10.1	6.6
Dislocation/subluxation	15.0	4.1	3.5
Infection	3.1	79.7	71.2
Periprosthetic fracture	9.2	3.5	3.8
Implant fracture	3.5	1.2	1.4
Implant wear	14.0	4.1	2.9
Malalignment	5.7	1.6	1.0
Head-socket size mismatch	0.8	0.4	0.2
Other indication	8.0	3.8	8.7
Adverse reaction to particle debris	10.4	3.0	2.1

There have been several ceramic and ceramic composites used including zirconia, alumina and zirconia platelet toughened alumina (ZPTA) in the orthopaedic world. ZPTA or Biolox® delta as it is known by its brand name (Figure 2.8). The ceramic composite is made up of the following: 82% alumina, 17% zirconium oxide, 0.3% chromium oxide, and 0.6% strontium oxide (D'Antonio and Sutton 2009).

Figure 2.8: Biolox delta ceramic head and insert

CoC constructs have several advantages over MoM implants which include significantly lower taper corrosion, no metal ion release, no known pathogenic reaction to particles, resistance to third-body wear and excellent wettability (Chevalier and Gremillard 2009, D'Antonio and Sutton 2009, CeramTEC 2015). CoC bearings also show superior wear properties over all other bearing combinations with 500 fold wear reduction over polyethylene and a 50 fold reduction over MoM (Essner, Sutton et al. 2005, D'Antonio and Sutton 2009, Al-Hajjar, Leslie et al. 2010, Hamilton, McAuley et al. 2015). However, they share same similar concerns with regards to edge loading of the implant. This again can affect the tribology of the implant and increase wear which is often referred to as stripe wear (Figure 2.9) (Walter, Lusty et al. 2006, Al-Hajjar, Leslie et al. 2010, Sariali, Stewart et al. 2010).

Figure 2.9: Stripe wear (Walter, Lusty et al. 2006)

Implant placement can also cause fractures of the ceramic liner, the implant head or both. These failures are usually instaneous unlike polyethelene failure which can occur over several years. Ceramic failures have become less common in recent times due to the improvement in material, that said CoC use still has a steep learning curve for the surgeon and can be seen as the more difficult bearing construct to use with implant positioning requiring higher accuracy than that of a soft bearing (Toni, Terzi et al. 2000, Beaver, McCormick et al. 2002, Chevalier and Gremillard 2009, D'Antonio and Sutton 2009).

Audible squeaking has been a concern specfically in CoC but has been seen in other joint constructs such as MoM (Brockett, Harper et al. 2008). It has been demonstrated that this has been directly related to implant positioning with more anteverted positions at higher risk of squeaking when walking or bending (Walter, Lusty et al. 2006, Walter, O'Toole G et al. 2007, Jim W. Pierrepont. et al. 2014).

2.4 PEEK and CFR PEEK

With the significant developments observed in recent years with MoM the author investigated the use of an alternative bearing material to be used in conjunction with large diameter ceramic heads. The material in question is Carbon Fibre Reinforced (CFR) PolyEtherEtherKetone (PEEK). PEEK or polyoxy-1,4-phenylene-oxy-1,4-phenylenecarbonyl1-1,4-phenylene, as shown in Figure 2.10, (Rae, Brown et al. 2007) has been used in orthopaedics since the 1980s for trauma and spinal implants (Williams, McNamara et al. 1987, Kurtz and Devine 2007). PEEK is a semi-crystalline linear polymer with a good combination of strength, stiffness, toughness and environmental resistance (Robotti, Vedova et al. 2009, Chen, Ou et al. 2016). By the late 1990's PEEK had emerged as the leading high-performance thermoplastic candidate for replacing metal components, especially in orthopaedics and trauma (Steven M. Kurtz 2012). There are several other advantages that are beneficial with this material, it is radiolucent, CT compatible and Magnetic Resonance Imaging (MRI) compatible, non-cytotoxic, it has a modulus of elasticity close to that of bone and is biocompatible (Williams, McNamara et al. 1987, Zhang, Breidt et al. 2004, Kurtz and Devine 2007, Link 2008, Robotti, Vedova et al. 2009, Langohr, Gawel et al. 2011, Chen, Ou et al. 2016).

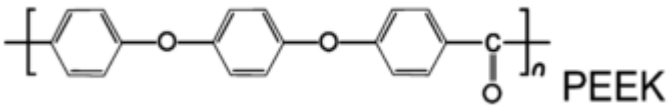

Figure 2.10: Chemical formula of PEEK (Kurtz and Devine 2007)

PEEK has demonstrated its benefits of mechanical stability with intervertebral cages in load bearing applications (Ferguson, Visser et al. 2006) and is widely accepted that it has the greatest clinical impact in the field of spinal implants (where it was chosen for its radiolucency and MRI compatibility) which has led it to be used in several other applications (Kurtz and Devine 2007). An example of such an implant is shown below in Figure 2.11.

Figure 2.11: PEEK intervertebral cage (Steven M. Kurtz 2012)

Carbon fibres are manufactured in two ways, one being a synthetic organic polymer fibre as the base material which is commonly referred to as polyacrylonitrile (PAN) fibres. The second uses coal tar pitch and is commonly referred to as PITCH fibres (Unsworth and Scholes 2009, Steven M. Kurtz 2012). Typically, there are two types of fibres, the first being short fibres; as the name suggests they are short with a length of 1mm to 6mm (Figure 2.12) and secondly continuous fibres which have a length greater than 6mm. The term continuous in this context means that they are long in relation to the diameter. These can both be processed with PEEK by injection moulding, compression moulding, hot pressing, etc.

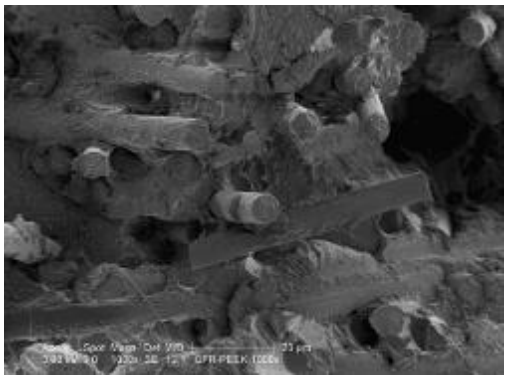

Figure 2.12: Electron micrograph of fractured short fibres reinforced PEEK (Green 2011)

While the initial tooling cost for injection moulding can be very high it also gives very reliable and repeatable results. This process allows for excellent surface finishing whilst omitting the need for excess traditional machining such as milling or turning. PEEK and carbon fibres can be blended during moulding; PEEK pellets (Figure 2.13) are poured into a hopper of the injection moulding machine and fed through the machine by a heated screw which melts and pressurizes the molten polymer, and at the same time the chopped fibres (Figure 2.14) are introduced through a second port before the composite flows into the heated mould. The fibres are further reduced during this process due to the compounding and injection moulding stages to a size of approximately 0.4mm. More commonly, particularly for medical applications, the PEEK and carbon fibres are provided ready blended by the manufacturer (Kurtz and Devine 2007, Steven M. Kurtz 2012); that was the approach taken in this project.

Figure 2.13: PEEK Pellets (Steven M. Kurtz 2012)

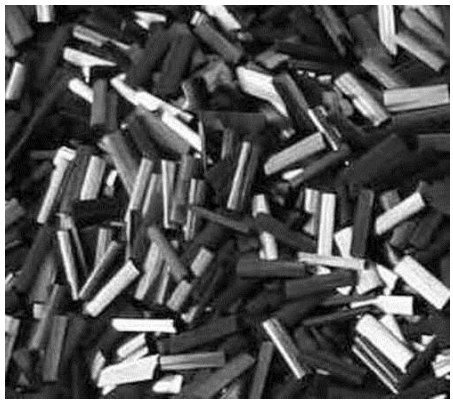

Figure 2.14: Chopped carbon fibres (Steven M. Kurtz 2012)

2.5 Mechanical Properties of PEEK and CFR PEEK

The structure of PEEK allows it to be chemical and radiation resistant, able to withstand temperatures exceeding 300ºC and it is compatible with several reinforcing materials such as glass and carbon fibre (Kurtz and Devine 2007, Robotti, Vedova et al. 2009). It is a tough semi-crystalline thermoplastic polymer with excellent mechanical properties (Table 2.3). CFR PEEK provides an inherently strong bond between fibres and matrix, with a fibre-to-matrix interfacial bond strength of at least on order of magnitude stronger than UHMWPE and carbon fibres. Additionally, CFR PEEK has shown to be highly resistant to creep with less than 0.4% of creep measured under loads of 50MPa, maintaining implant shape and contact area under constant stress (Jones, Leach et al. 1985, Zhang, Breidt et al. 2004, Rae, Brown et al. 2007, Invibio 2009).

Table 2.3: CFR PEEK Polymer Material Properties

Property	Test Method	Units	CFR PEEK Polymer
Tensile Strength	ISO 527	MPa	155
Tensile Elongation	ISO 527	%	2.2
Flexural Modulus	ISO 178	GPa	12.5
Flexural Strength	ISO 178	MPa	240
Notched Izod Impact Strength	ISO 180	KJ/m	5.7

2.6 Biological properties of PEEK and CFR PEEK

Wear particles generated by hip replacement components, with certain material bearing combinations, can have a negative effect on a patient (Ingham and Fisher 2000). Billions of wear particles are generated annually and migrate to the periprosthetic tissue (Catelas, Wimmer et al. 2011). UHMWPE wear particles have been implicated in osteolysis, implant loosening, and long-term failure of THA in vivo (Howling, Sakoda et al. 2003, Williams, Butterfield et al. 2003, Fang, Yang et al. 2006). Because wear particle characteristics (including size, shape and chemical composition) have been shown to influence the tissue response, these parameters are critical to any discussion about biological impact on the body (Catelas, Wimmer et al. 2011). It is not the wear volume that determines the biological response to the debris, but the concentration of the wear volume that is within the critical size range (0.2–0.8 mm) for macrophage activation (Ingham and Fisher 2000). MoM implants have been associated with metallosis which again results in aseptic fibrosis, local necrosis or loosening of the implant secondary to metal corrosion and release of wear debris (Oliveira, Candelária et al. 2015), whilst these constructs have shown to exhibit less volumetric wear than equivalent polyethylene systems. However while the particles generated by MoM bearing couples are smaller, their number is 13,500 times higher (6-7 x 10^{12} to 2-5 x 10^{14} particles/year) than a Metal on Polyethylene (MOP) bearing, the MoM particle debris are smaller than polyethylene ± 10 to 120μm (mean 40 μm), perfectly soluble and the cobalt (Co) and chromium (Cr) ions are bioactive (Delaunay, Petit et al. 2010).

It is well known that a reduction in the volume of wear produced by articulating surfaces in artificial joints is likely to result in a lower incidence of failure due to wear particle induced osteolysis (Scholes and Unsworth 2009). PEEK and its composites are recognised as alternative bearing materials for use in arthroplasty because of their suitable mechanical properties (Utzschneider, Becker et al. 2010). It has been demonstrated that PEEK and CFR PEEK compounds are biocompatible and meet ISO and ASTM standards (Morrison, Macnair et al. 1995, Pace, Marinelli et al. 2005, Kurtz and Devine 2007, Pace, Marinelli et al. 2008, Kurtz and Nevelos 2012). Hunter et al. (1995) demonstrated biocompatibility in an animal study and found that PEEK had no deleterious effect on the cells used. This is further supported by evidence that the in-vitro biocompatibility assessment of the composite showed initial osteoblast attachment at least comparable to that of titanium alloy Ti6Al4V (Katzer, Marquardt et al. 2002,

Garle 2003). It has been demonstrated in wear and particle analysis that CFR PEEK debris was less than 100-nm in size, which is much smaller than polyethylene with improved wear characteristics over UHMWPE and less cytotoxicity than Co Cr wear debris (Howling, Sakoda et al. 2003, Borruto 2010).

2.7 CFR PEEK as an Implant – Femoral Stem

Since the early 19th century studies were undertaken to understand the mechanical properties of bone and noted that the structure of the trabecular bone followed the lines of stress, which was observed in engineering structures (Steven M. Kurtz 2012). Julius Wolff and Wilhelm Roux both looked at the theory of bone remodelling or "Wolffs's Law" although Wilhelm Roux was first to accurately describe the adaption of bone to altered load (Lee and Taylor 1999). This theory led to the concept of "stress shielding". Typically when a metallic implant is used in the acetabulum or femur this provides structural reinforcement to the joint resulting in lower stress being applied to the living bone and can result in bone resorption (Huiskes, Weinans et al. 1992, Yamako, Chosa et al. 2014).

Research and development began in the early 1980's to reduce stress shielding and improve the bone resorption, for example the Zimmer VerSys® Epoch® stem which was a polymer composite stem that was made from a forged CoCrMo core with a PEEK and titanium fibre metal outside layer for bone ingrowth and long term fixation. This stem is the only successful low-stiffness stem for which long-term clinical performance has been reported (Yamako, Chosa et al. 2014) as shown in Figure 2.15.

Figure 2.15: Epoch® stem (Steven M. Kurtz 2012)

At the same time as the Epoch® stem was in development by Zimmer®, Orthodynamics Ltd were also developing a stem to prevent stress shielding. Again the inner core was CoCrMo with a CFR-PEEK outer layer and a hydroxyapatite proximal body as shown in Figure 2.16. This was prosthesis was implanted in 65 patients between 1996 and 1998. An in vitro study was conducted to investigate the human osteoblast-like cell and macrophage response to this material. The in vitro biocompatibility assessment of this composite undertaken in this study showed initial osteoblast attachment at least comparable to that of the tissue culture plastic and Ti6Al4V controls (Giannikas, Din et al. 2002, Garle 2003).

Figure 2.16: Bradley hip stem (Steven M. Kurtz 2012)

2.8 CFR PEEK as an Implant – Acetabular bearing

2.8.1 ABG II

There are two published CFR PEEK bearing constructs that have been used in vivo at the time of writing, the ABG II and the Mitch PCR™ Cup, the first being a modular construct and the second being a monobloc. Figure 2.17 shows the ABG II construct in post-operative X-ray. Figure 2.18 shows the unassembled liner which would fit into the appropriate shell and held in place with a locking ring. The liner was only available with a head size of 28mm and articulated against an alumina ceramic head. The composite material was PEEK and 200µm long carbon fibres, with inserts ranging from 50mm through to 58mm which were assembled to the pre-existing titanium shell. (Giannikas, Din et al. 2002, Pace, Spurio et al. 2002, Rogers, Kulkarni et al. 2003).

Figure 2.17: ABG II (Pace, Marinelli et al. 2008)

Figure 2.18: ABG II liner unassembled

Pace et al. presented a 36 month follow up study where by 28 patients were available for clinical review, none of the implants had been revised because of septic loosening (Pace, Marinelli et al. 2005). A further study by Pace *et al* looked at the technical and histological analysis of a retrieval of the aforementioned implant. This was retrieved because of post trauma infection from a patient who had the components in place for 28 months. Figure 2.19 shows the revised implant, where it was observed that there was a highly polished finish covering two thirds of the implant. The bearing surface with the unworn zone still shows the machining grooves, typically associated with conventional machining.

Figure 2.19: CFR PEEK insert revised from patient (Pace, Marinelli et al. 2008)

Surface topography measurement was undertaken to look at surface finish of the inner surface, which showed that the polished zones had a lower R_a value than the machined zone (0.2µm and 0.8µm respectively); it also showed fibre protrusion as shown in Figure 2.20 which the author would expect on this composite due to the longer fibres; this problem may be less severe with the short fibres used in the author's design (Pace, Marinelli et al. 2008).

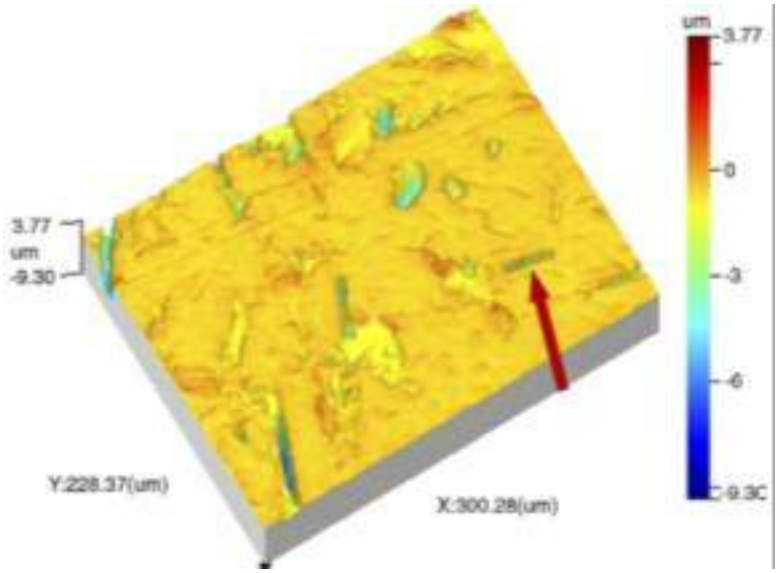

Figure 2.20: Fibre pull out (Pace, Marinelli et al. 2008)

Analysis was also undertaken of the sphere to detect wear patterns and this showed the deviation from the nominal dimension to be 0.130mm at 28 months (0.057mm/year) as shown in Figure 2.21.

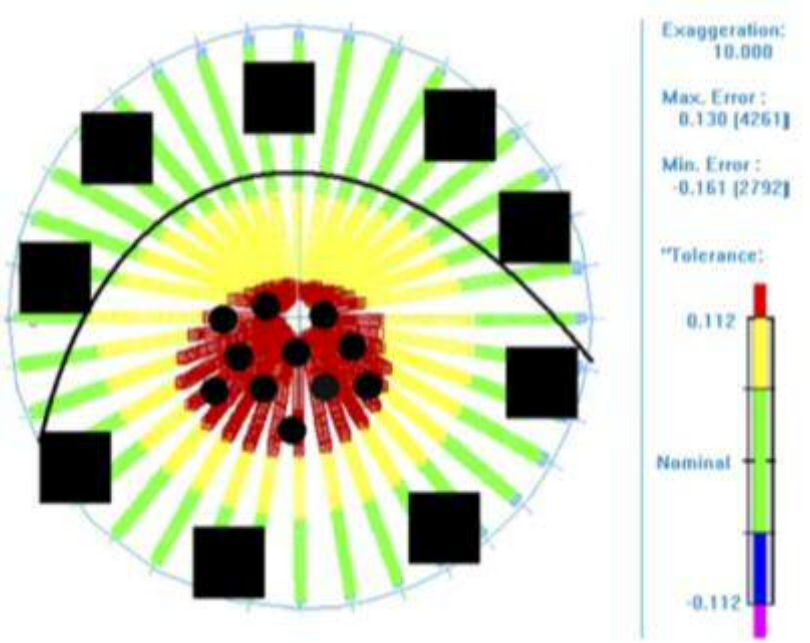

Figure 2.21: Coordinate measuring machine measurement of worn cup (Pace, Marinelli et al. 2008)

The author questions the accuracy of this data due to the piece of equipment used as this will take an average based on the sphere. The author was able to get access to a retrieved ABG II sample and drew comparison on the visual wear pattern seen with a highly polished contact patch and unworn machined zone. Whilst the author does not know how long the implant was in the patient, the results of the surface measurement were very similar; polished zone measuring 0.2924µm and machined 0.7087µm respectively as shown in Figure 2.22 and 2.23.

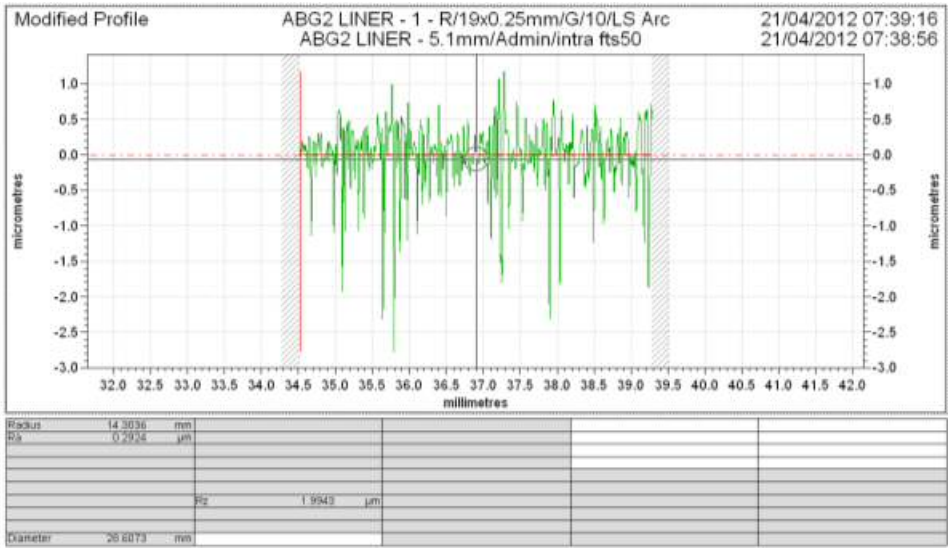

Figure 2.22: Surface measurement of ABG II – Polished zone

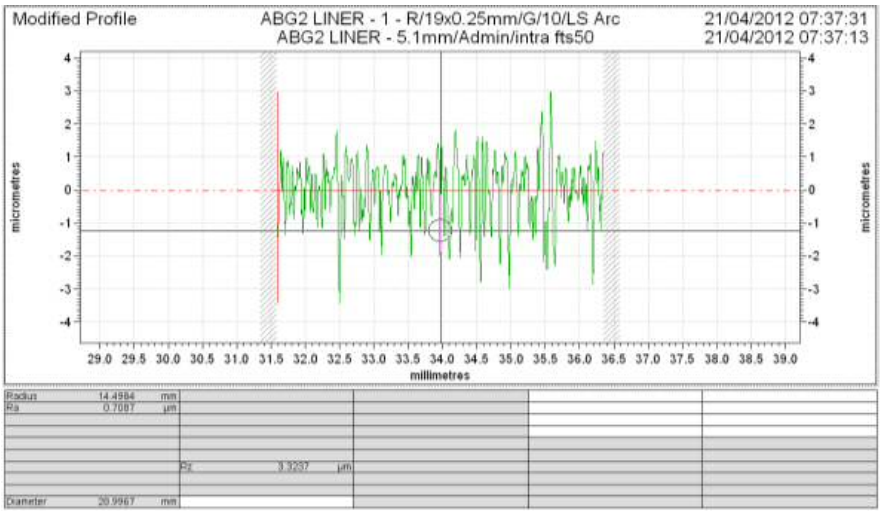

Figure 2.23: Surface measurement of ABG II – Machined zone

The author was also able to look at the wear and measure the roundness of the component using a Talyrond by Talyor Hobson. Figure 2.24 shows the out of roundness to be 47.78 µm in the top section of the prosthesis.

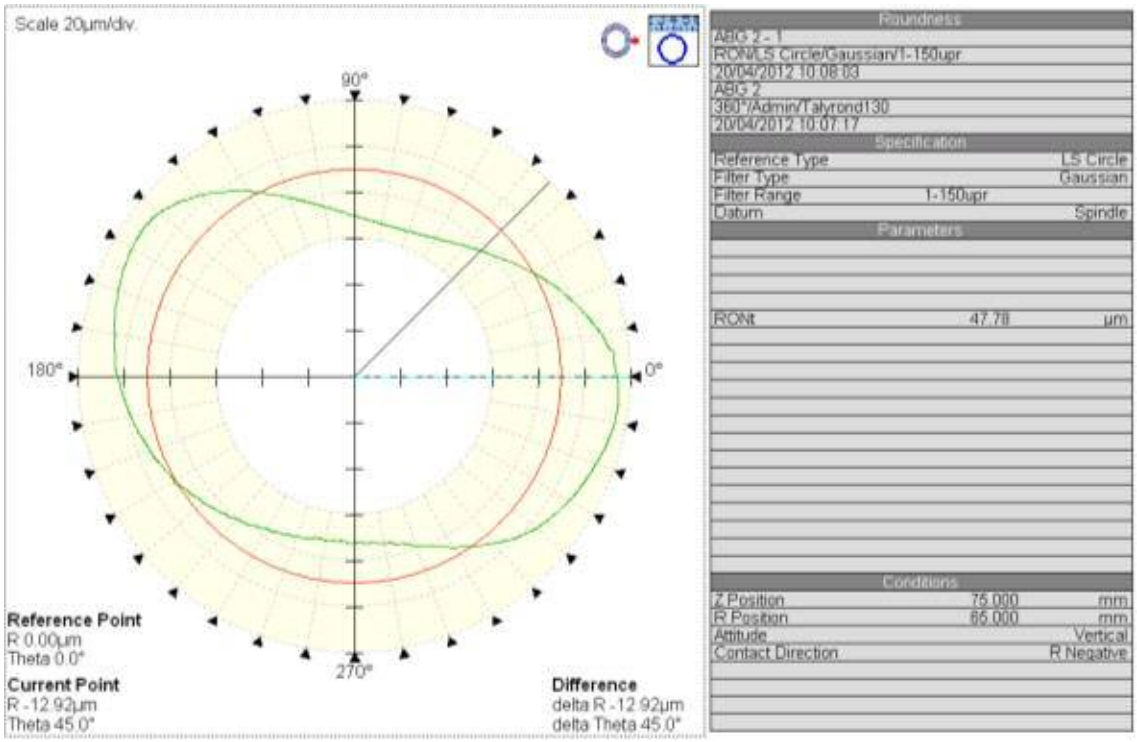

Figure 2.24: Top profile of ABG II

Figure 2.25 shows the out of roundness to be 53.08µm in the middle section of the prosthesis, with Figure 2.26 showing the out of roundness at the bottom of the prosthesis to be 35.86 µm. Given that the author has no patient or implant information it is difficult to draw any firm conclusions about the performance of the implant.

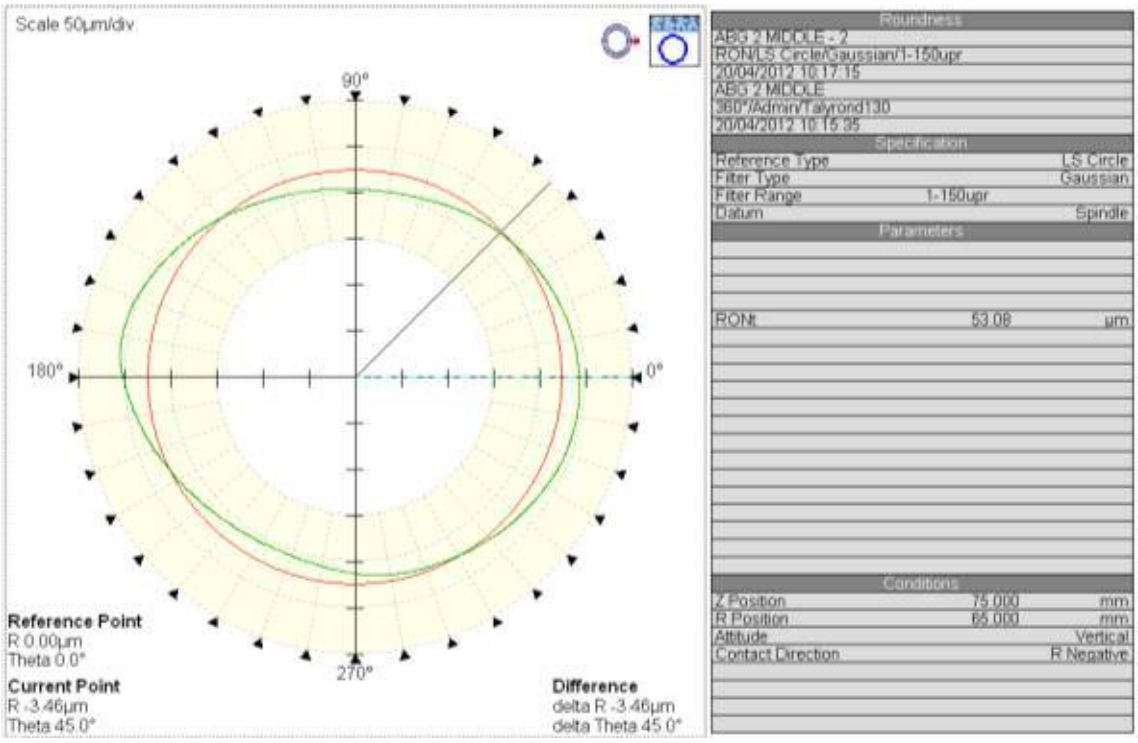

Figure 2.25: Middle profile of ABG II

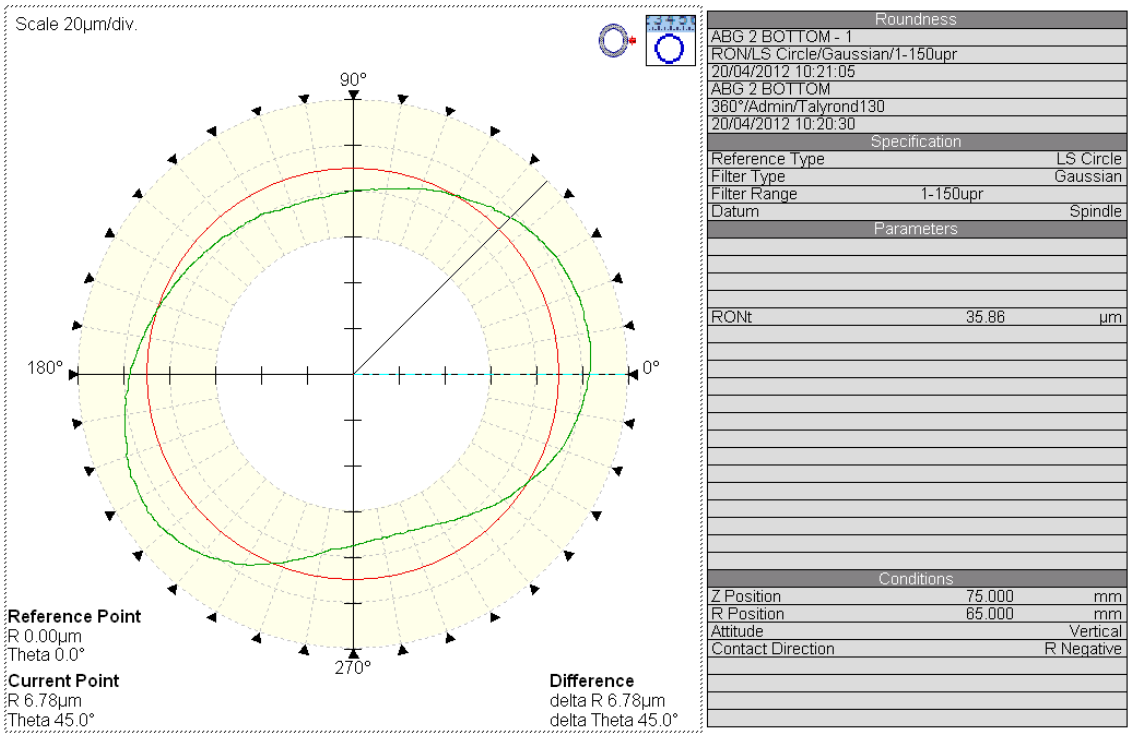

Figure 2.26: Bottom profile of ABG II

2.8.2 **Mitch PCR Cup™**

Figure 2.27 shows the predecessor to the Mitch PCR Cup™ on the left; the Cambridge cup. The Mitch PCR Cup™ is shown on the right. The Cambridge cup had been

designed to replace the horseshoe-shaped articular cartilage of the acetabulum and the underlying subchondral bone. It is intended to provide physiological loading with minimal resection of healthy bone. The bearing surface is a layer of 3mm thick UHMWPE with an injection moulded backing of Poly Butylene Terephthalate (PBT) reinforced with 30% carbon fibre measuring 1.5mm and a coating of hydroxyapatite (HA). A five year clinical study showed good early results as well as bone preservation following a two year dual energy X-ray absorptiometry (DEXA) study (Brooks, Jones et al. 2004, Field and Rushton 2005, Field, Cronin et al. 2006). Based on this success the Mitch cup was developed which was thinner because of the superior material properties of CFR PEEK (*Manley 2007).

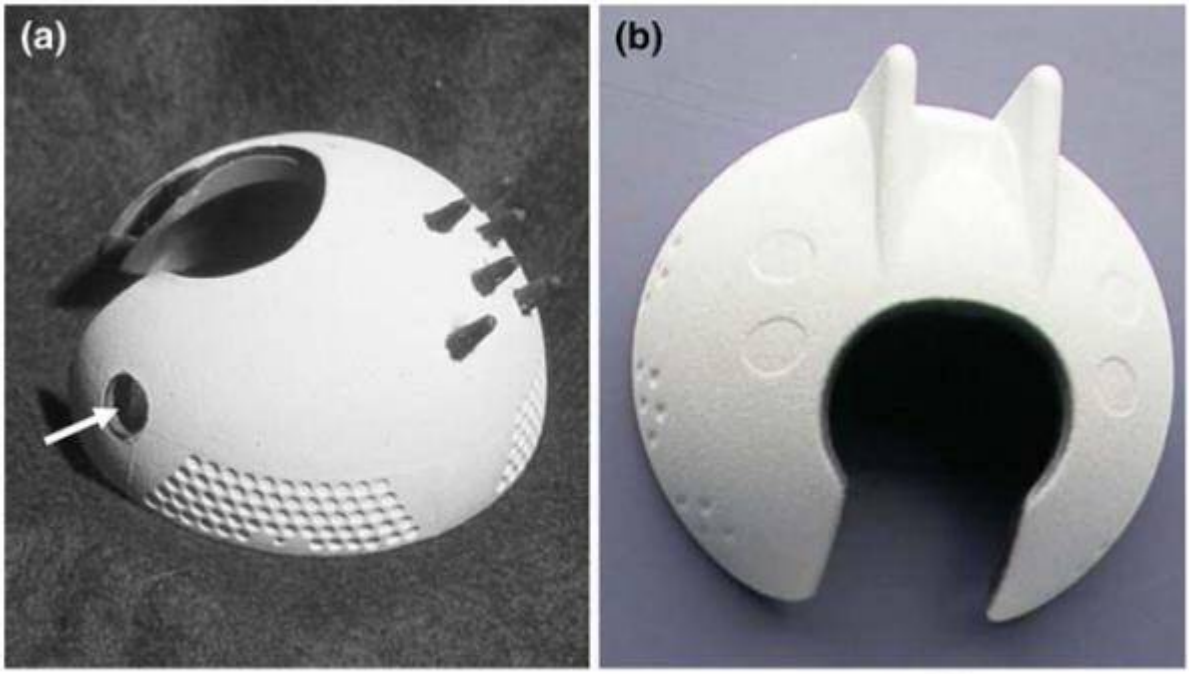

Figure 2.27: Cambridge and Mitch PCR™ cup (Latif, Mehats et al. 2008)

The Mitch cup measured 3mm in thickness, a reduction of 1.5mm over the Cambridge cup; increased stiffness, increased strength and improved creep resistance, allows thinner sections (Tai, Ma et al. 1995, Ferguson, Visser et al. 2006, Rae, Brown et al. 2007, Link 2008, Robotti, Vedova et al. 2009, Sobieraj, Murphy et al. 2010, Avanzini, Donzella et al. 2013).

2.9 Wear Properties of CFR PEEK

UHMWPE has been the most widely used bearing surface in THA and total knee arthroplasty TKA since the 1960's. However, in recent years it has been recognised that the wear of UHMWPE may be the limiting factor for the long term success of the prostheses (Wang, Lin et al. 1999). Wang *et al* conducted wear testing for five million cycles on three different materials; UHMWPE, Pitch CFR PEEK and Pan CFR PEEK which articulated against three different materials, CoCrMo, alumina and zirconia 32mm heads. The results showed the best bearing couple to be the pitch CFR composite against a zirconia femoral head which had a wear rate thirty times smaller than UHMWPE. Pin on plate testing has been conducted on the following materials shown in Table 2.4. Pin on plate does not replicate loads and motions both achieved in the human body and wear test simulators but looks at the wear that will occur once the materials come in to contact. Wear test simulators are expensive and typically run for a much longer period of time; the pin on plate provides quick results when testing new material combinations (Scholes and Unsworth 2009).

Table 2.4: Pin on Plate Materials

Pin Material	Plate Material
PEEK	Low Carbon (LC) CoCrMo
CFR PEEK – PAN	Low Carbon (LC) CoCrMo
CFR PEEK – PAN	High Carbon (LC) CoCrMo
CFR PEEK – Pitch	High Carbon (LC) CoCrMo

These tests ran for two million cycles at a cycle frequency of 1 Hz with new bovine calf serum diluted to 25% with distilled water being the lubricant. The results supported Wang *et al* with Pitch based carbon fibre showing superior wear over the other material combinations, as shown in Figure 2.28.

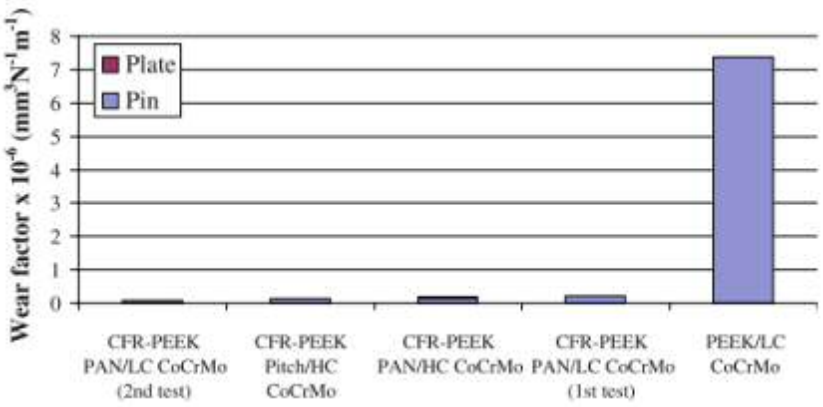

Figure 2.28: Wear results for all material combinations (Scholes and Unsworth 2009)

The author has to question the use of CoCr as a combination with CFR PEEK as analysis of the CoCrMo showed surface scratches, in pin on disc tests, due to protruding carbides. This may indicate that once the PEEK is removed by the CoCrMo that the protruding carbon fibres are in fact scratching the surface and further supports the notion that a ceramic counter face should be used in conjunction with this material (Scholes and Unsworth 2009, Wang, Wu et al. 2012). To further support this theory a wear simulation test was conduct with a 36mm Biolox Delta ceramic head and a CFR PEEK acetabular component manufactured form CFR PEEK™, the same material the author has used in his design of the implant. This test ran for 10 million cycles following the ISO standard 14242-1; "*Implants for surgery. Wear of the total hip-joint prostheses. Loading and displacement parameters for wear testing machines and corresponding environmental conditions for test*".

The mean volumetric wear rate was $0.3mm^3/Mc \pm 0.07mm^3/Mc$ which is very similar to the results obtained by A Wang *et al* and Q.Q Wang *et al* (Wang, Lin et al. 1998, Wang, Wu et al. 2012) , indicating the ceramic on CFR PEEK bearing to be a very low wear option for total hip replacement. A separate wear test simulation using the Mitch PCR™ cup against a large 54mm alumina head was conducted as shown Figure 2.29

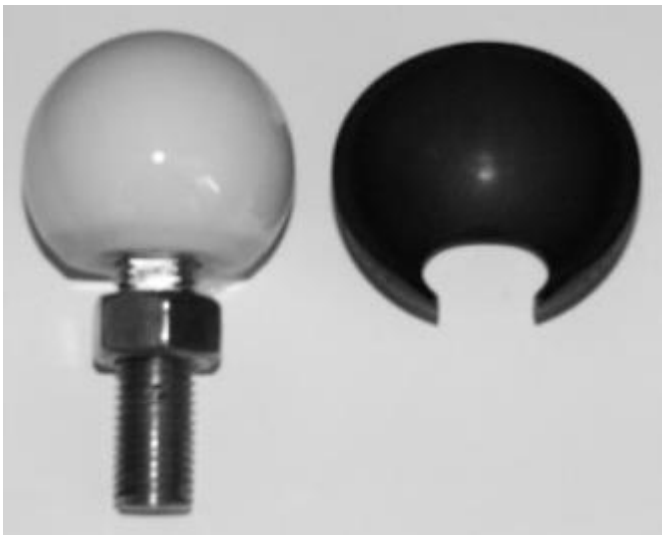

Figure 2.29: Mitch PCR™ and 54mm alumina femoral head (Scholes, Inman et al. 2008)

The test ran for 25 million cycles, which is approximately equivalent to 25 years *in vivo* use. A volumetric wear rate of 1.16mm^3/10^6 cycles was recorded, which whilst higher than the previous wear test results is still far lower than UHMWPE acetabular component of 28mm diameter against a ceramic head which had a volumetric wear rate of 38.6mm^3/10^6 . The author believes that the increased wear rate of the Mitch PCR™ cup could be down to several factors including surface finish, radial clearance and the thickness of the component itself.

2.10 Tribology in Orthopaedics

Synovial fluid is a clear, pale yellow, viscous liquid. The volume of synovial fluid present in the human body its sufficient both to lubricate the joint and to supply nutrition to the articular cartilage (Cooke, Dowson et al. 1978). As early as the 1940s amniotic fluid from animals was used in the joints and tissues of patients with joint disease (Rigdon and Warren 1941). In the 1970s silicone fluid was advocated as a synthetic lubricant, results showed that these synthetic fluids are suitable because of their similar rheological properties to synovial fluid (Cooke, Dowson et al. 1978). There is a strong correlation between experiment and theory when employing Carboxy Methyl Cellulose (CMC) fluids or silicone fluids as the lubricant (Scholes and Unsworth 2000). Further testing by Unsworth et al. investigated aspects of lubrication of artificial hip joints so that some indication of the modes of operation could be found, this involved various material combinations, radial clearances and surface areas tested when lubricated and when dry. The results showed that artificial joints operate under different

mechanics (Unsworth 1978, Roberts, Unsworth et al. 1982, S.C. Scholes a 2000). Unsworth et al. showed that frictional resistance in a joint was not dependent on viscosity but seemed to depend on the presence of a protein in the synovial fluid, hence new-born bovine calf serum is added to the lubricant used for wear tests as it has similar protein levels to human synovial fluid.

2.11 Mixed fluid regime

The mixed fluid lubrication regime is the term used to describe how the joint operates mechanically. Load is partially supported by the lubricating fluid but with some direct interaction between surfaces as shown in Figure 2.30. This is demonstrated by plotting a Stribeck curve (Figure 2.31), in which a decrease in friction factor with increase in Sommerfeld number is indicative of a mixed lubrication regime. The Stribeck curve describes the transition between different lubrication regimes with increasing speed for liquid lubricated sliding surfaces, which consist of three lubrication modes.

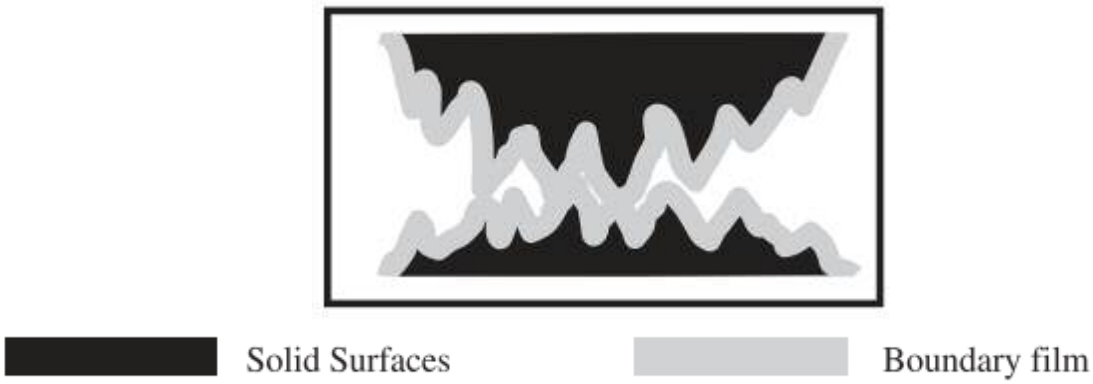

Figure 2.30: Schematic of mixed lubrication regimens (Jin, Stone et al. 2006)

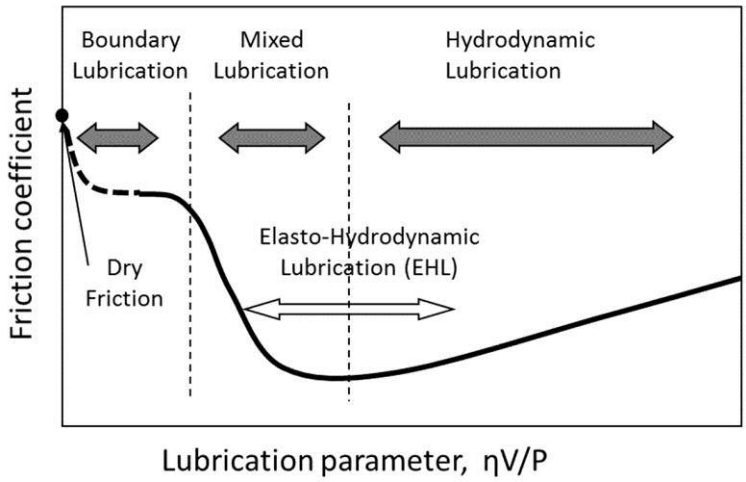

Figure 2.31: Example Stribeck curve (Kondo, Koyama et al. 2013)

2.12 Boundary regime

Some joints operate in the boundary lubrication regime; this involves substantial direct interaction between surfaces. Lubrication is provided by slippery molecules adhered to the surface as shown in Figure 2.32. This is again, demonstrated by plotting a Stribeck curve, in which a constant friction factor points towards a boundary lubrication regime.

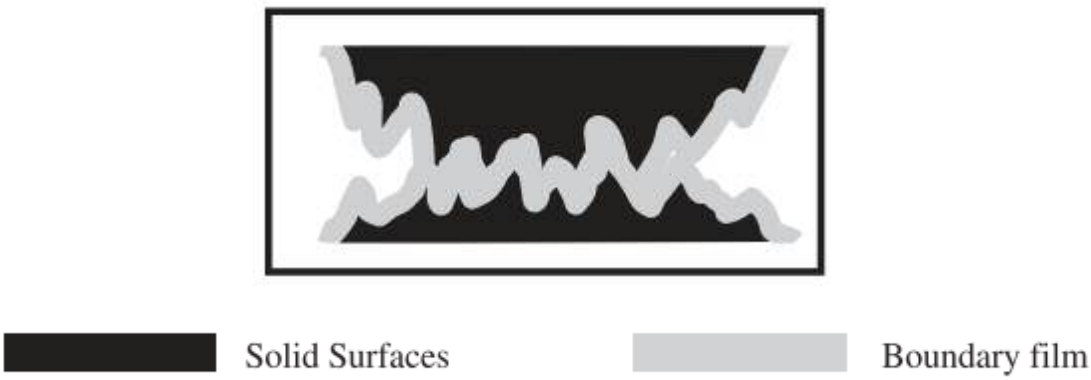

Figure 2.32: Schematic of boundary lubrication regime (Jin, Stone et al. 2006)

2.13 Fluid film regime

Some joints may operate in the fluid film lubrication regime (Figure 2.33), in which there is complete separation between the two surfaces. Lubricant viscosity becomes very important; there is minimal wear and low friction. A rising trend from a low friction factor with increasing Sommerfeld number is indicative of full fluid-film lubrication in a Stribeck curve.

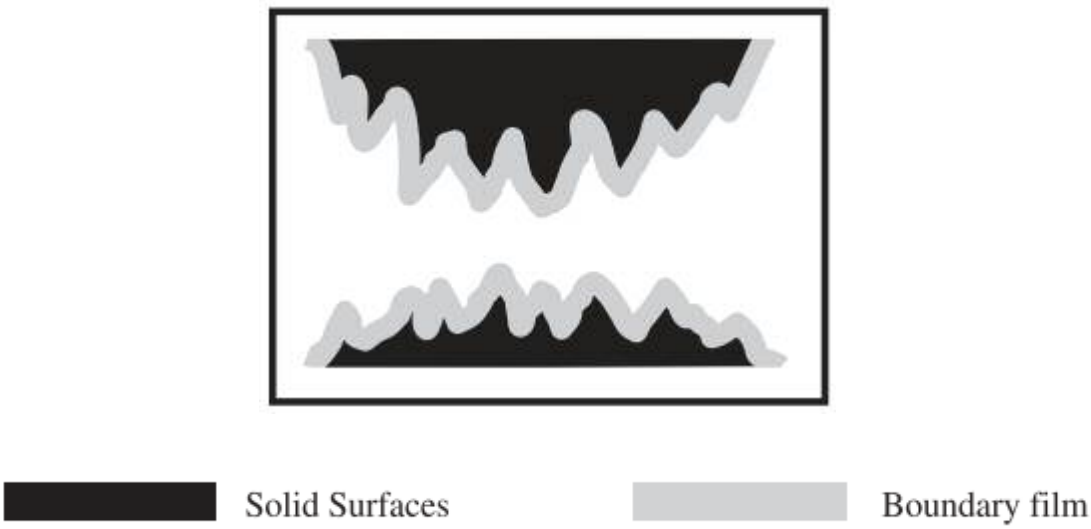

Figure 2.33: Schematic of fluid lubrication regime (Jin, Stone et al. 2006)

2.14 Cadaveric Experiments

Implant deformation really became a cause for concern with the introduction of hard-on-hard bearings specifically CoC and MoM bearing couples, although cup deformation was a concern with the introduction of modular acetabular components, which have the ability to accept different bearing options into one acetabular shell as shown in Figure 2.34.

Figure 2.34: Modular components (Squire, Griffin et al. 2006)

Deformation of the cup raises the risk of equatorial loading with increased wear, ceramic fracture and femoral clutching of the components; it can cause increased wear, interruption of the fluid regime and increased torque causing the implant to become removed from the patients acetabulum (Jin 2006, Squire, Griffin et al. 2006, Langdown, Pickard et al. 2007, Markel, Day et al. 2011). For CoC monobloc constructs this was less of a problem as these constructs are generally thicker due to the titanium shell required to grip the ceramic insert; ceramic inserts require a titanium shell in order for it to support a biological fixation method such as Porous Plasma Spray (PPS). MoM implants, specifically for resurfacing, were designed to be thinner walled constructs that could support a large femoral head to help reduce dislocation (van Heumen, Heesterbeek et al. 2014), much like what is seen in the human body (Liu, Jin et al. 2006, Shimmin, Beaule et al. 2008). To obtain initial fixation the surgeon can prepare the acetabulum anything from 1mm to 4mm below the final diameter of the implant depending on bone quality (Squire, Griffin et al. 2006). Grimes et al. analysed 11 Durom cups and modular heads (Zimmer, Warsaw, Indiana) which were retrieved at 13.5± 6.7 months, *in vitro* studies conducted along with the Birmingham Hip

Resurfacing (Smith & Nephew, Memphis) which served as a control. The mean diametric deformation of the Durom was 89.8 ± 14.8μm, significantly greater than the BHR, 57.2 ± 25.0μm (P b .002). More in-depth *in vitro* analysis by Jin *et al* using cadaveric models and similar 2-point acetabular urethane foam models to that of Grimes *et al* found that for a relatively thin cup with a press fit interference of 1 mm, the maximum diametric cup deformation was 80-96μm, compared with a nominal diametric clearance of 80–120μm generally required for an MoM prosthesis to provide satisfactory tribological performance. Utilising a different test setup it was shown that component deformation ranged from 15 to 300μm. Larger cups with thinner walls to allow for larger femoral heads had the greatest deformation, exceeding the radial clearances from the manufacturers (Springer, Habet et al. 2012).

2.15 Finite Element Analysis

Computational models may have the ability to quantify the relationship between hip morphology, cartilage mechanics and osteoarthritis (Anderson, Ellis et al. 2010) and is widely used in orthopaedic biomechanics. Finite Element Analysis (FEA) or finite element method/modelling (FEM) as it is also known is a computer technique of structural analysis developed in engineering mechanics, first being introduced to orthopaedics in 1972 to evaluate stresses in human bones (Brekelmans, Poort et al. 1972, Huiskes and Chao 1983). It is a tool that can be used to validate design features and explore the potential effects of design changes such as cup geometry and materials on the implant whilst also being able to analyse what potential effect the design has on the patient and how the prosthesis positioning in the acetabulum can improve or impair the surrounding bone.

In 1983 FEM was undertaken to compare two models, the first being the human pelvis, the second being a human pelvis but with the removal of cartilage and subchondral bone and replaced with alumina ceramic. The purpose of this study was to analyse the various deformations and displacements of the whole pelvis, the pelvic ring and the acetabulum and the principal stress, the maximum shear stress along with Von Mises stress on the surface of the whole pelvis and in the various horizontal sections of the whole pelvis. This study is one of the first that started to look at how the pelvis responses to different gait cycles by means of a three dimensional model (Oonishi, Isha et al. 1983).

In 1995 further research was undertaken to improve accuracy in the three dimensional model looking at cortical and trabecular bone thicknesses within the model. Computer tomography (CT) scans were taken of several pelvis bones looking at bone density and thickness, this in turn was added to the three dimensional model. To validate this FE model, two fresh pelvic bones were fitted with strain gages and loaded in a testing machine. Stresses calculated from the strain data of this experiment were compared to the results of a simulation with the developed pelvic FE model (Dalstra, Huiskes et al. 1995). This method has been improved on and undertaken in several separate studies (Anderson, Peters et al. 2005, Barink, van Kampen et al. 2005, Bevill, Bevill et al. 2005, Ferguson, Visser et al. 2006, Shultz, Blaha et al. 2006, Cilingir, Ucar et al. 2007, Majumder, Roychowdhury et al. 2007, Moser and Lightner 2007, Phillips, Pankaj et al. 2007, Cox, Driessen et al. 2008, Shim, Pitto et al. 2008, Kluess, Souffrant et al. 2009).

Using cadaveric specimens was paramount to the author's development of this implant as it aided in determining the predicted amount of deformation that could potentially occur *in vivo* and validating this with tribology testing, this supported validating the FEA model to support an optimum design.

2.16 Dynamic Fatigue Testing

There have been significant advancements in implant materials used in the manufacturing of orthopaedic implants in general, with joint replacement implants in the hip, knee, shoulder and spine sharing the same material options. An important mechanical factor is the ability of the implant to withstand the continual application of load which may exceed the body weight of the patient by several folds. To ensure that these implants do not fail prematurely due to fatigue, a draft standard was created in 1975, with the first British Standards Institution (BSI) and International Organisation for Standardization (ISO) standard being introduced in 1984 (Semlitsch and Panic 1983, Teoh 2000). Aseptic loosening is the term used to explain the late failure of the implant and the bond to the bone in the absence of infection (Heaton-Adegbile, Zant et al. 2006). Both mechanical failure and some aspects of aseptic loosening can be assessed by means of dynamic fatigue testing. As a general rule one million cycles *in vitro* equates to approximately one year *in vivo.* Depending on materials used the frequency will have to be adjusted accordingly; a hard bearing such as a ceramic can operate up to 20Hz, where polymers such as polyethylene and CFR PEEK need to be tested below 5Hz to prevent heating and softening of the material (Teoh 2000).

3 Design Evolution of Prosthesis

The author of this thesis was solely responsible for the initiation of the project within Zimmer Biomet and the determination of the fundamental design parameters and design evolution.

3.1 Introduction

As MoM implants started to show signs of significant mechanical failures and life changing effects for the patients the author started to examine alternative bearing materials. Initially when anatomic MoM devices were created they allowed for a thin walled acetabular component to be used in conjunction with a large anatomic femoral head, which allows several benefits:

- Increased Range of Motion (RoM);
- Joint stability with the reduction of dislocation and subluxation (the neck is narrow compared to the diameter of the head and so less likely to impinge on the edge of the cup);
- Optimised Internal Diameter (ID) to Outer Diameter (OD) ratio (e.g. 60 mm femoral head into a 66 mm cup);
- The use of anatomic sized bearing couples that will allow for the least bone removal and gain the largest head size possible.

The CFR PEEK Monobloc has been through several design iterations to develop the optimum solution possible for the patient and surgeon. This involved analysing and evaluating all elements of geometries, bearing surface finish and radial clearance. The aim was to produce the lowest wear and friction as possible in this bearing combination of CFR PEEK and ZPTA ceramic heads.

3.2 Design Specification

The concept behind the author's design is to allow a monobloc construct to utilise novel screw-hole designs directly through the bearing surface in order to obtain secondary fixation by means of CFR PEEK cancellous locking screws. The thinned wall construct minimises bone removal and trauma to the patient, and allows for large anatomic heads to be used to replicate the natural anatomy. In summary the fundamental design specification points are:

- The CFR PEEK monobloc will be used in un-cemented THA/THR;
- Correct clearance to achieve lowest wear and friction rates;
- CFR PEEK monobloc will need to withstand impaction into the acetabulum;
- Prosthesis to retain geometric tolerances when impacted into the acetabulum;
- Shell must survive fatigue testing when the cup is implanted at a high inclination angle (60º) and as a result loaded through the rim;
- CFR PEEK monobloc to be used in conjunction with ceramic heads only;
- CFR PEEK monobloc must have biological fixation;
- Good biocompatibility is essential;
- Bearing articulating surface must have a R_a 0.02µm - R_a 0.5µm;
- Construct must have potential for injection moulding.

3.3 Design Evolutions

3.3.1 Design Version One

Version one was a hemispherical design profile with a 3mm internal offset, and a large radial clearance of 800µm. The internal offset has two main features, the first being to bring the internal bearing centre outwards so that the cup is thicker at the apex and thinner at the rim of the cup the second reason why this is implemented is to reduce the risk of femoral impingement when used as a resurfacing construct. The outside geometry had a layer of Biomet's proprietary PPS applied. The design envelope of a hemispherical design with an internal offset was based on a traditional monobloc construct, which at the time were MoM. The internal offset allows the construct to be used in conjunction with resurfacing implants without the risk of impingement. This design was initially selected for the following reasons:

- A benchmark to compare against MoM monobloc;
- To evaluate the properties and limitations of the CFR PEEK material;
- To ascertain orthopaedic surgeon feedback as a monobloc and alternative material;
- The author believes that resurfacing as a technique is still viable and will be needed due to the population living longer, leading active lives and wanting to return to an active life after hip arthroplasty.

Based on an initial investigation the author organised a cadaveric experiment (Chapter 5) with five specimens of Design One. To ensure that the specimens were inserted

correctly an orthopaedic surgeon supported the activity. The test results were positive, however specific feedback from the surgeon was that aesthetically the large radial clearance was of concern, as typical clearances for monobloc constructs are much smaller. The practical results showed more deformation than that of traditional monobloc constructs, but still met the criteria set by the author. However, it was noted that this still could lead to femoral clutching as maximum deformation occurred in a 2mm press fit scenario, based on reaming parameters. This lead to the author altering radial clearance and investigating the outside geometry profile with the aim of obtaining an enhanced primary press fit. During this phase friction tests to evaluate various radial clearances were being conducted The tests covered a wide range of clearances to look at the effects these have on the friction factor and the regime that the bearing couple would perform under i.e. boundary, fluid or mixed regimes. The tests are presented in Chapter 6 and enabled the author to fully understand the material and further core development of the design. The radial clearance was subject to further changes based on further cadaveric and tribology testing. The final result was validated using FEA.

3.3.2 **Design Version Two**

This is again a hemispherical design profile, however with axial and circumferential grooves. The design had a 3mm internal offset and a radial clearance of 330µm. The outside geometry again had a layer of Biomet's proprietary PPS. A second cadaveric experiment was completed in conjunction with Dr Stephen Vehmeijer, a Dutch orthopaedic surgeon. The surgeon implanted four out of the six specimens, with the remaining two being installed by the author. The initial results confirmed the findings from the first cadaveric study that the defined reaming parameters affected the degree of deformation that can occur to the implant on impaction. The reduction in radial clearance reduced deformation, which is an obvious assumption to make. The variability in reaming parameters and the amount of deformation occurring was a concern for the author. The second cause for concern was that on impaction the author managed to fracture the implant in several place which highlighted the notch sensitivity of PEEK.

3.3.3 **Design Version Three**

Version Three had an elliptical profile, the pole of the implant was reduced by 1mm and the periphery increased by 1mm. It too had the same axial and circumferential grooves as Version Two; the grooves were retained as there was an overall increase in wall

thickness which would prevent fracture on impaction. The radial clearance was 230µm. with again a layer of Biomet's proprietary PPS. Due to the author's findings on cadaveric and tribology testing, 230µm was selected as the optimum radial clearance for all sizes of monobloc. From a tribology perspective 230µm offered the best performance but would need validation for the level of deformation in a cadaver to ensure that it would work correctly.

3.3.4 Design Version Four

This was the same as Version Three, but the axial and circumferential grooves were removed, based on surgeon feedback. Surgeons stated that they were not beneficial to the implant with the new profile geometry, secondly the author still had reservations that they are stress risers which would increase the risk of early fatigue failure or fracture under impaction. The cadaveric experiment undertaken with Design Four demonstrated that the implant showed the least deformation and from a surgical perspective provided superior press fit and initial stability.

3.4 Thread and screw design

3.4.1 Thread design

The author proceeded to develop a new screw for securing the implant. The screw has two threaded sections, the shaft and the head. The cup thread design has a radius type geometry, removing sharp corners. The thread form is also tapered so that when the mating screw is engaged an interference fit occurs. The screws will be tightened to a pre-determined torque to ensure that the threads do not become damaged (Figure 3.1).

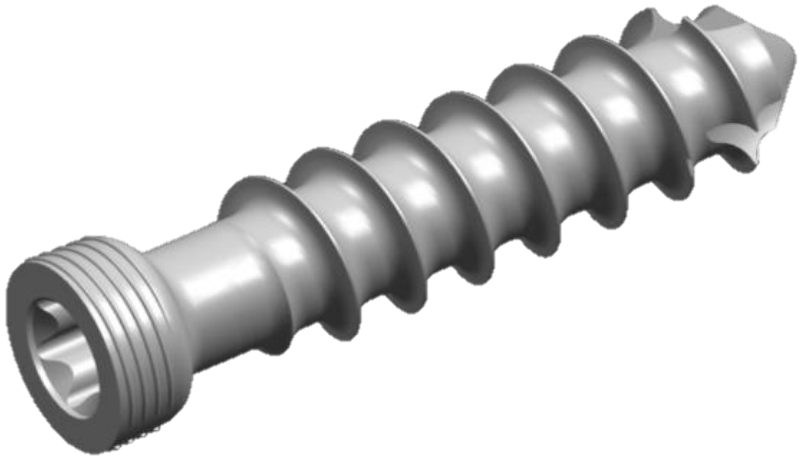

Figure 3.1: CFR PEEK Cancellous Screw

The thread on the shaft is a typical cancellous screw thread measuring 6.5mm in diameter. The screw geometry on the head matches the thread in the cup, as mentioned previously there is an interference fit between the thread in the monobloc and the thread on the screw head. This ensures that the threads engage and it prevents the risk of the screw migrating back out directly on the femoral head as shown in Figure 3.2 and 3.3. Detailed drawings of screw and cup can be found in Figures 3.4 and 3.5.

Figure 3.2: CFR PEEK locking screw thread

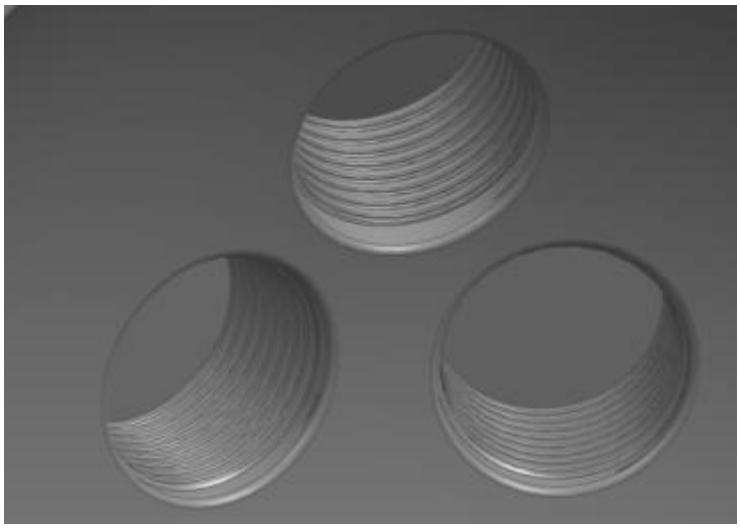

Figure 3.3: Screw thread geometry in the cup

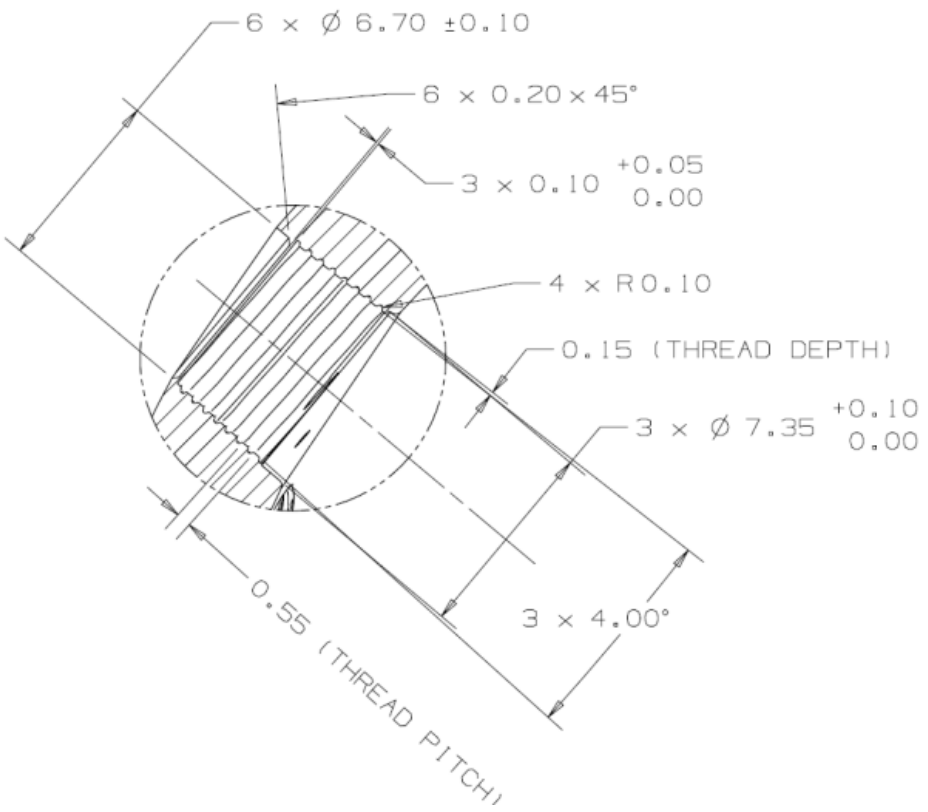

Figure 3.4: Screw thread geometry (All dimensions in mm)

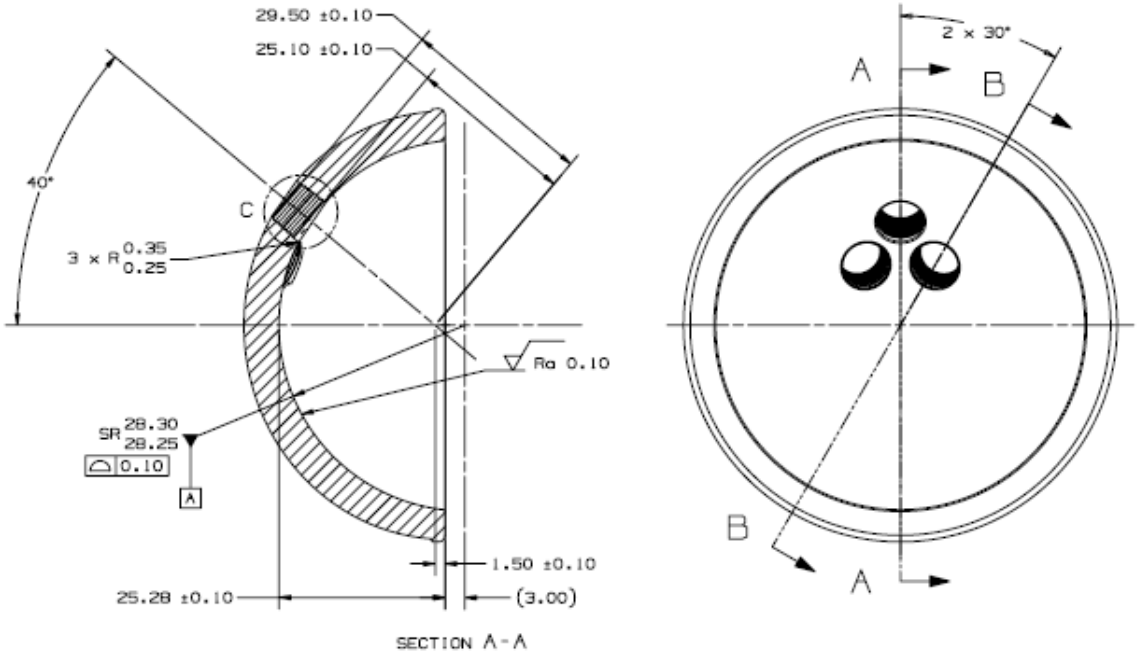

Figure 3.5: CFR PEEK Monobloc with screws (All dimensions in mm)

3.5 Frangible Elements

Screw fixation in hip surgery is based on a patient's requirements. Screw fixation is usually dependent on bone quality whereby primary fixation is inadequate. In this situation screws are used to support the cup until biological fixation develops. Frangible elements were designed to close the screw holes and allow flexibility in implant installation. Frangible elements would prevent third body wear penetrating the bearing surface and the femoral head, and stop wear debris from the bearing travelling through the unused holes to the bone-implant interface. The holes are designed in such a way that there is a thin piece of CFR PEEK machined into the shell. On the outside of the shell the hole is chamfered; this is for a practical reason, CFR PEEK is typically notch sensitive (Sobieraj *et al*., 2010). Whilst every effort has been taken to remove sharp corners from the design, this chamfer has been strategically added so that when the surgeon punches out the blank with the specific instrument the frangible element breaks (Figure 3.6).

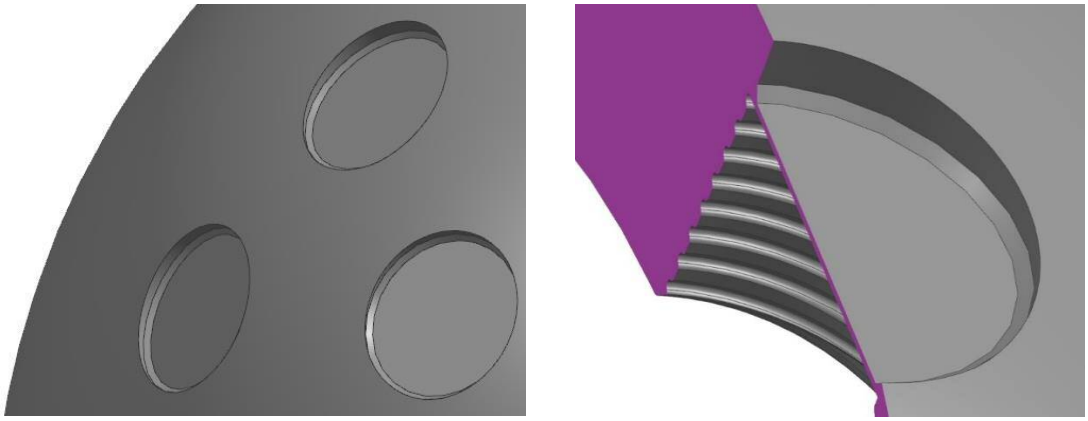

Figure 3.6: CFR Frangible elements

An important part of the development of the design was tribological testing to investigate the effect of radial clearance and other variables and hence optimise the design. This is described in the following chapter.

4 Tribology Testing

4.1 Introduction

Initial designs of the CFR PEEK monobloc showed that varying degrees of deformation occurred during implantation into a cadaveric specimen. Deformation of an acetabular cup results in changes of the diametric clearance; in severe cases clutching of the femoral head can occur with the acetabular cup pinching the femoral head. Furthermore, the literature shows that the combination of a CFR PEEK cup and a ZPTA femoral head may result in lower friction than conventional materials (Garle 2003, Fisher, Jin et al. 2006).

The purpose of this study was therefore:

1. To determine the optimum clearance for the entire size range;
2. To determine the lubrication regime of the implant against a femoral ceramic head under typical loading conditions;
3. To determine the optimum surface finish to produce the lowest friction.

4.2 Methods

4.2.1 Radial clearances

In order to determine an appropriate range of clearances to be tested, an effective radius was considered as given by Equation 4.1:

Equation 4.1

where:

R_{eff} = effective radius (m)

R_1 and R_2 = radius of surface 1 and 2 respectively (m)

For convex surfaces R_1 and R_2 are positive, for a concave surface they are negative. Therefore, for a ball and socket arrangement the formula becomes Equation 4.2:

Equation 4.2

Where R_1 = head radius (m) and R_2 = cup radius (m).

Ceramic on CFR PEEK bearings have been previously shown to operate under mixed or boundary conditions (Scholes et al., 2008, Scholes and Unsworth, 2000, Unsworth and Scholes, 2009). In these studies, a wide range of clearances was tested to evaluate how the material performed. Using equations 4.1 and 4.2 the effective radius of a Biomet UK ceramic on polyethylene cup was calculated. The largest effective radius was found from the tolerance combination which gives the smallest clearance, i.e. minimum cup size - max head size, and vice versa for the smallest effective radius. The largest effective radius of a 28mm polyethylene bearing was calculated as follows using Equation 4.3.

Equation 4.3

This effective radius was then used to calculate a maximum cup inside diameter (ID) given the head size (Magnum C, Biomet UK). The smallest effective radius was used to calculate the minimum cup diameter. Given these two values and the known size of the head, the maximum and minimum clearances were found. Initial friction testing was conducted at the University of Durham using an internationally recognised test facility. Due to availability subsequent testing was completed at the University of Bradford.

4.2.2 Experimental procedure at Durham Facility

The friction test set up consists of an oscillating upper frame in which the femoral head is mounted (Figure 4.1 and 4.2). The acetabular cup is then fixed inverted, to the anatomical position at 33°, in the measuring carriage. The CFR PEEK monobloc cups were mounted in a custom made fixture as shown in Figure 4.2.

Figure 4.1: Friction testing machine

Figure 4.2: Friction testing fixture

The PEEK cups were stored in a 60°C water bath for three days before the friction tests commenced, this is necessary as CFR PEEK is porous so needs to reach saturation, so no further liquid is absorbed into the material which could affect results. The CFR PEEK cup is placed into the plastic ring shown in (Figure 4.2). The CFR PEEK is secured by a cap with is screwed on this ensures the CFR PEEK cup is also levelled out. A servo hydraulic system applies a simple-harmonic oscillatory motion comprising of a low load swing phase, the maximum and minimum forces exerted on the prosthesis were 2000 N and 100 N respectively. A sinusoidal motion was applied to the femoral component in the flexion - extension plane with an amplitude of ±24° and at a frequency of 0.8Hz. Load, frictional torque and angular displacement were recorded during the 1st, 21st and 41st cycle. Testing was conducted using various viscosities of lubricant as shown in Table 4.2 (Unsworth et al., 2006, Unsworth, 1978, Scholes et al., 2000a). CMC solution was used to alter the viscosity to produce Stribeck plots, as it has similar properties to synovial fluid (Scholes and Unsworth, 2006a, Scholes and Unsworth, Fam et al., 2007). The viscosity is very important for synovial fluid because

it determines the type of lubrication that occurs; by nature, it is non-Newtonian, hence the viscosity decreases as the shear-rate increases. For patients with osteoarthritis or rheumatoid arthritis, the viscosity of the synovial fluid decrease, and the combination of CMC and bovine serum covers this range (Cooke et al., 1978, Unsworth et al., 2006, S.C. Scholes a, 2000, Auger et al., 1993, Birkinshaw et al., 2010, Wang et al., 2012, Unsworth, 1978). Bovine serum is used as the proteins present within the serum are representative of the proteins in the synovial fluid, which are important in boundary lubrication, hence it is generally used in wear studies (Cooke et al., 1978). Each cup was tested three times.

Table 4.1: Lubricant and viscosities

Lubricant	Viscosity [Pas]
100% bovine Serum (BS)	0.00153
25BS+75 distilled water	0.00118
25BS+75DW+0.5g CMC	0.00524
25BS+75DW+1g CMC	0.0128
25BS+2g CMC	0.043
25BS+3.5g CMC	0.12
25BS+5g CMC	0.229

4.2.3 Experimental procedure at Bradford University

A further series of experiments were completed at a different facility due to limited availability of the Durham laboratory. The set-up was similar, but a different simulator was used, the swing angle was larger (±30° instead of ±24°) and the rotation frequency was slightly higher (1 Hz vs 0.8 Hz). The loading cycle was set as in the previous experiment at 2000 N to 100 N. In both test cases friction factor results were made in the maximum load at 2000N. In these experiments the system was run at 1Hz giving an entraining velocity of 0.02 m/s compared with the previous test of 0.015 m/s.

Figure 4.3: Biolox Delta Ceramic Head & CFR PEEK Cup

In the Bradford experiments a ProSim Friction Simulator was used (Figure 4.3). The ProSim friction simulator is a single station servo-hydraulic machine that consists of:

- A fixed frame which comprises of a friction measuring carriage that is placed on two externally pressurised hydrostatic bearings. The bearings allow negligible friction within the carriage, with respect to the friction generated between the articulating counter faces of the joints.
- A loading frame in which the femoral head is attached through a motion arm.

In order to achieve the true value of frictional torque between the bearing surfaces for the duration of the experiment, correct alignment of centres of rotation of the head and cup within the friction carriage and the loading frame is necessary. The acetabular cup is placed in the lubricant seat within the friction carriage, such that the hip implant is inverted with respect to the in vivo condition as shown in Figure 4.4

.

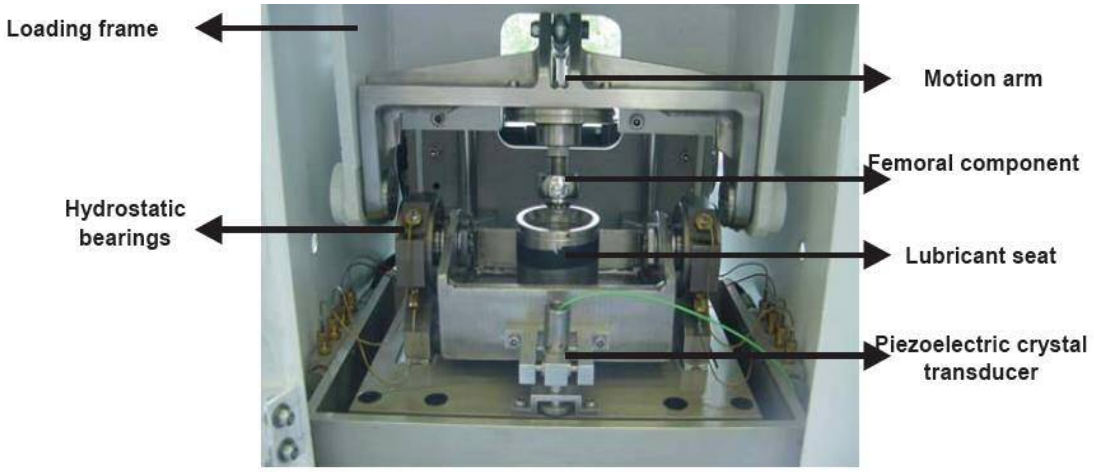

Figure 4.4: The friction measuring carriage and loading frame (Adapted from ProSim (Yan, Neville et al. 2009))

It should be noted that the alignment procedure must be carried out external to the machine. Alignment of the centre of rotation of the femoral component takes place by adjusting the femoral component using a stem holder. Furthermore, a specially designed rig is used in order to match the distance between the centre of the femoral head and the base of the stem holder, with the distance between the centre of rotation of the motion arm and the base of the stem holder. The femoral head height is then adjusted using slip gauges, to give a clearance between the top of the head and the roof of the rig. This clearance was determined using Equation 4.4:

$$\text{Clearence} = (99.43 - 72.91 + R_1)$$

Equation 4.4

where:

R_1 is the radius of the femoral head (mm)

99.43 = the distance (in mm) between the base and the foot of the stem holder jig

72.91 = the distance (in mm) between the centre of the femoral head to the base, which matches the centre of rotation of the motion arm and the base of the holder.

The position and height of the acetabular cup within the lubricant seat is adjusted by positioning a ceramic ball of a diameter less than the radius of the acetabular cup and using the adjustment screw in the base of the seat. The calculated value from Equation 4.5 is set on a depth gauge which can then be placed in the lubricant seat.

$$\text{Depth gauge setting} = (R_2 - 2R_{ball} + 14.92)$$

Equation 4.5

where:

R_2 = radius of the acetabular cup (mm)

R_{ball} = radius of the ball bearing (mm)

14.91 = distance (in mm) from the centre of rotation of the friction measuring system to the top edge of the lubricant seat.

The acetabular cup is adjusted correctly when the edge of the ceramic ball reaches the tip of the depth gauge shown in Figure 4.5.

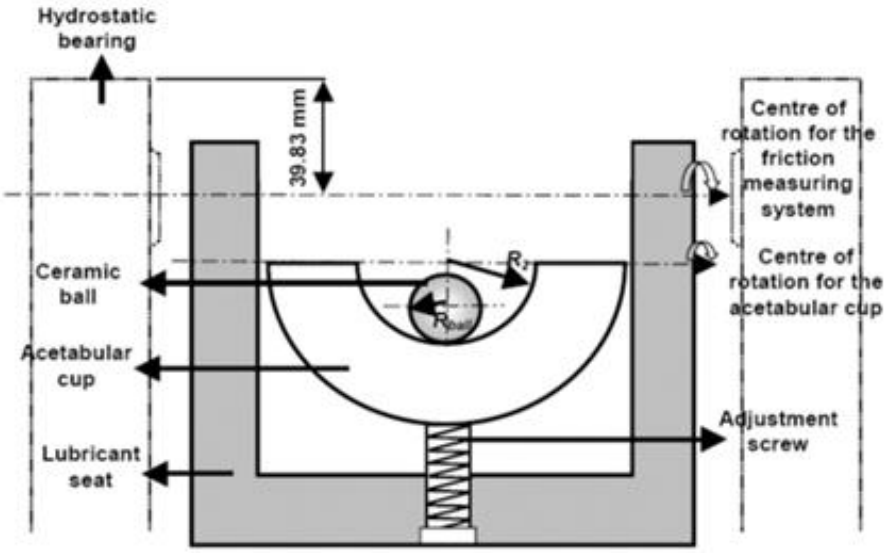

Figure 4.5: Schematic of setup

4.2.4 **Kinetics and Kinematics**

Like the Durham simulator, the ProSim friction simulator has two controlled axes of motion; rotation and load. In order to simulate the dominant flexion/extension action of the natural hip joint in the hip friction simulator, the motion arm of the loading frame is used to flex and extend the femoral head in a range of ±30°. A hydraulic pressure system controls the loading cycle that has been applied vertically through the femoral head. A cam-follower mechanism applies the pressure to the hydraulic system as the femoral head undergoes flexion/extension motion. This pulls the loading frame

downwards and consequently will apply a load to the acetabular cup in the fixed frame. Only fixed frequencies of 0.5, 1 and 2 Hz are available, hence the change in frequency from the previous experiments. The loading cycle is shown in Figure 4.6.

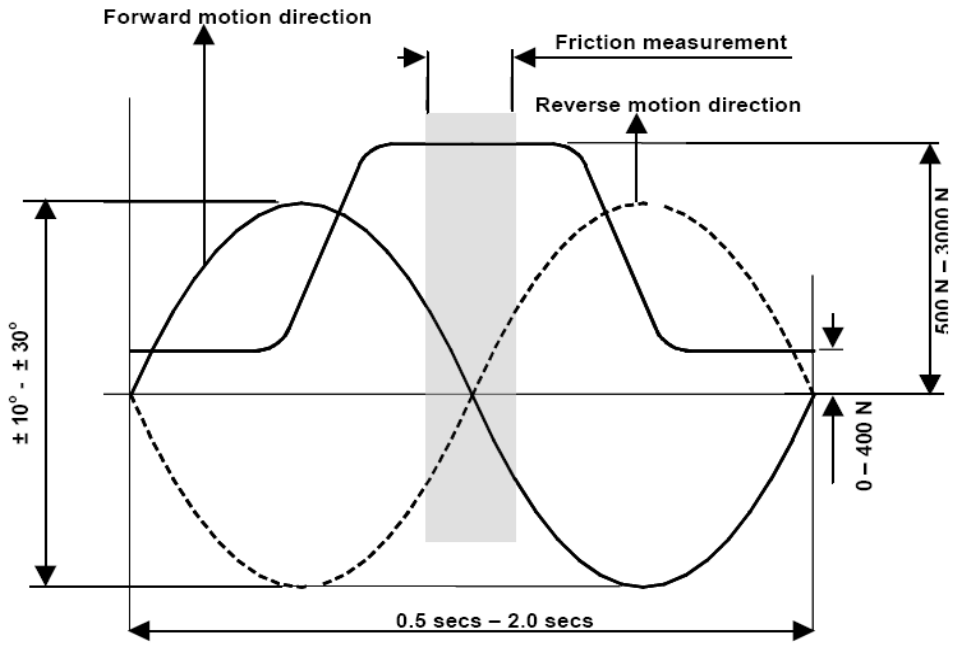

Figure 4.6: Loading and motion test profile

4.2.5 **Stribeck Analysis**

The results were presented as a Stribeck curve. In order to minimise any small misalignment within the simulator, the tests were repeated in both forward and reverse directions and the kinetics, kinematics and frictional torque were recorded. The data were logged every 10 cycles at 256 points per cycle. Data generated by ten measurements were then selected in order to calculate the friction factor. The friction factor (*f*) was then calculated from Equation 4.6.

$$f = \frac{T}{rL}$$

Equation 4.6

where:

T is the measured frictional torque (Nm)

L = applied load (N)

r = femoral head radius (m)

The Sommerfeld number (z) was calculated and plotted against the friction factor, using Equation 4.7.

$$z = \frac{\eta u r}{L}$$

Equation 4.7

where:

η = the viscosity of the lubricant

u = entraining velocity between the two bearing surfaces (m/s)

r = radius of the femoral head (m)

L = applied load (N)

The Sommerfeld number was varied by altering the viscosity of the lubricant (Unsworth et al., 2006, Unsworth, 1978, Scholes et al., 2000a) whilst the entraining velocity, femoral head radius and load were kept constant.

4.2.6 Theoretical calculation of minimum film thickness (hmin) and λ ratio for the prediction of the lubrication regime

The film thickness and λ ratio were calculated using the analysis of Hamrock and Dowson as shown in equations 4.8 to 4.15. The λ ratio is a dimensionless parameter which can be calculated by determining the minimum film thickness and knowing the surface roughness using the following Equation 4.8.

Equation 4.8

Where

Rq1 = roughness of head (μm)

Rq2 = roughness of cup (µm)

h_{min} is the minimum film thickness (m).

The lubrication regime can be predicted by the λ value, i.e. when λ is less than or equal to one, boundary lubrication is predicted. When λ value is more than or equal to three, fluid film lubrication is the likely prediction, and when the λ value is less than three but more than one, then mixed lubrication is predicted.

Using Reynolds Equation 4.9 for the hydrodynamic pressure p, the least film thickness can be determined for head and cup articulations with spherical coordinates (Dowson and Jin 2006).

$$\sin\theta\frac{\partial}{\partial\theta}\left(h^3\sin\theta\frac{\partial p}{\partial\theta}\right)+\frac{\partial}{\partial\phi}\left(h^3\frac{\partial p}{\partial\phi}\right)=6\eta R_1^2\sin^2\theta\left(\omega\frac{\partial h}{\partial\phi}+2\frac{\partial h}{\partial t}\right)$$

Equation 4.9

For elastic deformation, the film thickness can be calculated using Equation 4.10.

$$h=(c-e_x\sin\theta\cos\phi-e_y\sin\theta\sin\phi-e_z\cos\theta)+\delta$$

Equation 4.10

When the film thickness is between 12nm to 20nm, there is drastic reduction in wear rate, but if the film thickness is more than 20nm there is an increase in wear rate (Liu et al., 2006b). For an implant, the Hamrock and Dowson Equation (4.10) (Hamrock and Dowson, 1981) is used for predicting the lubrication regime. The parameters required for this prediction are femoral head diameter (m), diametric clearance (m), elastic modulus (GPa), Poisson's ratio, entraining velocity (m/s), viscosity (Pas), and surface roughness (µm). By applying these parameters to the formula, the minimum film thickness and then the lambda ratio can be obtained, which helps to predict the lubrication regime. The equations and the steps to calculate the film thickness and lambda ratio are as follows:

Step 1: Calculate the equivalent elastic modulus using the elastic modulus and Poisson ratio for the head and cup in using Equation 4.11.

Equation 4.11

Where:

and are the Poisson ratio of head and cup, respectively.

And are the elastic modulus of head and cup, respectively.

Step 2: Calculate the entraining velocity (u=0.02m/s) by knowing the angular velocity and joint diameter using Equation 4.12:

Equation 4.12

Step 3: Calculate the equivalent radius (R) by using the head diameter and diametric clearance in Equation 4.13:

Equation 4.13

Where:

d is the diameter of the implant, with diametric clearance .

Step 4: The minimum film thickness has to be calculated using the above equivalent radius, equivalent elastic modulus and entraining velocity. By using the formula below and knowing the applied load and viscosity, the minimum film thickness can be calculated Equation 4.14:

$$\frac{h_{\min}}{R} = 2.8\left(\frac{\eta u}{E'R}\right)^{0.65}\left(\frac{w}{E'R^2}\right)^{-0.21}$$

Equation 4.14

Where:

h_{min} is the minimum film thickness and W and η are the applied load and viscosity, respectively.

Step 5: Finally, by using the calculated minimum film thickness values and the surface roughness of the head and cup, the lambda ratio can be calculated using Equation 4.15:

$$\Lambda = \frac{h_{min}}{\sqrt{(R_a)^2_{head} + (R_a)^2_{cup}}}$$

Equation 4.15

Where:

R_a head and R_a cup are the surface roughness of the head and cup, respectively.

4.3 Components for Tribology Testing

4.3.1 Stage 1

For the first set of friction testing only one ZPTA ceramic head was available, this was a 52mm diameter head manufactured by Morgan Advanced Ceramics for Biomet UK (Figure 4.8). This ceramic head was selected as it represented the implant combination that would be used in vivo.

Figure 4.8: Magnum C Head with Taperloc Stem

The samples were machined from a CFR PEEK extruded CFR PEEK rod (60mm diameter). Using a CNC lathe, 200, 300 & 400 µm radial clearances were machined. Diamond paste was then used to polish the bearing surface of the cup to achieve a surface roughness (R_a) of 0.1µ. This was completed by securing the cup back into the lathe, applying the diamond paste and using a polishing pad whilst the cup rotated at 1500 RPM. The surface finish was measured using a contact profilometer (Talysurf, Taylor-Hobson ultra). While a highly polished surface finish was achieved the diamond paste proved to be too aggressive and removed a substantial amount of material from

the bearing surface. The inside diameter was measured using a CMM which showed clearances were 257, 661 & 706 µm. This was only discovered after initial testing was completed at Durham, hence the subsequent investigation.

4.3.2 **Stage 2 & 3**

Due to manufacturing issues with large diameter extruded CFR PEEK rod an alternative method was required to manufacture the raw material. Based on the proposed size range of the CFR monobloc a design was developed with Invibio to create three injection moulded pre forms which could be used to manufacture cups. The preforms come in three sizes small, medium and large (Figure 4.9); with the possibility to produce four sizes from each preform.

Figure 4.9: CFR PEEK NNS

Four radial clearances were machined using a CNC lathe: 30, 330, 630, & 930µm. These were again assessed using a CMM to check dimensions and a profilometer was used to check surface roughness which showed an (R_a) of 0.5µm. At this stage there was no reliable way of altering the surface finish without affecting the clearance. The same components were tested at both Durham and Bradford University.

4.3.3 **Stage 4**

Four bearing diameters were manufactured using identical manufacturing and inspection methods. The bearing diameters were 38, 46, 52 & 60mm and all had the same radial clearance of 930µm. The (R_a) value produced was in the region of 0.5µm to 0.8µm on the larger sizes. This was due to manufacturing constraints, CFR PEEK is very abrasive to machine and while polycrystalline diamond (PCD) tool inserts were used to minimise this, surface roughness was affected.

4.3.4 **Stage 5**

The CFR monobloc shell was further developed from a hemispherical profile to a bispherical profile. In addition, a new clearance and surface finish to test based on cadaveric studies and previous friction data was identified. Head diameters were also changed due to the availability of ceramic heads that have excellent clinical history (D'Antonio and Sutton, 2009, Chevalier, 2006, Chevalier and Gremillard, 2009, Meinhard Kuntz, 2014, Kuntz et al., 2005, Kuntz, 2006). The new heads made from CeramTec's Biolox® Delta ceramic are shown in Figure 4.10.

Figure 4.10: Biolox® Delta Ceramic Heads

This included the six head diameters of 36, 40, 44, 48, 52 & 56mm in diameter. The CFR PEEK monobloc cups were machined in an identical manner to previous components to produce a radial clearance of 230µm. Eight components were produced; six were machined and had an average (R_a) 0.5415 µm. Two components (36mm & 56mm) were polished with an average (R_a) 0.0882 µm to validate previous work which suggested that a better surface finish will reduce friction factor. The ceramic heads used had an average (R_a) 0.0065 µm. A summary of all the fiction testing completed is shown in Table 4.2.

Table 4.2: Friction testing summary

Test	Radial clearance [µm]	Head Size [mm]	Ra Value [µm]	Manufacturing process	Location
Stage 1	0.257 0.661 0.706	52	0.1	CNC Machined Diamond polished	Durham
Stage 2	30 330 630 930	52	0.5415	CNC Machined	Durham
Stage 3	30 330 630 930	52	0.5415	CNC Machined	Bradford
Stage 4	930	38 46 52 60	0.5415	CNC Machined	Bradford
Stage 5	230	36 40 44 48 52 56	0.1381	CNC Machined & Polished	Bradford

4.4 Results and Discussion

The author applied the Hamrock and Dowson to theoretically predict film thickness and λ ratio to compare against the practical results. Each femoral diameter was calculated utilising the full range of viscosities (Tables 4.3-4.8) used in the practical friction testing and to plot the theoretical Stribeck curves. Typical values for friction factors for various bearings for artificial hip joints in presence of bovine serum are presented in Table 4.9 (Jin et al. 2006).

Table 4.3: Theoretical calculations of fluid film thickness and lubrication regimes for 56mm head

Viscosity [Pas]	Minimum film thickness ^{h}min [mm]	Lambda λ	Head Diameter [mm]
0.00153	0.001708	0.012351	56
0.00118	0.001442	0.010433	56
0.00524	0.003801	0.027494	56
0.0128	0.006792	0.049131	56
0.043	0.014931	0.107999	56
0.12	0.029094	0.210442	56
0.229	0.044283	0.320301	56

Table 4.4: Theoretical calculations of fluid film thickness and lubrication regimes for 52mm head

Viscosity [Pas]	Minimum film thickness ^{h}min [mm]	Lambda λ	Head Diameter [mm]
0.00153	0.001683	0.012177	52
0.00118	0.001422	0.010285	52
0.00524	0.003747	0.027105	52
0.0128	0.006697	0.048437	52
0.043	0.014720	0.106474	52
0.12	0.028683	0.207470	52
0.229	0.043657	0.315777	52

Table 4.5: Theoretical calculations of fluid film thickness and lubrication regimes for 48mm head

Viscosity [Pas]	Minimum film thickness ^{h}min [mm]	Lambda λ	Head Diameter [mm]
0.00153	0.001658	0.011991	48
0.00118	0.001400	0.010128	48
0.00524	0.003690	0.026692	48
0.0128	0.006594	0.047698	48
0.043	0.014496	0.104849	48
0.12	0.028246	0.204304	48
0.229	0.042991	0.310959	48

Table 4.6: Theoretical calculations of fluid film thickness and lubrication regimes for 44mm head

Viscosity [Pas]	Minimum film thickness ^{h}min [mm]	Lambda λ	Head Diameter [mm]
0.00153	0.001630	0.011792	44
0.00118	0.001377	0.009960	44
0.00524	0.003629	0.026249	44
0.0128	0.006485	0.046906	44
0.043	0.014255	0.103109	44
0.12	0.027777	0.200915	44
0.229	0.042278	0.305800	44

Table 4.7: Theoretical calculations of fluid film thickness and lubrication regimes for 40mm head

Viscosity [Pas]	Minimum film thickness ^{h}min [mm]	Lambda λ	Head Diameter [mm]
0.00153	0.001601	0.011578	40
0.00118	0.001352	0.009779	40
0.00524	0.003563	0.025772	40
0.0128	0.006367	0.046053	40
0.043	0.013996	0.101235	40
0.12	0.027272	0.197262	40
0.229	0.041509	0.300240	40

Table 4.8: Theoretical calculations of fluid film thickness and lubrication regimes for 36mm head

Viscosity [Pas]	Minimum film thickness ^{h}min [mm]	Lambda λ	Head Diameter [mm]
0.00153	0.041509	0.300240	36
0.00118	0.001568	0.011345	36
0.00524	0.001325	0.009583	36
0.0128	0.003491	0.025253	36
0.043	0.006239	0.045128	36
0.12	0.013715	0.099200	36
0.229	0.026724	0.193296	36

Table 4.9: Typical friction factors for various bearings for artificial hip joints in presence of bovine serum (Jin et al. 2006)

Lubrication Regimes	Friction Factor
Boundary Lubrication	0.1-0.7
Mixed Lubrication	0.01-0.1
Fluid Film Lubrication	0.001-0.01

4.4.1 **Stage 1**

Figures 4.11- 4.15 show the results for stage one of the tribology measurements, details of the parameters are presented in Table 4.2. As shown in Figure 4.11, friction factors of 0.071, 0.0441 and 0.057 were recorded for the radial clearances 257µm, 661µm and 707µm respectively. Figure 4.12 shows the friction factors with the introduction of 25% bovine serum. The friction factors with bovine serum are slightly lower as Scholes and Unsworth (2006b) previously demonstrated. The results show there was no clear trend with a low friction factor throughout the range of Sommerfeld numbers that was tested, and this suggests that at least partial hydrodynamic lubrication occurred. The results from Stage 1 are similar to those for UHMWPE-on-metal and UHMWPE-on-ceramic (Jin et al., 2006, Auger et al., 1993, Scholes and Unsworth, 2000, Scholes and Unsworth, 2006b).

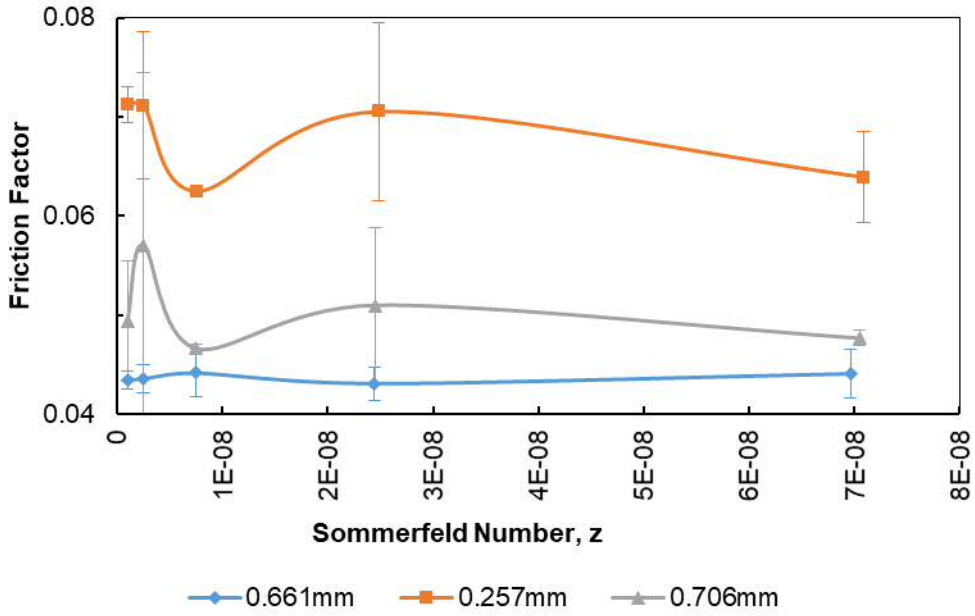

Figure 4.11: Stribeck Curve with three different clearances with a 52mm ZPTA head against CFR PEEK

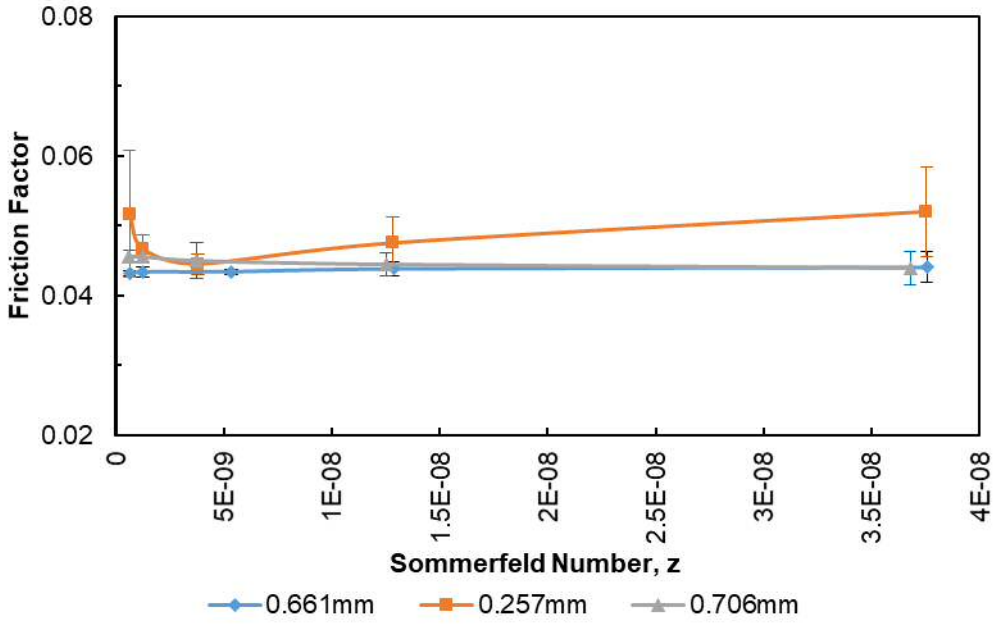

Figure 4.12: Stribeck Curve with three different clearances with a 52mm ZPTA head against CFR PEEK - CMC & 25% BS

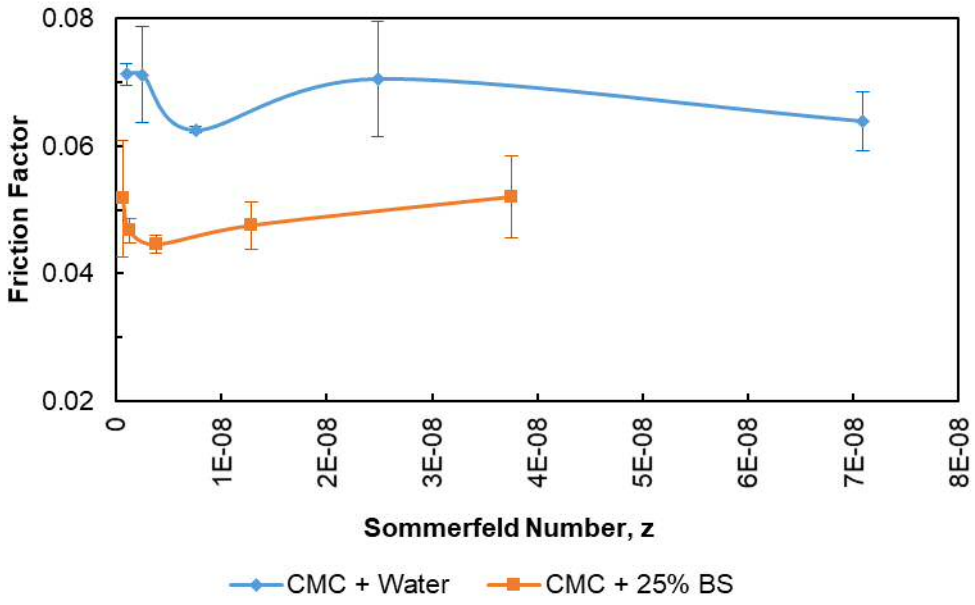

Figure 4.13: Stribeck Curves for 0.257mm radial Clearance

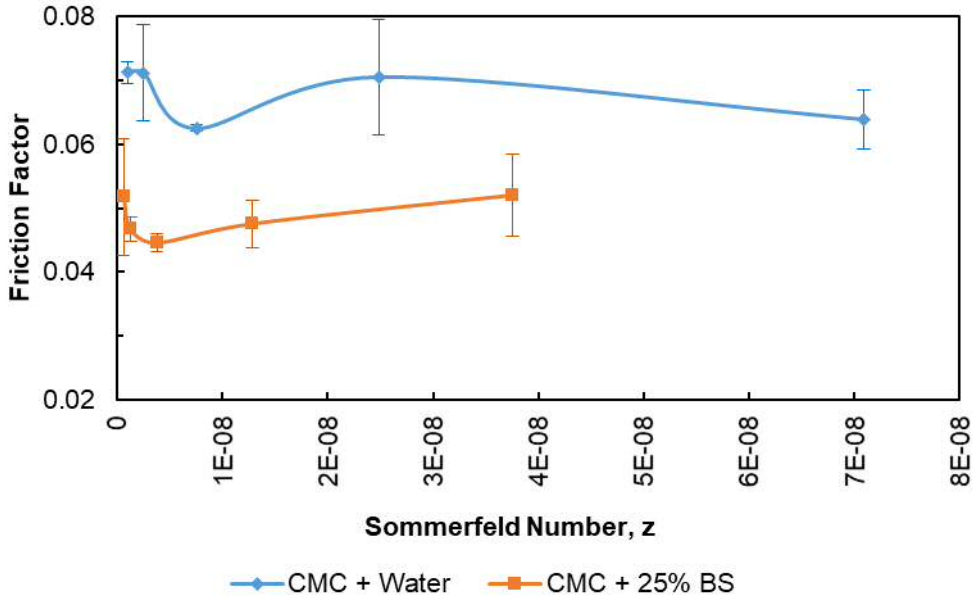

Figure 4.14: Stribeck Curve 0.661µm radial Clearance

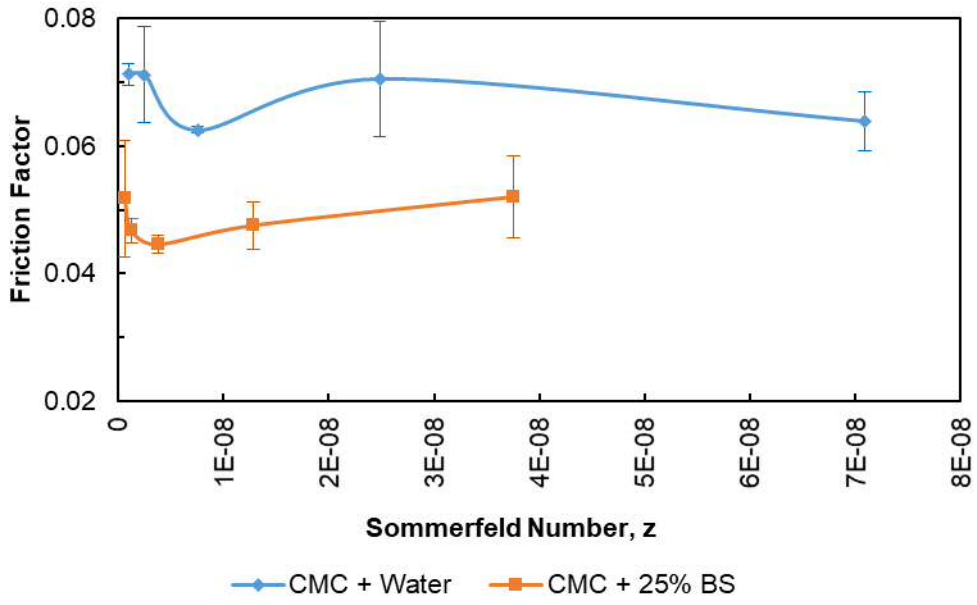

Figure 4.15: Stribeck Curve 0.706µm radial Clearance

4.4.2 **Stage 2**

Figures 4.16 and 4.17 shows the results for Stage 2 of the tribology analysis (Table 4.2). This was the first study with cups with a higher roughness average (R_a) measurement, the figures show a rising trend in the friction which is indicative of full fluid film lubrication (Scholes and Unsworth, 2006b); more viscosities would have to be compared to see if this still remains valid. 0.07585, 0.04024, 0.00302 and 0.04919 were friction factors recorded for the radial clearances 930µm, 630µm, 330µm and 30µm respectively shown in Figure 4.16. 0.07348, 0.0765, 0.0733 and 0.0762 were friction factors recorded for the radial clearances 930µm, 630µm, 330µm and 30µm respectively shown in Figure 4.17, whilst the friction values increase typical full fluid lubrication friction factors fall between 0.001-0.01 and mixed lubrication between 0.01-0.1 (Scholes and Unsworth, 2006b). However the friction factors are higher in Figure 4.17 this is thought to be due to the proteins which adsorb to the surfaces and break down the lubricant film formed by the micro elastohydrodynamic lubrication, causing protein-to-protein rubbing and therefore higher friction (Scholes and Unsworth, 2006b,

Cheng, 1984) this can be seen in the smallest of radial clearances 0.30µm where by the friction factor almost doubled with the introduction of bovine serum (Birkinshaw et al., 2010).

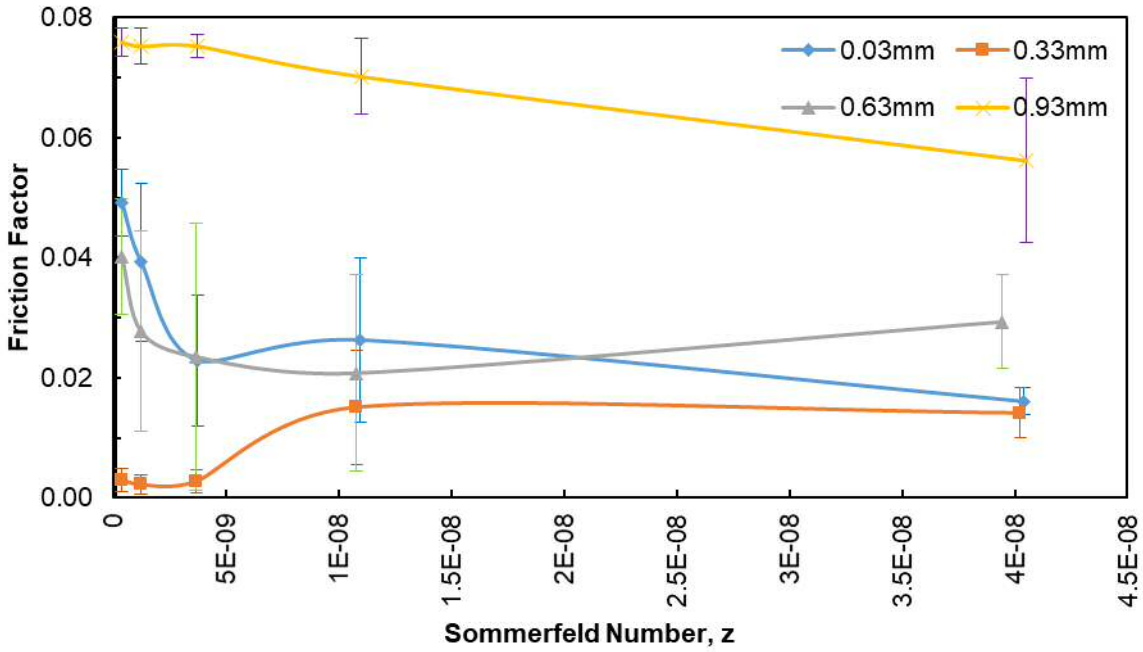

Figure 4.16: Stribeck Curve of a 4 Radial Clearances, 52mm ZPTA head against CFR PEEK with CMC & DW

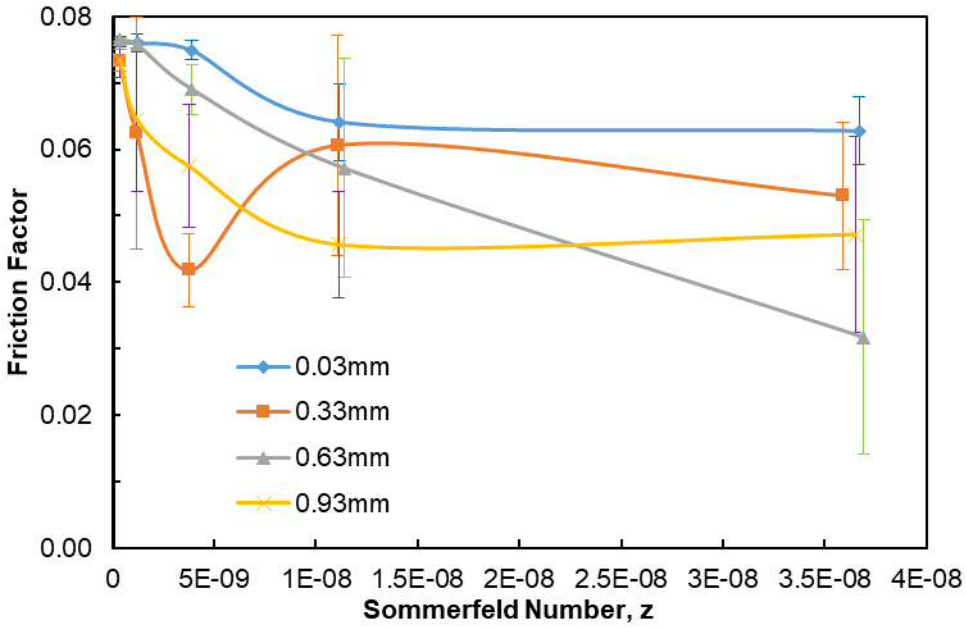

Figure 4.17: Stribeck Curve of a 4 Radial Clearances, 52mm ZPTA head against CFR PEEK – CMC & BS

4.4.3 **Stage 3**

Figure 4.18 shows the results for Stage 3 of the tribology analysis, details of the parameters as shown in Table 4.2. This study was a repeat of Study 2 but completed in Bradford University utilising a larger range of viscosities as shown in to compare friction and plot Stribeck curves accordingly. This produced much clearer results with less scatter. The highest friction factors of 0.25022, 0.1463, 0.2274 and 0.2352 were recorded for radial clearances of 930µm, 630µm, 330µm and 30µm respectively. However, the lowest friction factors of 0.02648, 0.05174, 0.0489 and 0.11636 were recorded for the radial clearances of 930µm, 630µm, 330µm and 30µm respectively. The friction values are similar to those that have been observed in metal on metal joints (Scholes and Unsworth 2000). The results are in line also with ceramic on CFR PEEK tests which showed values between 0.3-0.15 for the Mitch cup and Trinity multi-bearing shell system (Scholes et al., 2008, Wang et al., 2012, Latif et al., 2008a). The values for the larger clearances are also consistent with previous friction testing of CFR PEEK against ceramic (Birkinshaw et al., 2010). The plots are indicative of a mixed lubrication regime.

Stage Two testing results showed a different trend for the exact same clearances. It is believed that this may have been due to errors in the test setup as indicated by the plots and also the friction factors values which are very low when compared with those found in literature. It also showed in this stage of testing that the four clearances selected were consistent with the 930µm radial clearance showing the lowest friction factor with the 630µm radial clearance showing the most consistent plot throughout the viscosity range. This is the opposite to what may be found in MoM joints with the largest clearances offering the highest friction factor (Brockett et al., 2008) this is because the CFR PEEK is running under a mixed fluid regime whereas the MoM runs under fluid film regime.

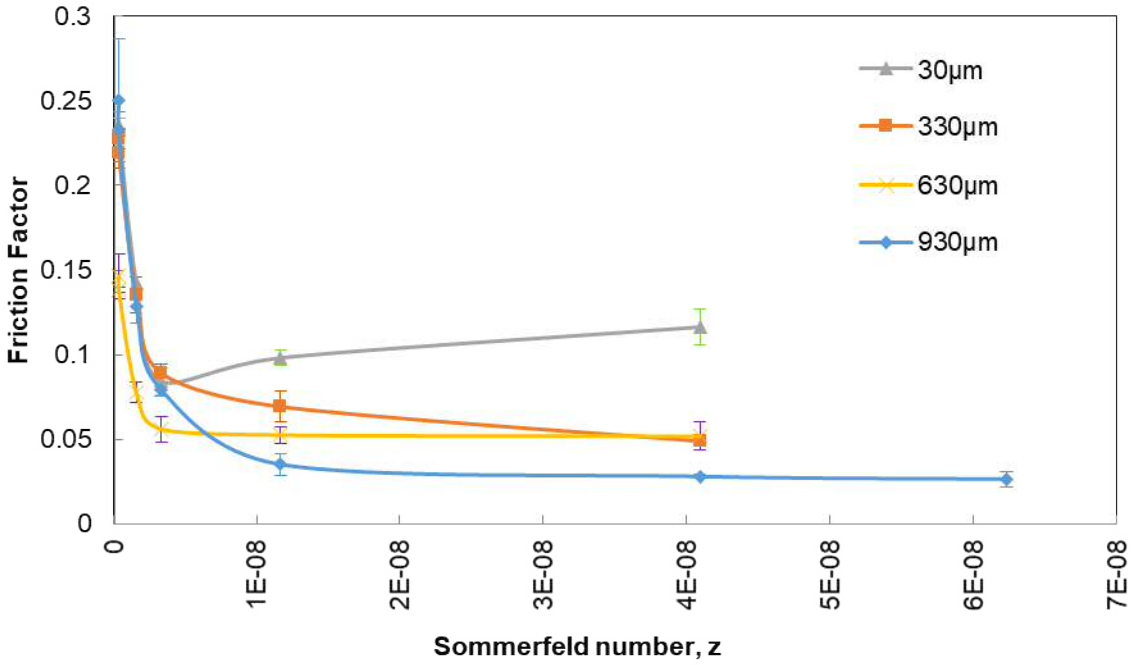

Figure 4.18: Stribeck Curve of a 4 Radial Clearances, 52mm ZPTA head against CFR PEEK – CMC & BS at Bradford University

4.4.4 **Stage 4**

Figure 4.19 shows the results for Stage 4 of the tribological testing (Table 4.2). A larger radial clearance which is not typically seen in orthopaedic bearings was investigated. This was motivated based on previous friction testing and cadaveric work to assess cup deformation once impacted into the prepared acetabular under different reaming parameters. It is common for surgeons to prepare the acetabulum based on bone quality to either create a press fit for osteoporotic bone by under reaming compared to the size of the final implant which can be from 1mm under to 2mm under, i.e. ream the acetabulum to 53mm insert a 54mm acetabular implant. Or typically in hard sclerotic bone ream line to line; ream the acetabulum to 54mm insert a 54mm acetabular implant. (Vendittoli et al., 2006, Hendrich et al., 2007). The larger clearance would allow deformation of the monobloc cup once impacted into the acetabulum without the risk of clutching of the femoral head, this is where the cup deforms greater than the radial clearance causing the mating head to become fixed (McKee, 1982, Hothan et al., 2011, Squire et al., 2006a). The larger clearances from Stage 3 were consistent throughout the Stribeck plot with the 930µm showing the lowest friction factors. Figure 4.19 shows that the highest friction factors of 0.2302, 0.25022, 0.3194 and 0.1502 were recorded for the 60mm, 52mm, 56mm and 38mm heads respectively. The lowest values were

0.16617, 0.02648, 0.20473 and 0.1215 for the 60mm, 52mm, 56mm and 38mm head respectively. Again these results are consistent with the previously highlighted research.

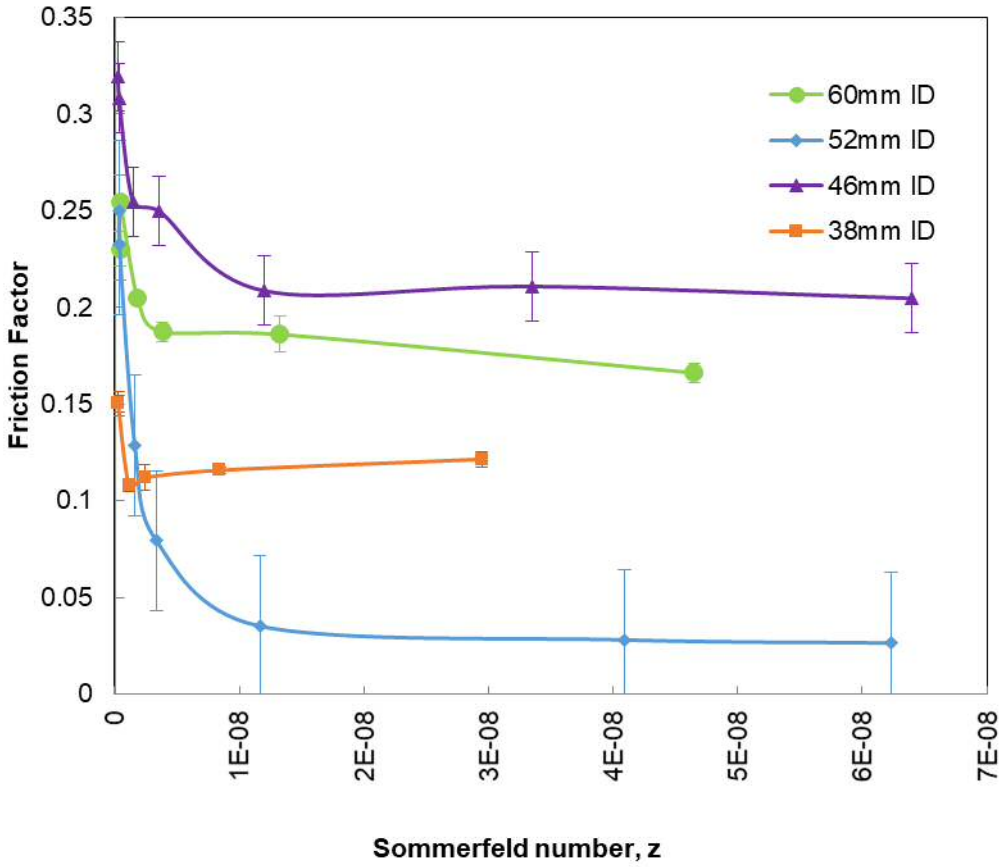

Figure 4.19: Stribeck Curve of 930µm Radial Clearance with 4 different IDs. ZPTA head against CFR PEEK – CMC & BS at Bradford University

4.4.5 **Stage 5**

Figures 4.20 to 4.32 show the results for Stage 5 (Table 4.20. Stage Five was the final set of testing, based on the development work of the outside geometry of the implant. A new clearance of 230µm radially, was selected, which equates to a 460µm diametric clearance between the articulating head. The final set of testing covered the head diameters used in the implant configuration 36mm, 40mm, 44mm, 48mm, 52mm and 56mm respectively. As the final implant will be injection moulded and based on testing results from Stage 1, unpolished and polished cups were tested as surface finish plays an important role in the friction factors both in hip and knee bearings (Birkinshaw et al.,

2010, Wang et al., 2012, Unsworth and Scholes, 2009). Table 4.10 summarises the minimum and maximum friction factor values for the 230µm radial clearance.

Figure 4.20 shows the results for the smallest articulating head in the implant range which is 36mm, this showed to have the highest friction factor of 0.28091-0.12563 which are similar to the Mitch implant (Latif, Mehats et al. 2008) but are slighter higher than published work on MoM joints of similar diametric sizes 1.5-2.0 (Scholes and Unsworth, 2000, Scholes et al., 2000a). In contrast to this, published data on the Trinity system, with a CFR PEEK bearing and Mitch cup show higher values of up to 0.3 (Scholes et al., 2008, Wang et al., 2012). Figures 21 to 23 show classic mixed fluid regime Stribeck plots with decreasing friction values and in an increase of the Sommerfeld number for the 40mm, 44mm, and 48mm articulating heads with the 230µm radial clearance. Figures 24 and 25 show the 52mm and 56mm articulating heads with the 230µm radial clearance. These plots show the lowest friction values throughout the range of implants tested with a reduction in friction and an increase of the Sommerfeld number (Scholes and Unsworth, 2000).

Figure 4.28 show the Stribeck plot for the 36mm implant with a highly polished surface which shows a significant decrease in friction factor values, the unpolished cup gave values of 0.28091-0.12563 as shown in Figure 4.20; in contrast the highly polished cup gave values of 0.10319-0.05597. The polished implant is more realistic of the final implant design which will have a highly polished injection moulded surface with the fibres following the cup geometry. Under tribological studies it has shown that surface finish improves friction factor values (Unsworth and Scholes, 2009, Scholes et al., 2008, Birkinshaw et al., 2010). A comparison between polished and unpolished is presented shown in Figure 4.29. Although the friction factor has spiked to 0.13067 showing what would appear to be a steady or slight increase in friction factor with Sommerfeld number at the lower end of the viscosity scale. This is because the lowest viscosity of 0.001 Pa s was measured with distilled water. Distilled water is Newtonian in nature and therefore its viscosity remains the same regardless of shear rate. (Scholes et al., 2000b). The synovial fluid from a patient with rheumatoid arthritis is around 0.005 Pa s (Cooke et al., 1978) measured at a shear rate of 3000 s−1, which corresponds to a Sommerfeld number of 1.7×10−9. This lies slightly to the left of the third point on each curve (Unsworth et al., 2006). At this viscosity, the friction factor within the joint was found to be 0.898 which further supports optimum clearance for the implant with

the enhanced surface finish, the comparison is shown in Figure 4.31. Due to a suspected manufacturing error in the injection moulding of the NNS, one of the largest shells displayed a crack in the pole of the implant, this implant was tested to assess what impact the defect has on the friction factor, the implant also maintained the highly polished finish and the results are shown in Figure 4.32 with the friction factor values ranging from 0.137012-0.07478 which is still very promising for the implant in that if it did become damaged through 3rd body wear the friction factor is still in the acceptable range of published bearing couples.

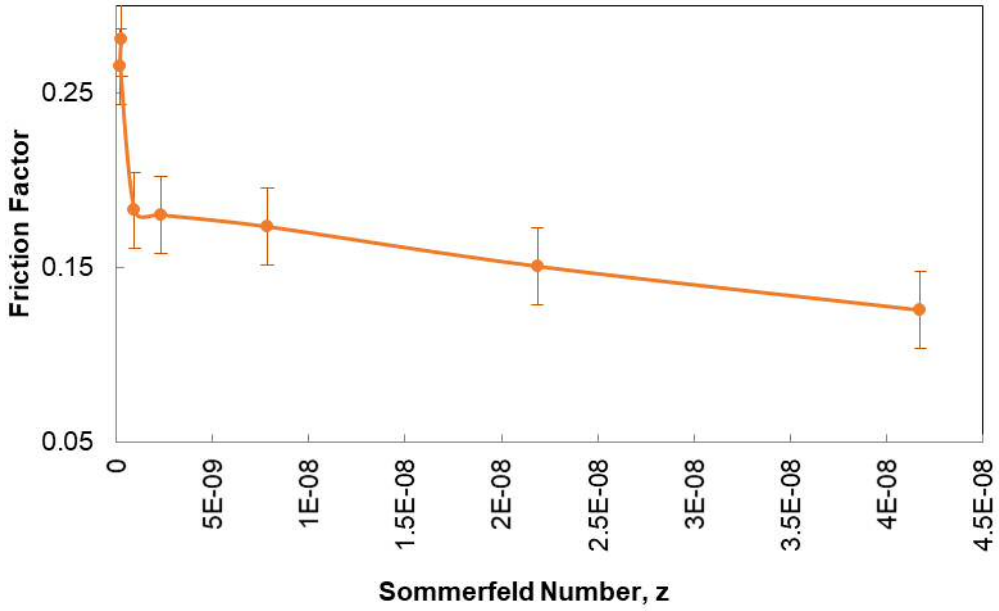

Figure 4.20: Stribeck curve for the 36mm ceramic head on CFR PEEK with 230µm radial clearance

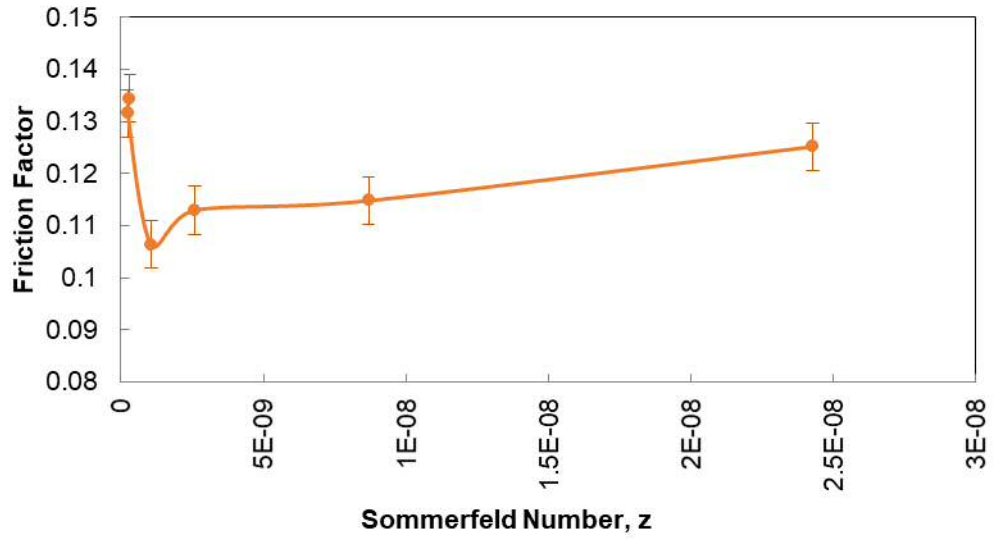

Figure 4.21: Stribeck curve for the 40mm ceramic head on CFR PEEK with 230µm radial clearance

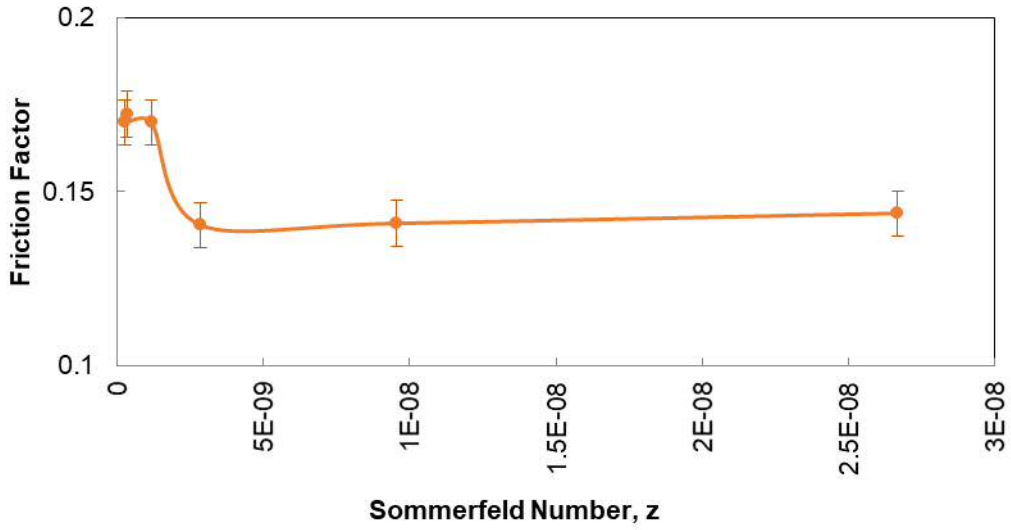

Figure 4.22: Stribeck curve for the 44mm ceramic head on CFR PEEK with 230µm radial clearance

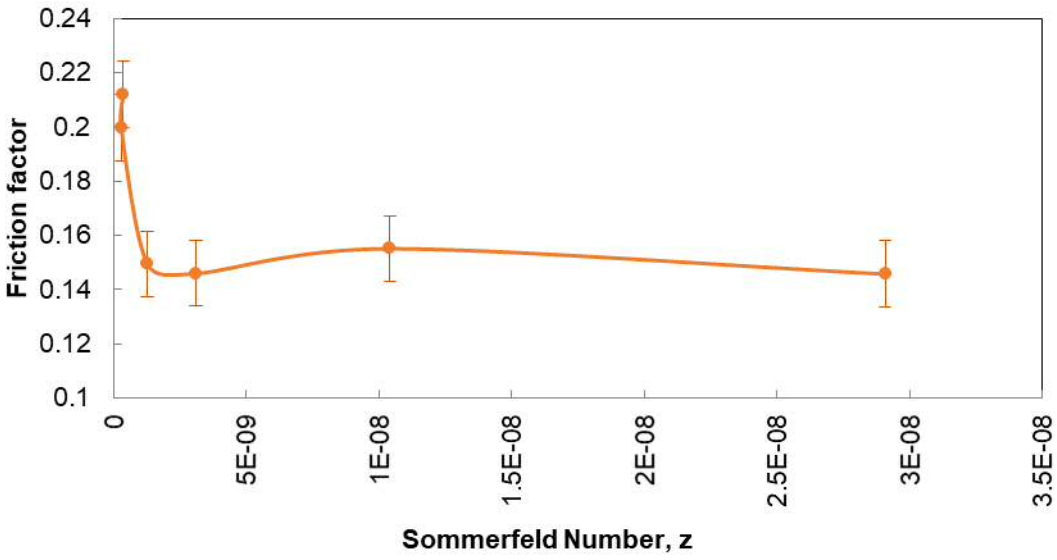

Figure 4.23: Stribeck curve for the 48mm ceramic head on CFR PEEK with 230µm radial clearance

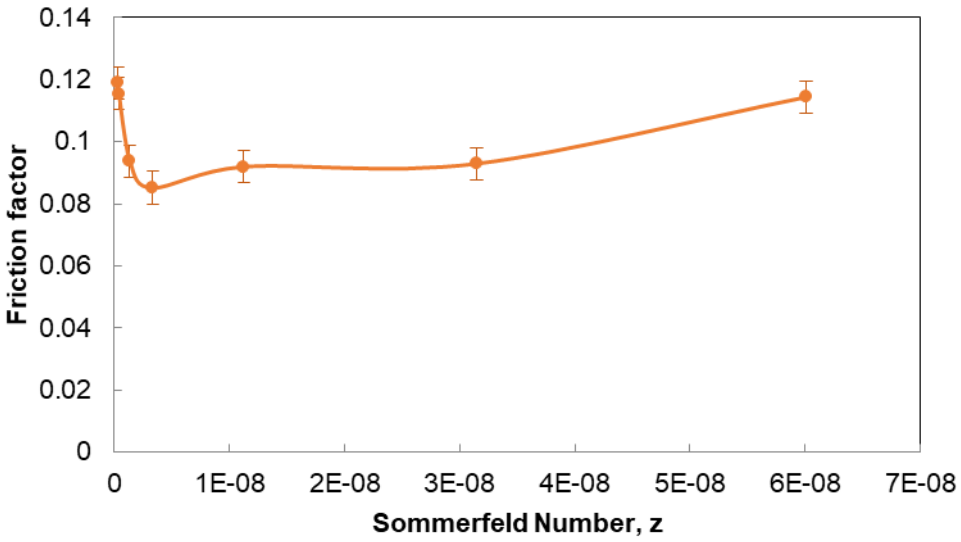

Figure 4.24: Stribeck curve for the 52mm ceramic head on CFR PEEK with 230µm radial clearance

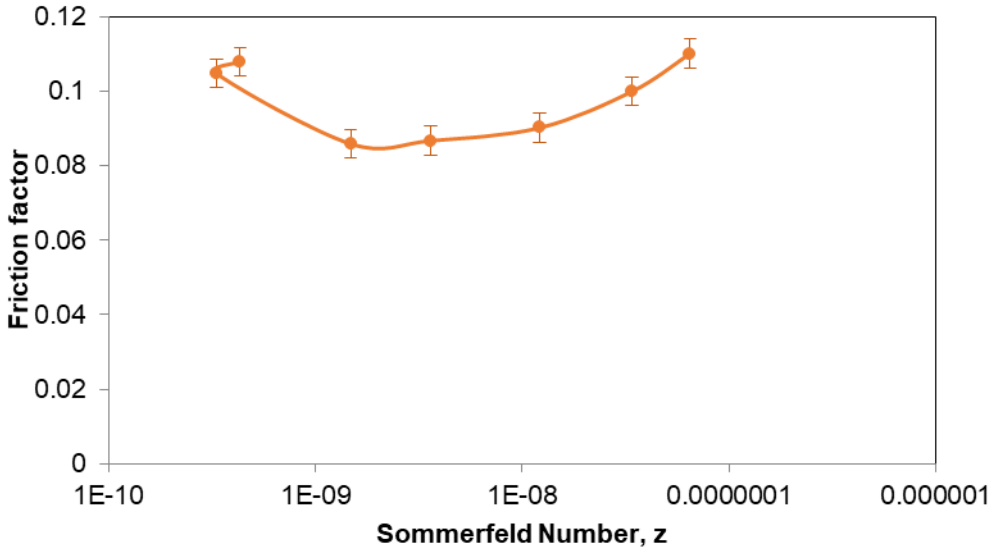

Figure 4.25: Stribeck curve for the 56mm ceramic head on CFR PEEK with 230µm radial clearance

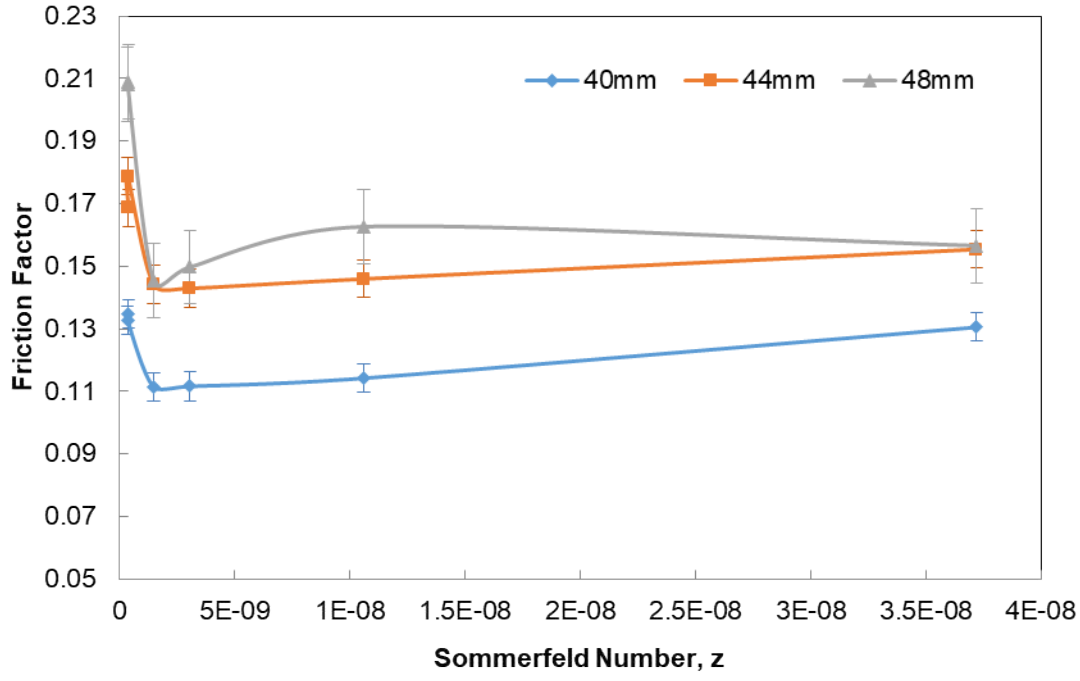

Figure 4.26: Stribeck curve for the 40, 44 & 48mm ceramic head on CFR PEEK with 230µm radial clearance

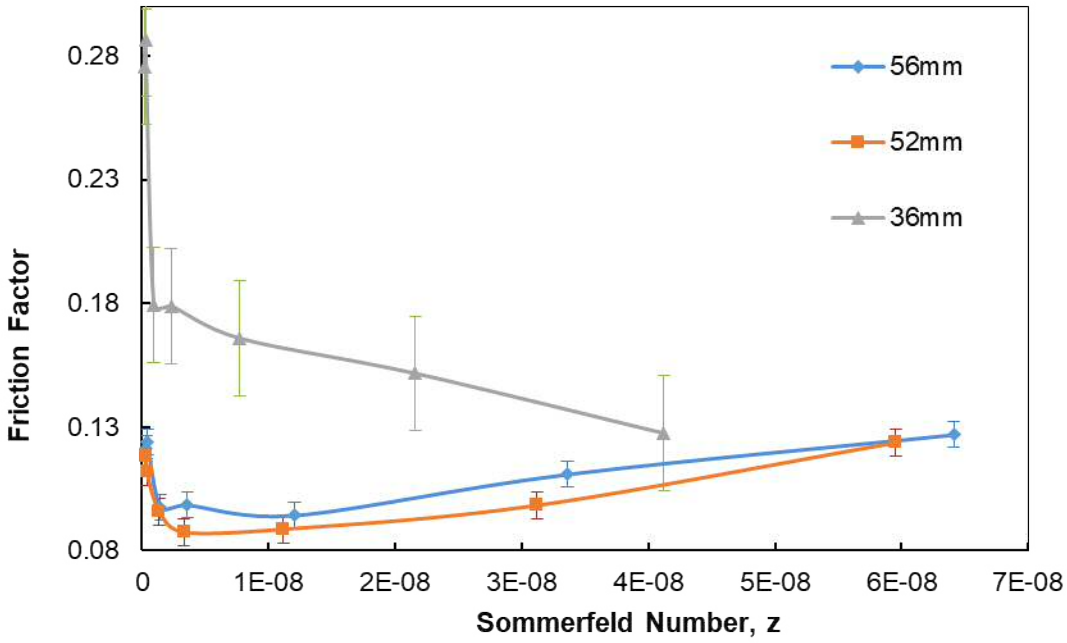

Figure 4.27: Stribeck curve for the 36, 52 & 56mm ceramic head on CFR PEEK with 230µm radial clearance

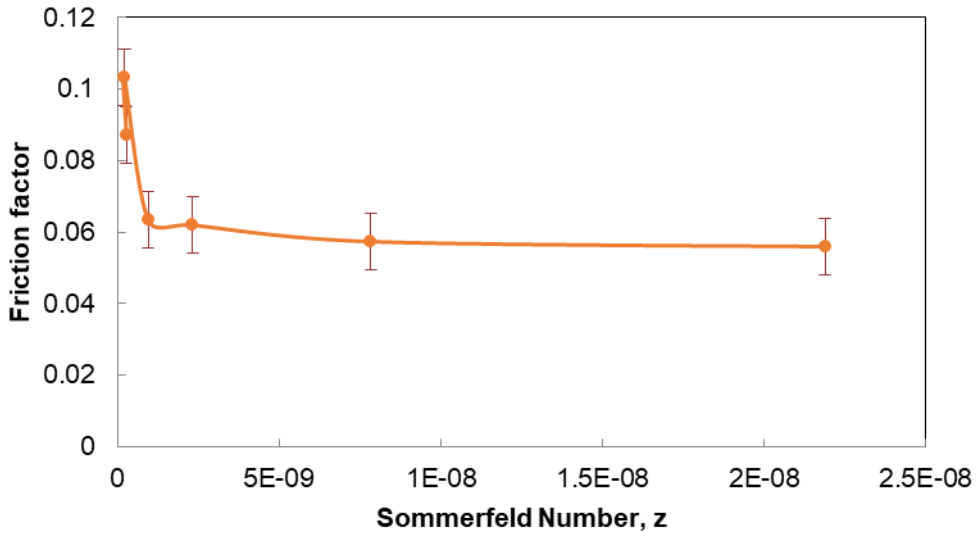

Figure 4.28: Stribeck curve for the 36mm ceramic head on polished CFR PEEK with 230µm radial clearance

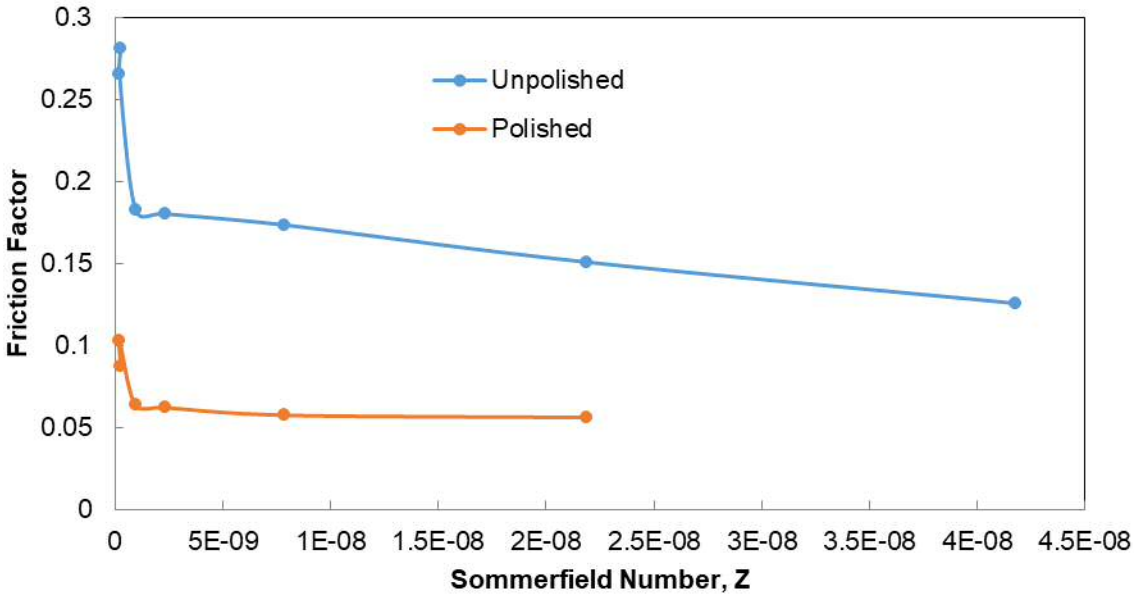

Figure 4.29: Stribeck curve for the 36mm ceramic head on unpolished & polished CFR PEEK with 230µm radial clearance

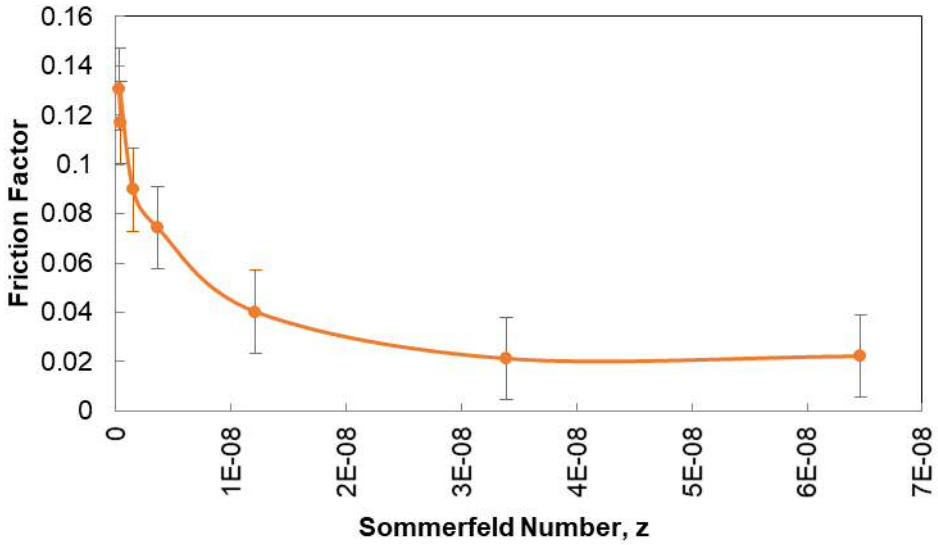

Figure 4.30: Stribeck curve for the 56mm ceramic head on unpolished & polished CFR PEEK with 230µm radial clearance

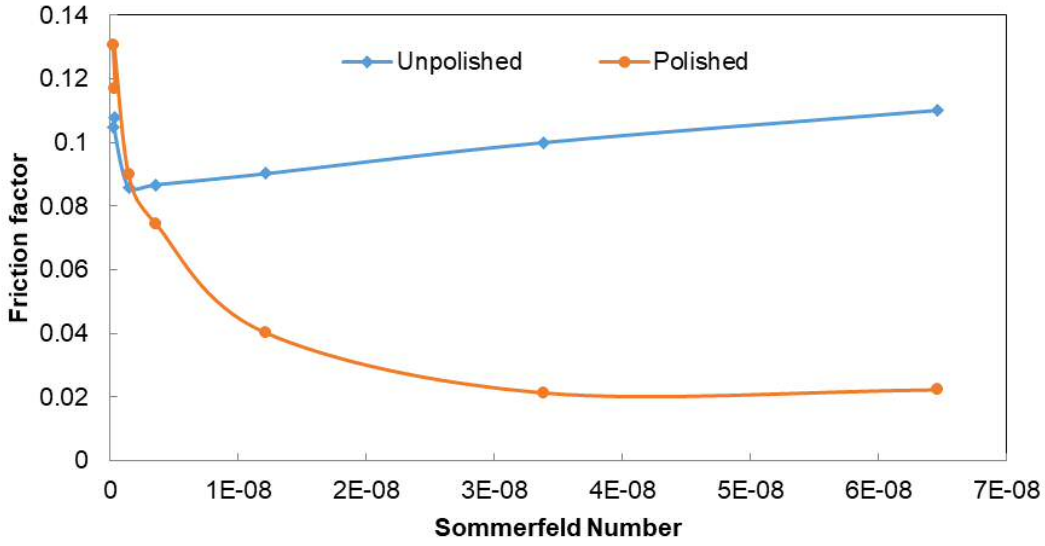

Figure 4.31: Stribeck curve for the 56mm ceramic head on unpolished & polished CFR PEEK with 230µm radial clearance

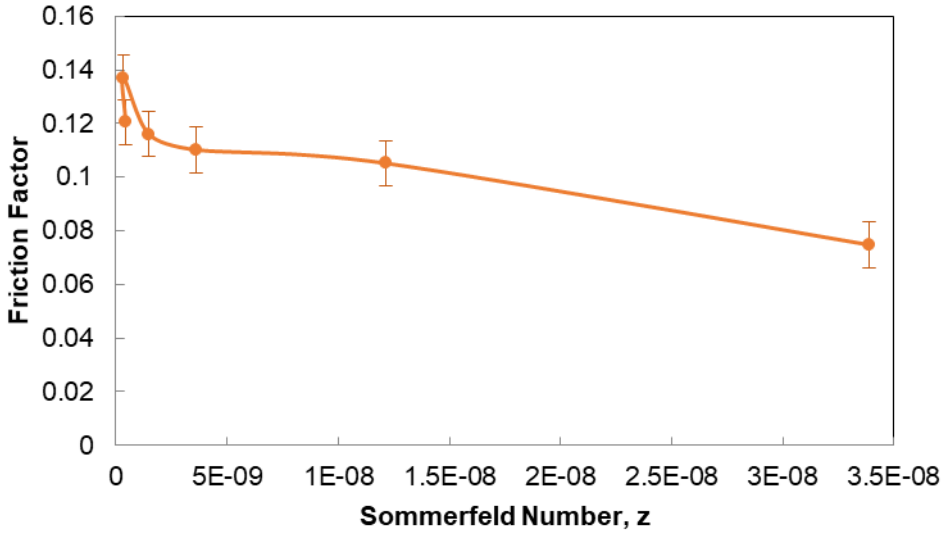

Figure 4.32: Stribeck curve for the 56mm ceramic head on polished CFR PEEK with 230µm radial clearance and a fracture on the inside diameter

Table 4.10: Summary of Friction factors for 230µm radial clearance

Head size [mm]	Features	Highest Friction Value	Lowest Friction Value
36	Unpolished and Polished	0.28091	0.12563
40	Unpolished and Polished	0.13440	0.12520
44	Unpolished and Polished	0.17230	0.14379
48	Unpolished and Polished	0.21196	0.14578
52	Unpolished and Polished	0.1189	0.11441
36	Unpolished and Polished	0.1079	0.1101
56	Unpolished and Polished	0.10319	0.05597
56	Unpolished and Polished	0.13067	0.02226
56	Fracture on inside diameter	0.137012	0.07478

4.5 Conclusion

The theoretical results support the practical results. There is mixed fluid lubrication and there is a trend that with the more viscous viscosity that the theoretical values place it in the boundary lubrication for all joint diameters. This is still an acceptable lubrication regime to achieve with this implant design.

The aim of this chapter was to establish the optimum radial clearance and surface finish for the CFR PEEK Monobloc cup. This was achieved by conducting five stages of tribological testing. The tests looked at several radial clearances and the how surface finish impacts on friction factor values. It has been shown that the large radial clearance is an effective clearance for the entire range of articulating heads which is in contrast to large bearings such as MoM and CoC where the smallest possible clearance optimises the bearing performance in vitro. MoM and COC bearings run between full fluid film regime and mixed regime depending on the bedding in phase of the implant. While in

vitro testing is vital for the evolution of reconstructive hip development these tests have been performed in optimum conditions, where parameters such as cup positioning, edged loading and implant deformation need to be taken into consideration.

Further testing needs to be undertaken on injection moulded parts with and without screw holes in the bearing surface to ascertain its effectiveness, as the bearing couple runs under mixed fluid regime with a much larger clearance than would have been typically seen in MOM joints it should further support the use of screw holes in the bearing surface without any adverse effects.

5 Cadaveric Testing

5.1 Introduction

In this Chapter, cadaveric specimens were used to evaluate the designs developed through this project. Cadaveric experiments were completed at each major landmark of design evolution to assess the implant and investigate cup deformation. Therefore, the aims of the studies were:

- To ascertain the level of deformation in the CFR PEEK Monobloc upon immediate impaction into the prepared acetabulum of a cadaveric specimen;
- Acquire accurate values of deformation to correctly evaluate the effectiveness of the implant;
- Determine the accuracy of acetabular reaming, performed by a qualified surgeon, to develop the correct inside and outside geometry of the implant.

5.2 Cadaveric Experiment One

5.2.1 Experimental Procedure

Due to manufacturing restrictions of large diameter extruded CFR PEEK CFR PEEK; further work was completed with Invibio to define a set of injection moulded near net shapes to be able to manufacture a range of implants based on existing sizes from Biomet's Magnum Brand. The near net shapes (NNS) consisted of three sizes; small, medium and large with each near net offering the ability to produce four sizes each.

In preparation for the cadaveric experiment four sizes of CFR PEEK implant were machined from the NNS at Biomet UK Ltd; the implants were then sent to Biomet UK Ltd Swindon for porous plasma sprayed (PPS) titanium coating which was completed manually. The reason for the different sizes is to ensure that the correct size implants would be available for each cadaveric specimen, the selection of cups are the most commonly used sizes shown in Figures 5.1 and 5.2.

Figure 5.1: CFR Peek Monobloc prototype one

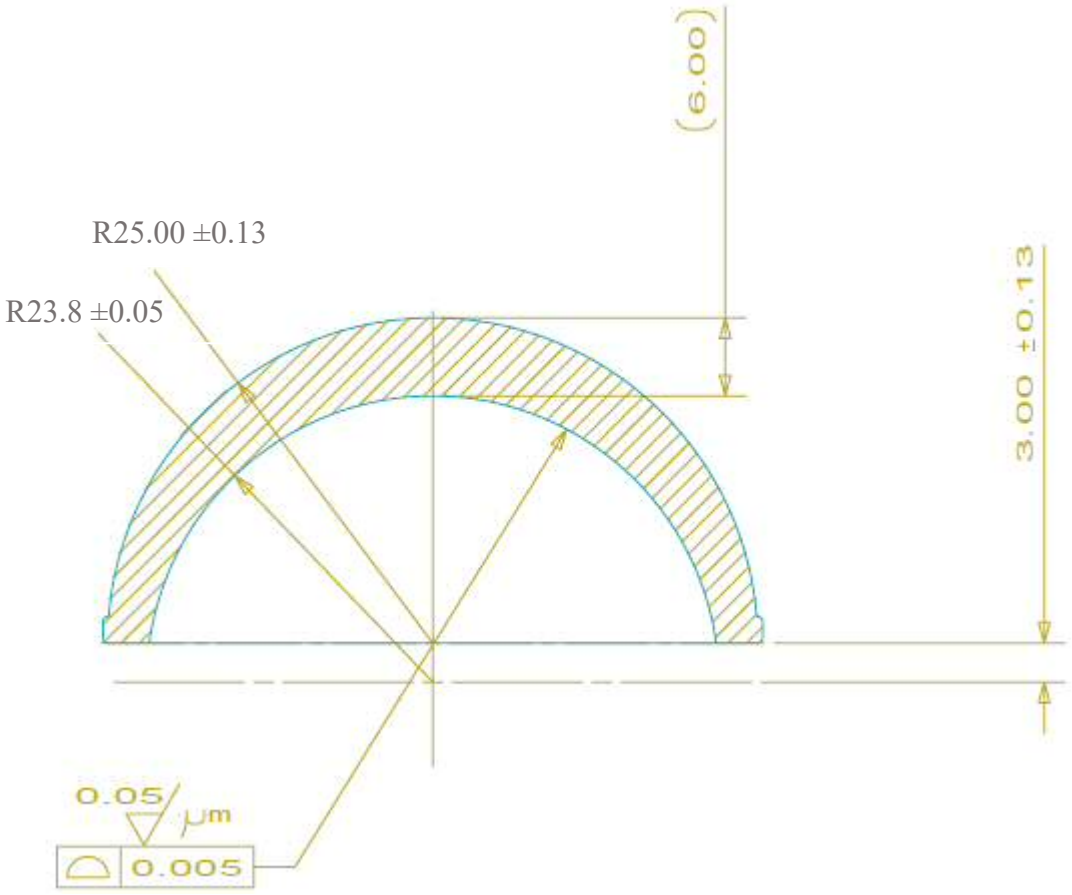

Figure 5.2: Schematic of CFR PEEK Implant version one (All dimensions in MM)

Morgan Advanced Ceramics supply Biomet with a range of ceramic heads from 36mm – 60mm in Diameter with 2mm increments, for the experiment cobalt chromium modular femoral heads were used due to availability. The final design will utilise ceramic heads only.

On the 14th of July 2010 the first cadaveric experiment was undertaken in the anatomy department of the University of Vienna in Austria. Five cadaveric specimens were prepared by surgeons to provide line to line reaming and a 2mm under ream. Line to line reaming is reaming of the acetabulum to the same size as the implant i.e. 52mm ream for a 52mm implant. A 2mm under ream is reaming the acetabular 2mm smaller than the implant i.e. 52mm ream for a 54mm implant. A surgeon prepared each specimen in an identical manner to the method that a total hip arthroplasty is completed in theatre. Standard orthopaedic instruments were used to prepare the cadaveric specimens. A prototype instrument however, was used to impact the CFR PEEK monobloc in to the acetabulum.

Once each ream was completed quick set Provil novo dental putty was used to take a cast of the prepared acetabulum (Heraeus Kulzer GmbH, Hanau, Germany), as shown in Figure 5.3. The dental putty consists of a catalyst and a primer, mixed together the putty becomes hard with heat. The following steps were then taken to record information.

- Once implanted, a mould was cast of the inside diameter of the cup, again using dental putty (Figure 5.4 and 5.5). The putty moulds were cleaned and disinfected using Virkon (Antec International Ltd, Sudbury, UK) and 3D scanned at Biomet UK Ltd, Swindon.
- To obtain immediate feedback on cup deformation, engineer's blue was utilised. Engineer's blue is a highly pigmented paste used to assist in the mating of two or more components. The correct femoral head was then rotated around the articulating surface of the implant. The head was then carefully removed and photographed (Figure 5.6). The presence of engineer's blue at the pole of the head indicates dome contact which is the desired outcome; if engineer's blue is present around the circumference this would imply that the implant has deformed to such a degree as to cause femoral clutching which is unacceptable.

It was not possible to test the largest of the CFR PEEK implants due to the sizes of the cadaveric specimen's acetabulum. Table5.1 presents the actual implanted cup sizes.

Table 5.1: CFR PEEK implants used

Implant Size	Number implanted
50mm x 44mm	1
52mm x 46mm	2
54mm x 48mm	3

Figure 5.3: Dental Putty inserted in to the prepared acetabulum

Figure 5.4: Implanted CFR PEEK monobloc into cadaveric specimen

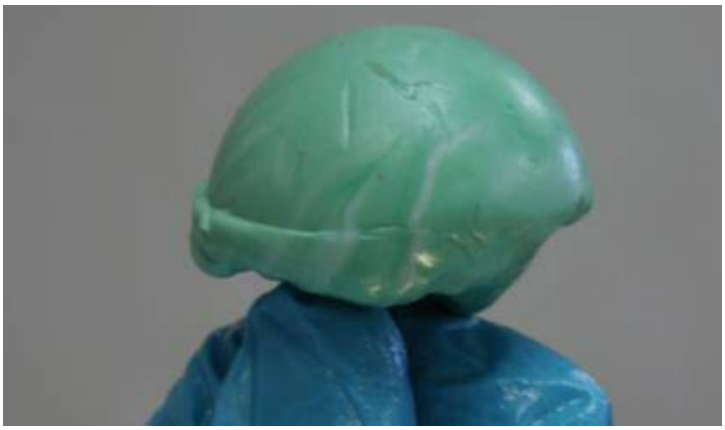

Figure 5.5: Dental Putty mould of the implant in situ

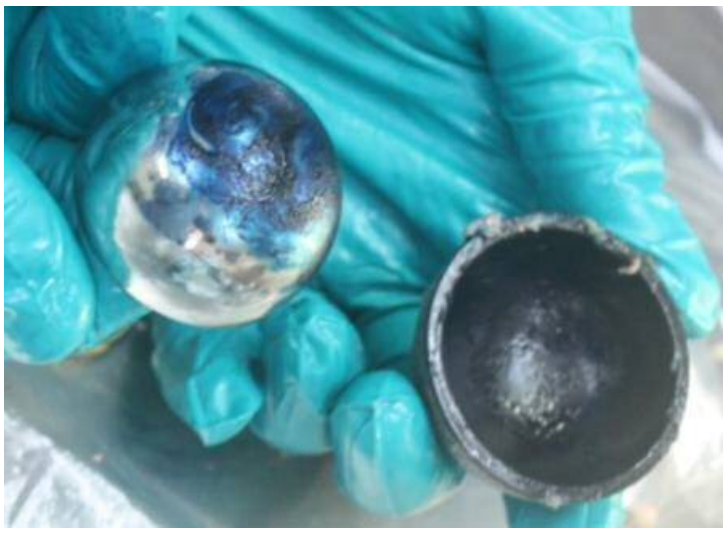

Figure 5.6: CFR PEEK implant with femoral head showing dome

5.2.2 Results and Discussion

The dental putty moulds in this instance required longer to harden due to the cold cadaveric specimens, while this did not present a significant problem it did take longer for the putty to set before removal. Surgical lamps were used to help cure the putty so that it could be removed safely without the risk of damage to the mould. After impaction all were tested using the appropriate mating femoral head and engineer's blue, all showed dome contact and no indication of femoral clutching.

Table 5.2 presents the results of the dental putty mould analysis for the reaming process. It can be seen that there was a significant difference between the final reamer selected and the cavity prepared by the surgeons, up to 0.75 mm in one example (Figure 5.7). When using the acetabular reamers, it was noted that some techniques used by the surgeon were to rotate the reamer in a circular motion which could explain the deviation

instead of using the reamer in a linear motion to provide an accurate acetabulum for the implant. These findings are in line with previous work that demonstrates inaccuracy of reaming (Alexander et al., 1999, Vaughan et al., 2010).

Table 5.2: Dental putty moulds or reamed acetabulum

Reamer size [mm]	Laser scan results [mm]		Cavity size [mm]
	Deviation	Deviation	
52	-0.9	+0.5	51.1 – 52.5
54	Mould not useable		
54	-0.39	-0.75	53.2 – 53.6
54	+0.4	+0.2	54.2 – 54.4
54	+0.5	-0.1	53.9– 53.5
50	-0.1	-0.05	49.9 – 49.9
54	Very flat – unable to scan		

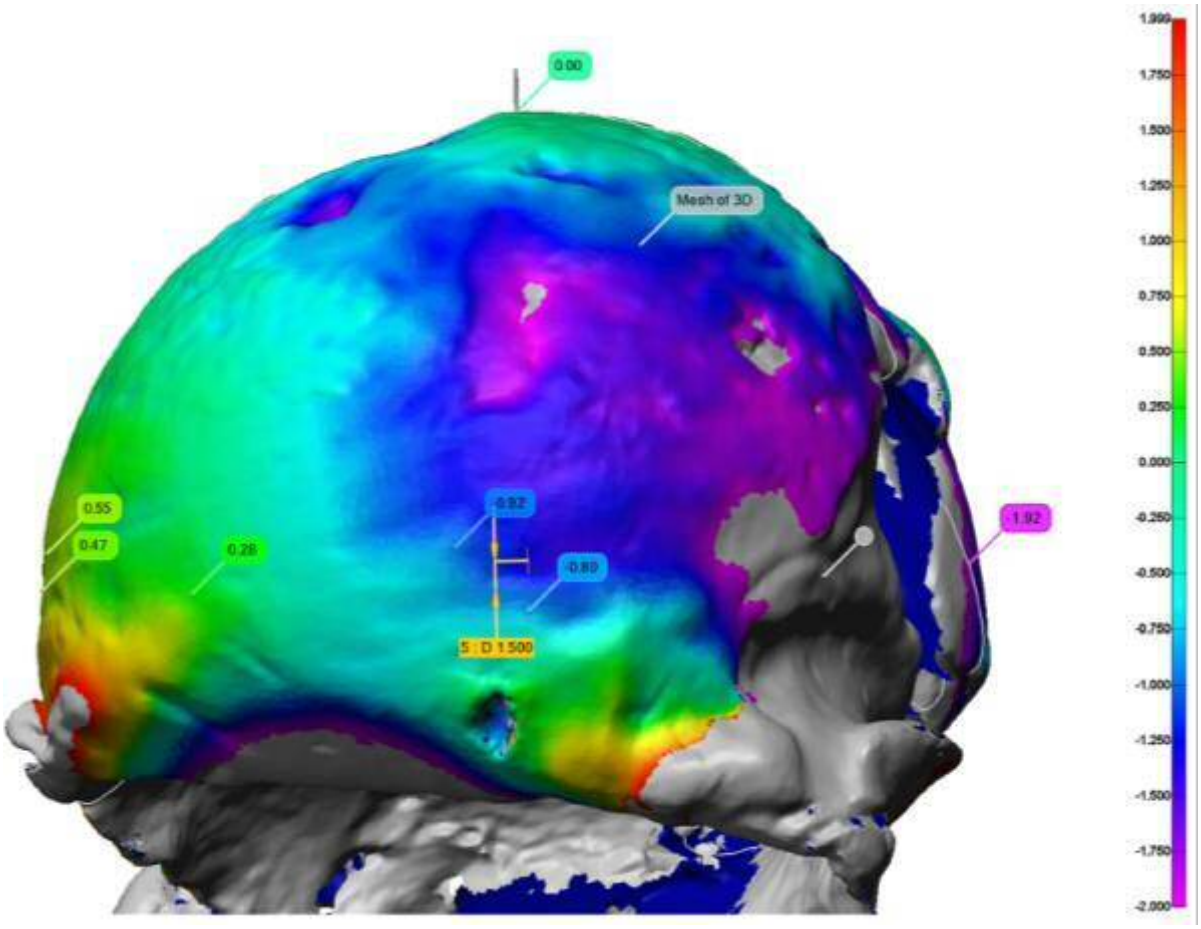

Figure 5.7: 3D Laser scan of dental putty mould from the acetabulum

Table 5.3 presents the results of the putty mould test on the implanted cups. As expected the results show deformation and expansion. Deformation occurring along the ilium and ischium column (Figure 5.8) as identified previously in the literature (Jin, 2006, Squire et al., 2006b, Kroeber et al., 2002, Hothan et al., 2011).

Table 5.3: Impaction results, first cadaveric experiment

Cup size [mm]	Head articulated	Dome contact	Laser scan results [mm]	
			Radial compression	Radial expansion
52	Yes	Yes	-0.31	+0.46
52	Yes	Yes	-0.10	+0.25
54	Yes but stiffer	Yes	-0.66	+0.46
54	Yes	Yes	-0.41	+0.31
50	Yes	Yes	-0.05	+0.11
54	Yes	Yes	-0.2	+0.40

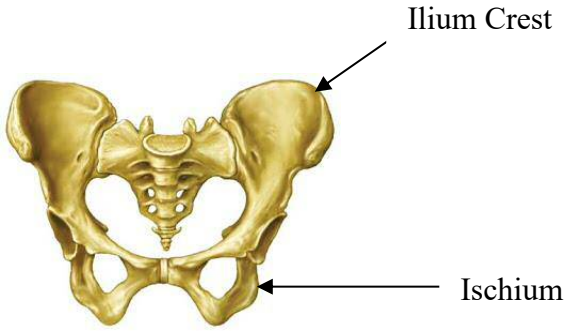

Figure 5.8: Human pelvis

As shown in Table 5.3 the maximum diametric deformation was 0.66mm. The maximum expansion, running anterior to posterior to the ilium and ischium column, was 0.46mm. While dome contact was indicated, the femoral head articulated with greater resistance than the remaining implants. Jin (2006) showed that deformation of cobalt chromium implants was significantly smaller with a maximum diametric value of 0.123mm; although much smaller deformation was recorded compared to the CFR PEEK monobloc this exceeded the diametric clearance of the implant which was 0.080 - 0.120mm. Given that the implant performs under a fluid film regime this would present issues for the implant as it would interrupt the fluid regime and cause femoral clutching. Similar results were recorded, although using a different implant concept by Squire et al. (2006b).

An example of the scan dental putty mould of the articulating surface with the CAD model of the implant, deviations in the mould is shown in Figure 5.9.

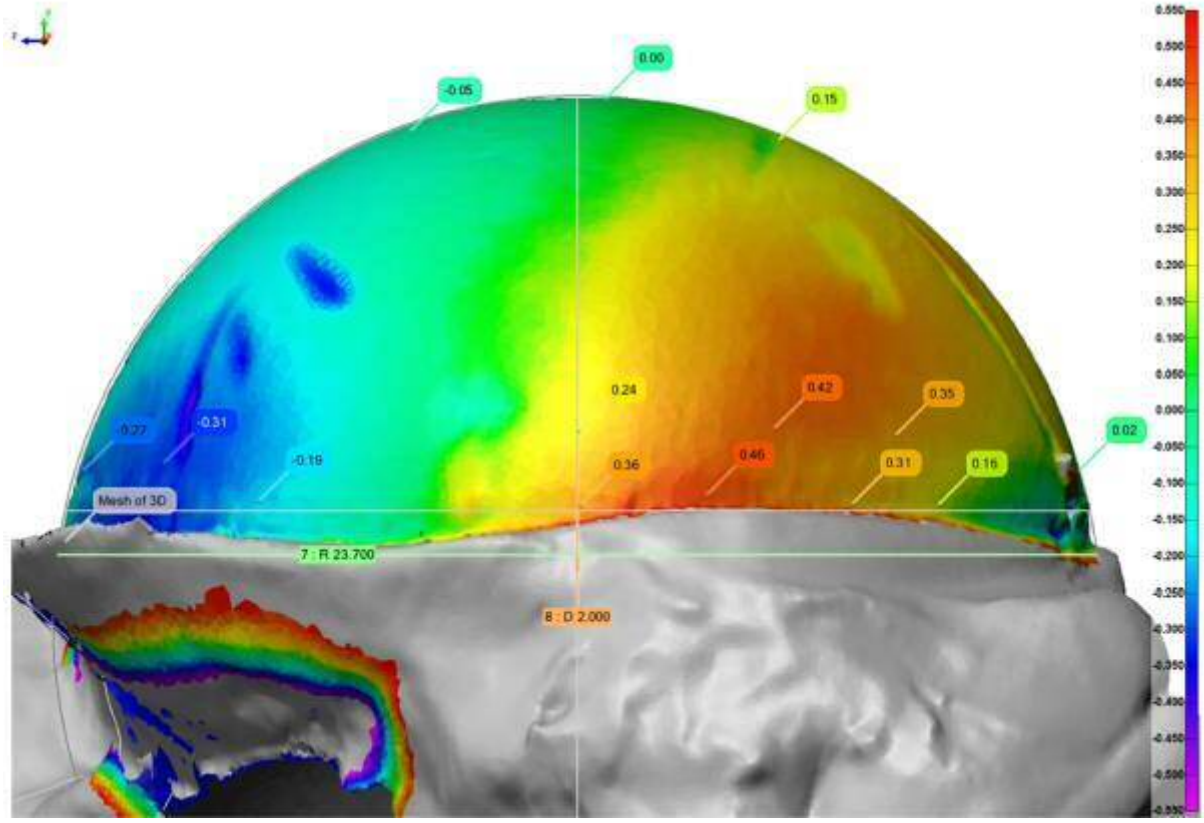

Figure 5.9: 3D laser scan with superimposed CAD model

5.2.3 Conclusion

The initial design was based on Biomet's Magnum MoM design; a hemispherical profile with a 3mm internal offset but with a larger diametric clearance, the results showed significant deformation with a 2mm under ream. While the deformation did not exceed the diametric clearance of 1.8 mm, there is concern about the level of deformation and how this may affect in vivo use. The diametric clearance is not a clearance that is widely used and is far greater than that of the Mitch cup (Latif et al., 2008a) although large clearances have been explored (Wang et al., 2001). Monobloc constructs are typically metallic and referred to as "hard bearings" due to the material either being ceramic or metal such as CoCrMo alloy. "Soft bearings" are typically polyethylene. CFR PEEK and its application in this instance crosses over between the two so a larger clearance than is clinically accepted was selected as a starting point. Based on these results a design evolution occurred and a further cadaveric experiment was completed.

5.3 Cadaveric Testing Experiment Two

5.3.1 Experimental Procedure

The initial implant design was altered to accommodate axial and circumferential grooves to aid in primary and secondary fixation. The diametric clearance was changed to 0.66mm (Figures 5.10 to 5.12). The addition of circumferential grooves would allow the cup to "bite" into prepared acetabulum, with the axial grooves acting as anti-rotation when osseointegration occurs.

Figures 5.10: CFR PEEK monobloc prototype two

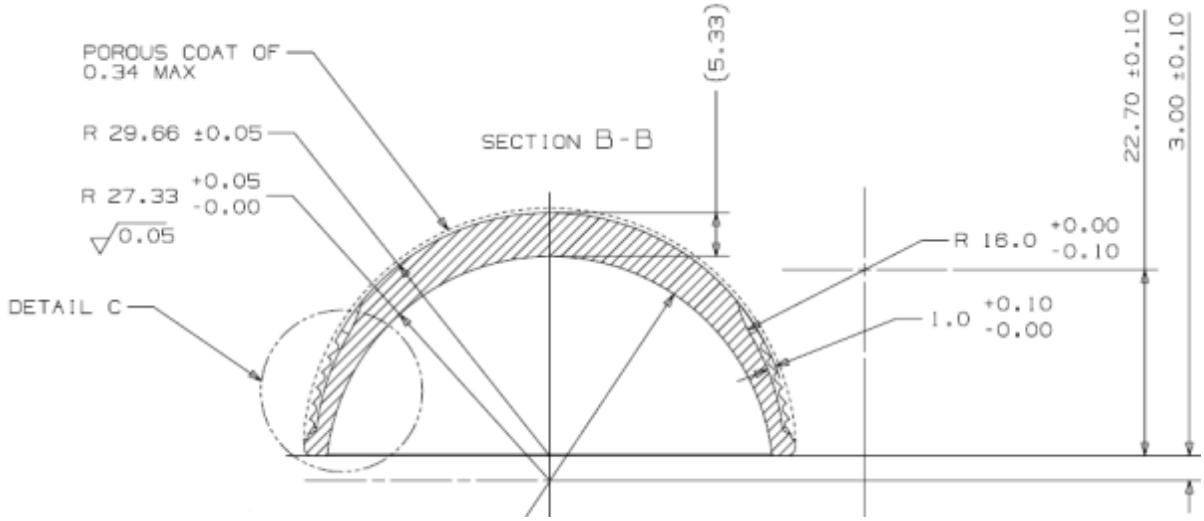

Figure 5.11: Schematic of CFR PEEK Implant version two (All dimensions in mm)

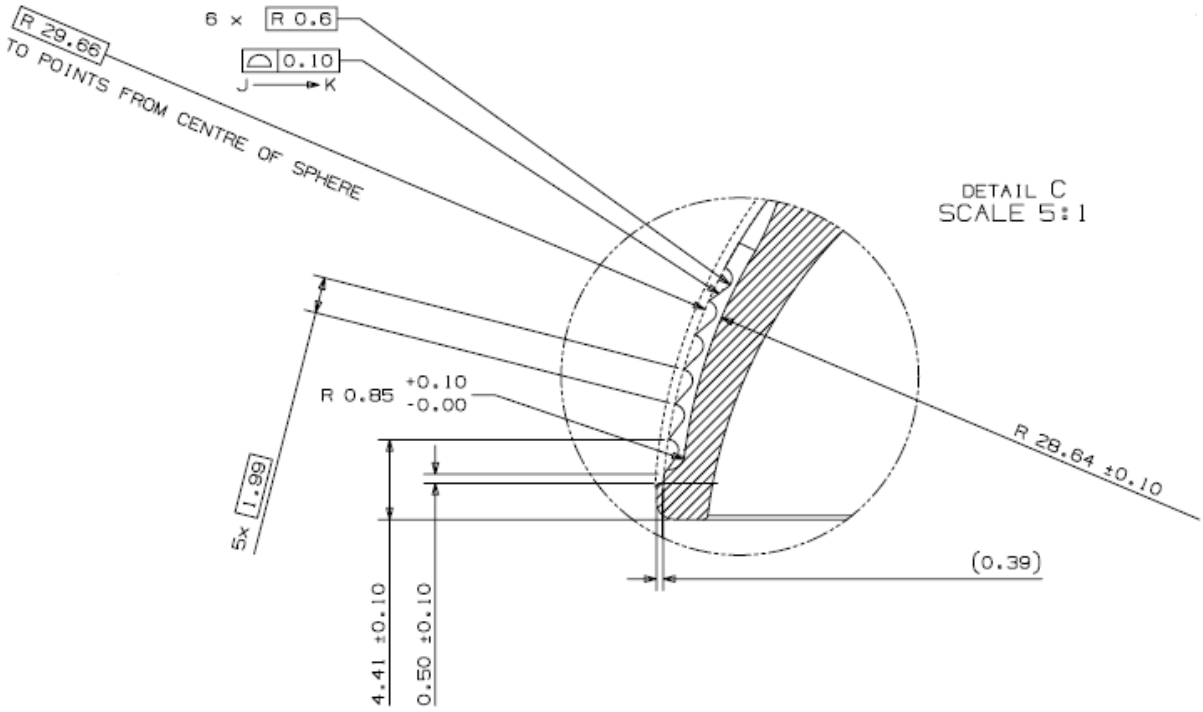

Figure 5.12: Schematic of CFR PEEK Implant version, two circumferential grooves (All dimensions in mm)

On the 6th December 2010 a cadaveric experiment was held in the anatomy department of the Vienna University. Dr Stephen Vehmeijer, a Dutch Orthopaedic surgeon, impacted four out of the six cups provided; the remaining two shells were impacted by the author. The surgeon used a small ASI (Anterior Supine Intramuscular) approach as shown in Figure 5.13. This approach allows the surgeon to avoid cutting muscles to expose the femur and acetabulum; although typically a small incision is used this is not always the case. Selective under-reaming techniques were used depending on bone quality of the specimens and also to represent worst case scenarios for the implant to create the largest amount of deformation.

Figure 5.13: ASI approach

5.3.2 Results and Discussion

Table 5.4 presents a summary of results from the putty moulds for the reaming process. Only three acetabulum moulds could be collected. This was due to difficulty in taking a suitable mould based on the surgical approach and the small incision.

Table 5.4: Results for putty moulds of reamed acetabulae

Acetabular reamer [mm]	Shell impacted [mm]	Ø in X Axis [mm]	Ø in Y Axis [mm]
52mm	54mm	53.474mm	53.069mm
54mm	56mm	57.105mm	55.640mm
52mm	54mm	51.579mm	52.139mm

The sixth and final cup implanted into the cadaveric specimen resulted in the fracture of the shell as shown in Figure 5.14. The author was using the cadaveric specimen after the ASI had finished and the retractors had been removed from the specimen. Due to time constraints, the incision was held open whilst the implant was impacted. The

impaction plate came away from the face of the cup and acted like a chisel. This highlights an important observation. PEEK is a notch sensitive material, although this is reduced with the introduction of carbon fibre (Sobieraj et al., 2010, Nisitani et al., 1992). As shown in Figure 5.15, the failure produced had a very clear precise fracture pattern. On closer inspection of the fractured implant it could be seen that the fractures occurred along the circumferential grooves, in essence these machined grooves acted as stress raisers to the implant (Sobieraj et al., 2010, Avanzini et al., 2013).

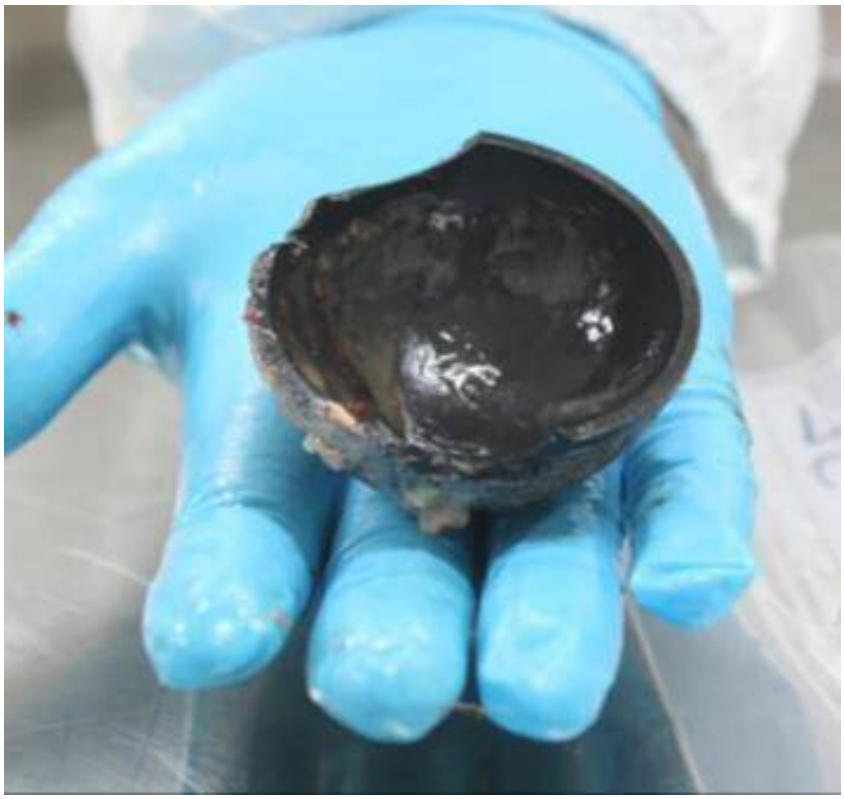

Figure 5.14: Fractured CFR PEEK monobloc

Figure 5.15: Notch sensitivity of PEEK

The results shown in Table 5.4 present the deformation findings of the implants and whether any dome or equatorial contact was present.

Table 5.5: Impaction results for second cadaveric experiment

Cup size [mm]	Head articulated [mm]	Dome contact [mm]	Laser scan results [mm]	
			Radial compression	Radial expansion
54x48	Yes	Yes	-0.30	0.53
54x48	Yes	Yes	-0.27	0.05
54x48	Yes	Yes	+0.07	0.13
56x50	Yes	Yes	+0.12	0.19
56x50	Yes	Yes	-0.11	0.39

5.3.3 Conclusion

The implant did not undergo enough deformation to cause femoral clutching of the head. One of the critical factors that have been observed to date with the cadaveric studies is that the reaming parameter selected by the surgeon affects the deformation

significantly; this level of deformation is comparable to the previous cadaveric experiment. The experiment demonstrated that the cup would have to be redesigned due to the fractured implant which is unacceptable.

5.4 Cadaveric Testing Experiment Three

5.4.1 Experimental Procedure

The implant design evolved, again based on the previous experiment, to include larger radii on the circumferential grooves to help minimise the risk of fracture. In addition, a smaller diametric clearance of 0.460mm was used. This was based on the results of Chapter 4 and an FEA investigation (Chapter 6). The outer geometry was adjusted to an elliptical profile as shown in Figure 5.16. Typically, hemispherical acetabular components are labelled their true size, i.e. 56mm acetabular component is labelled 56mm, elliptical or press fit implants are labelled differently (Biomet, 2015, Biomet, 2014) for example a 56mm acetabular component is labelled 54mm but in the case of the CFR PEEK monobloc it will measure 56mm at its widest point. The press fit is built into the design of the implant with more material situated at the periphery of the implant to minimise deformation on impaction into the acetabulum, it also supports with primary stability before osseointegration occurring (Streit et al., 2014, Ries et al., 1997, Kroeber et al., 2002).

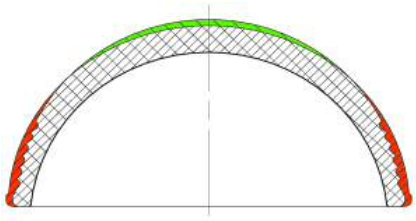

Figure 5.16: Difference between hemispherical and elliptical profiles

The green zone, in Figure 5.16, shows the reduction from a hemispherical profile, and the red areas show the expansion. The reason for the flattened pole is to prevent the implant impinging at the pole of the prepared acetabulum without compromising the press fit at the periphery. A detailed schematic of the implant is shown in Figure 5.17; this geometry will reduce deformation with extra material at the periphery.

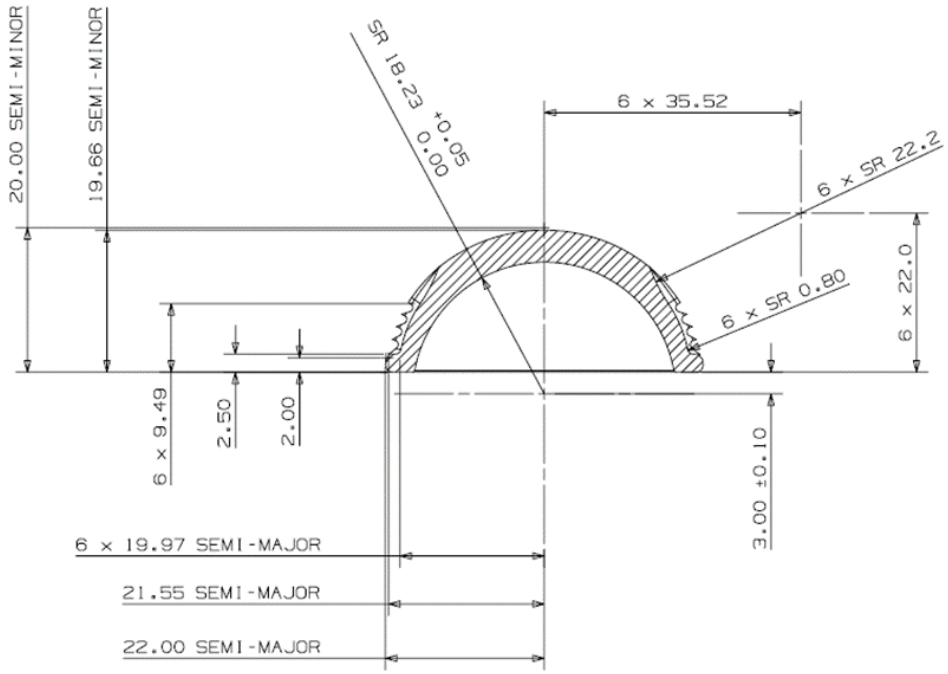

Figure 5.17: Schematic of CFR PEEK Implant version three (all dimensions in mm)

On the 24-25th February, 2011 a cadaver experiment was held in the anatomy department of the Vienna University. The method for this cadaver experiment was identical to the first and second experiments. Dr Pace, an Italian orthopaedic surgeon, was responsible for the surgical approach and implanting the implant. In addition, fluoroscopy was used to ascertain implant seating within the prepared acetabulum. The 3D scanning, in this investigation, was conducted by Re-Tec Engineering Solutions using a Nikon LC15Dx laser scanner mounted to a Reinshaw PH10M coordinate measuring machine (CMM). To obtain a precise overview of the deviations in reaming, the results of the laser scanning are presented in the X-X & Y-Y cross section.

5.4.2 **Results and Discussion**

The results from this investigation are consistent with the previous findings with deviations up to 0.80mm larger than the size of the reamer. Scan results showed that most of the over reaming occurred at the pole and not at the mouth of the acetabulum, which indicates a linear movement by the surgeon as shown by the red and yellow areas in Figure 5.18.

The first three cadaveric specimens were, unfortunately not fully defrosted. This potentially affected the results of the reaming and the impaction. It could be argued that this is a worst case as impaction has taken place in a very dense acetabulum. The stiffer

bone would then result in greater deformation of the shell than a less stiff thawed cadaver. The remaining cadaveric specimens were thoroughly defrosted using surgical lamps before the experiment continued. Figures 5.19 to 5.24 show the first three prepared acetabula. Figures 5.25 to 5.27 show the last four prepared acetabula, these specimens were allowed to thaw properly and were at room temperature when reamed. The reaming was more consistent with the last four acetabula when compared with the first three investigations.

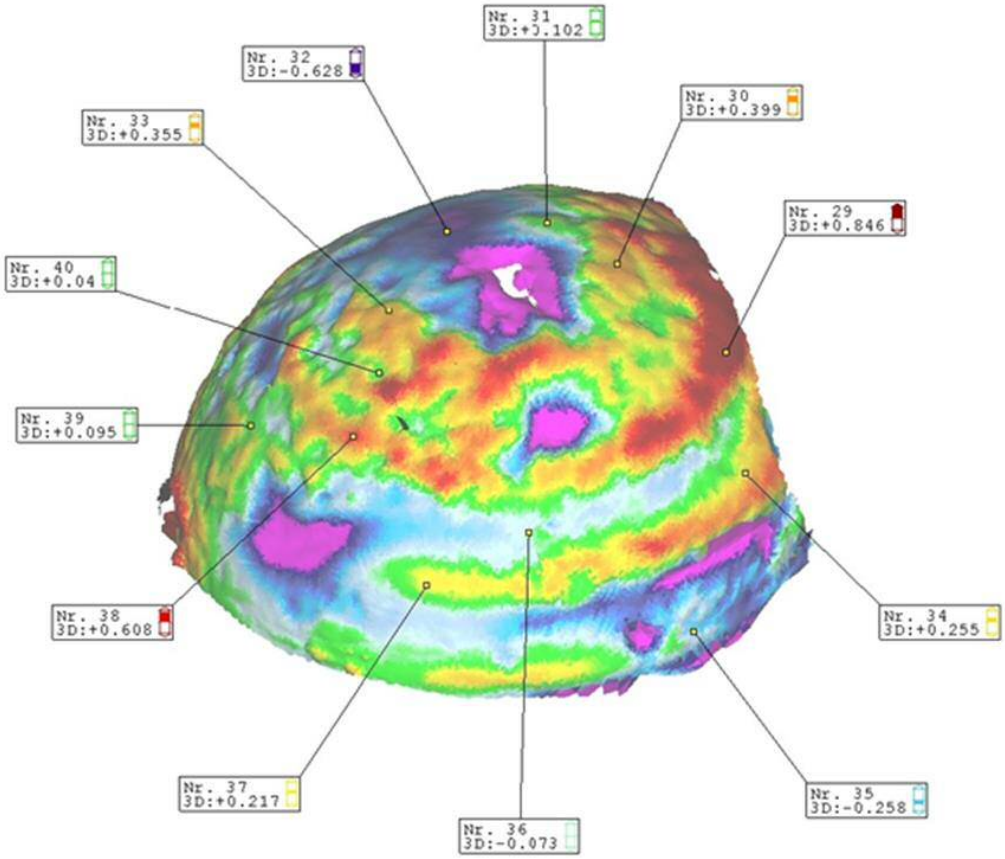

Figure 5.18: 3D scan of reamed acetabulum

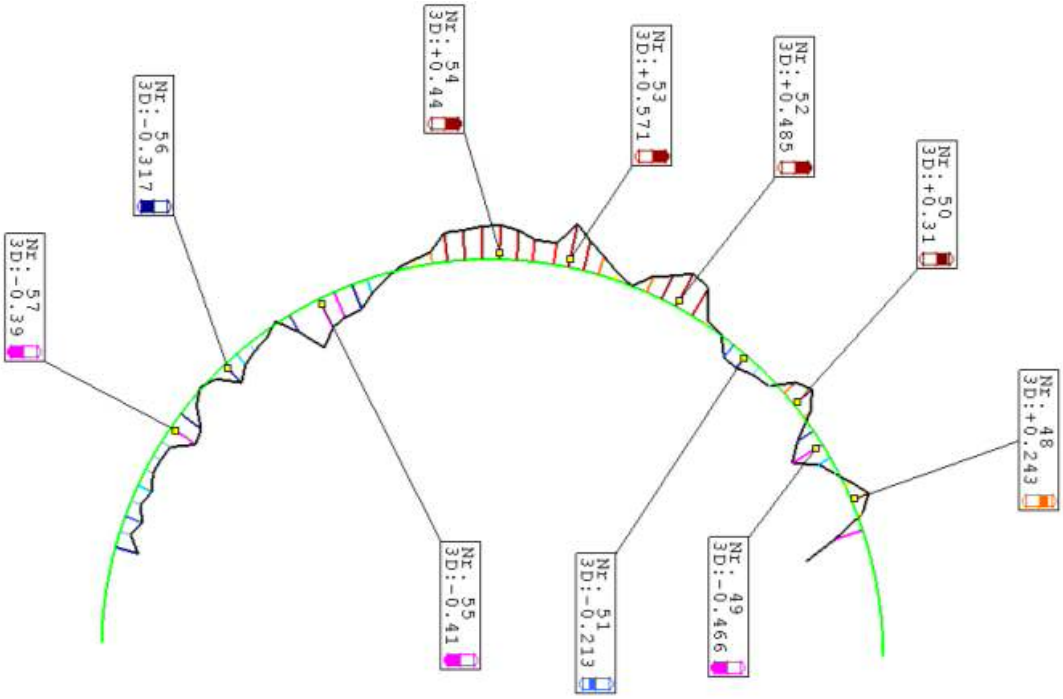

Figure 5.19: Scan of acetabulum 52mm Ream X-X

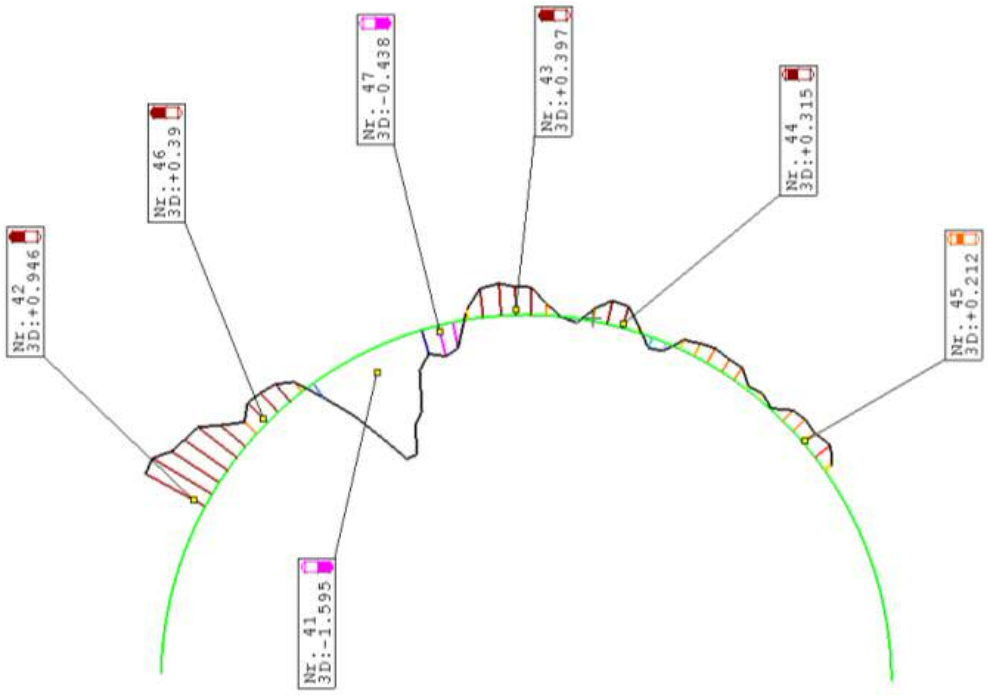

Figure 5.20: Scan of acetabulum 52mm Ream Y-Y

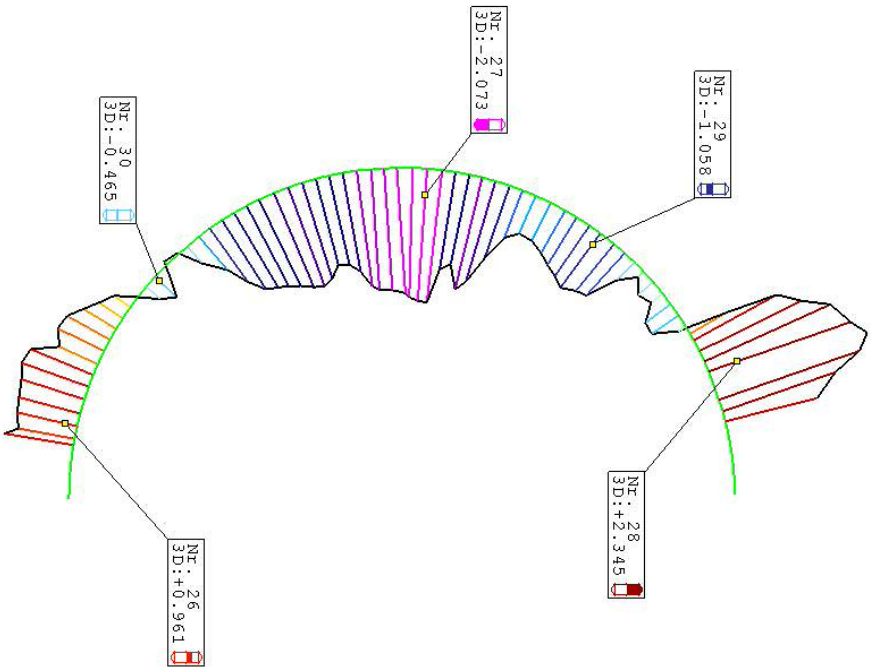

Figure 5.21: Scan of acetabulum 52mm Ream X-X

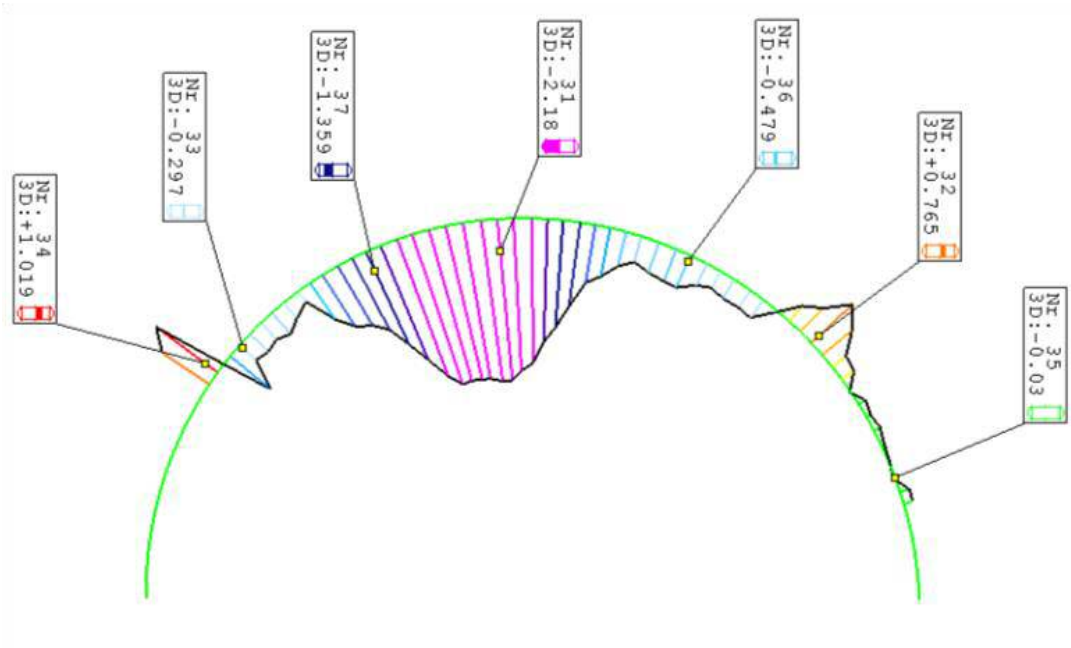

Figure 5.22: Scan of acetabulum 52mm Ream Y-Y

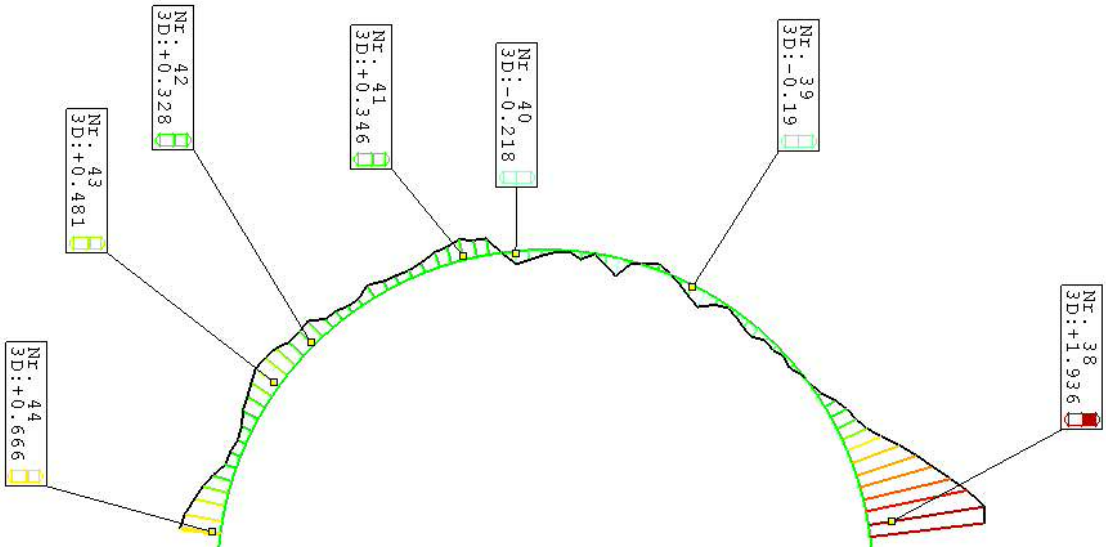

Figure 5.23: Scan of acetabulum 54mm Ream X-X

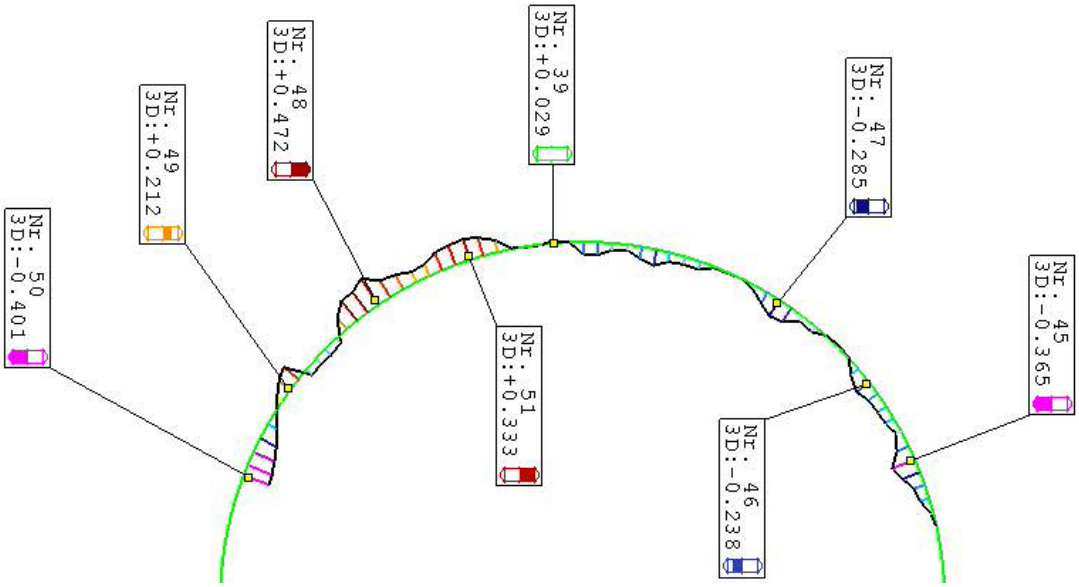

Figure 5.24: Scan of acetabulum 54mm Ream Y-Y

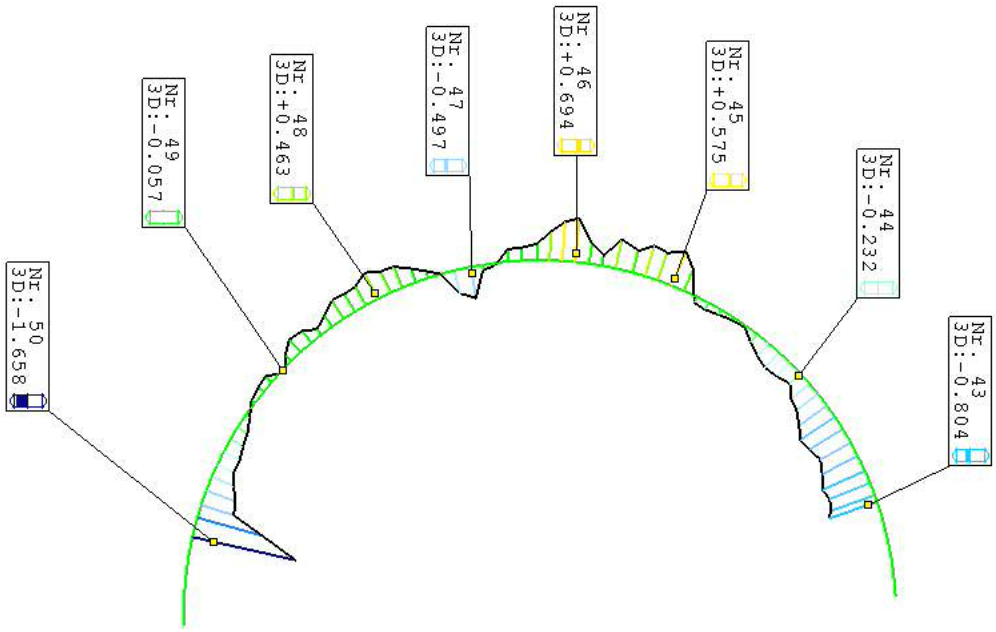

Figure 5.25: Scan of acetabulum 56mm Ream X-X

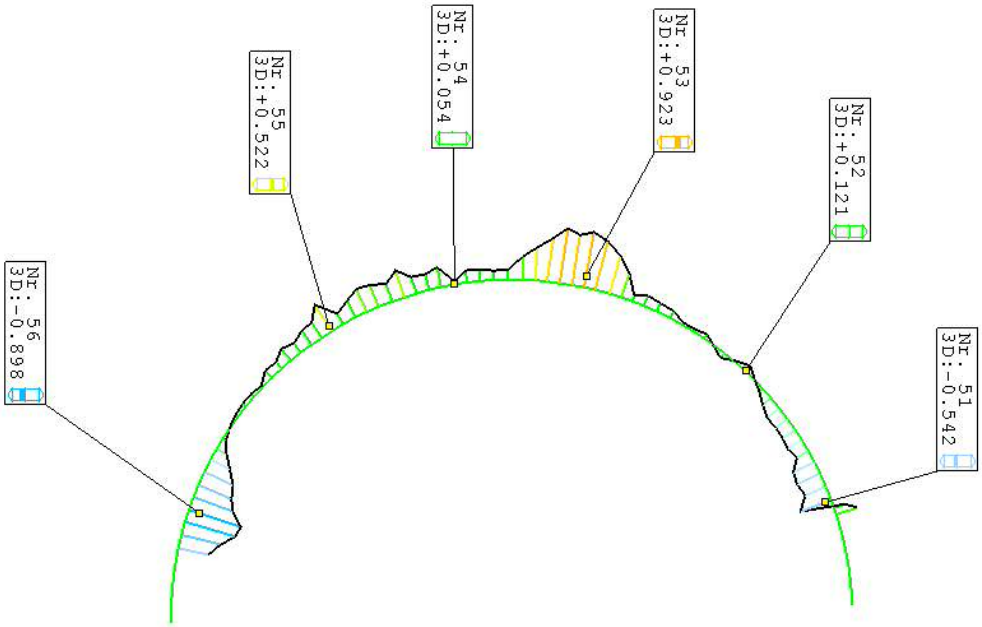

Figure 5.26: Scan of acetabulum 56mm Ream Y-Y

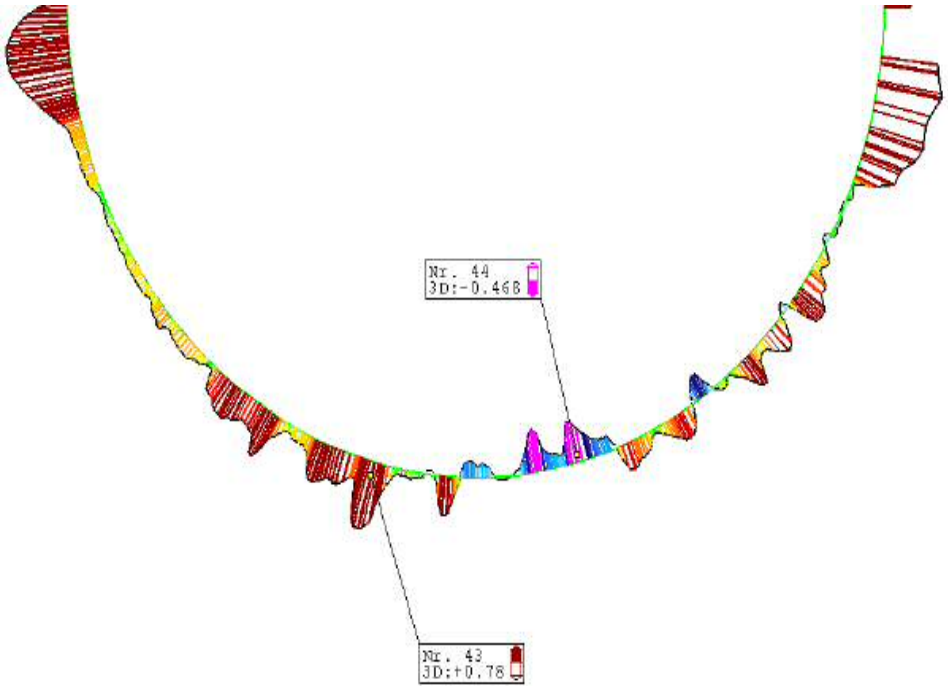

Figure 5.27: Scan of acetabulum 56mm Ream X-X

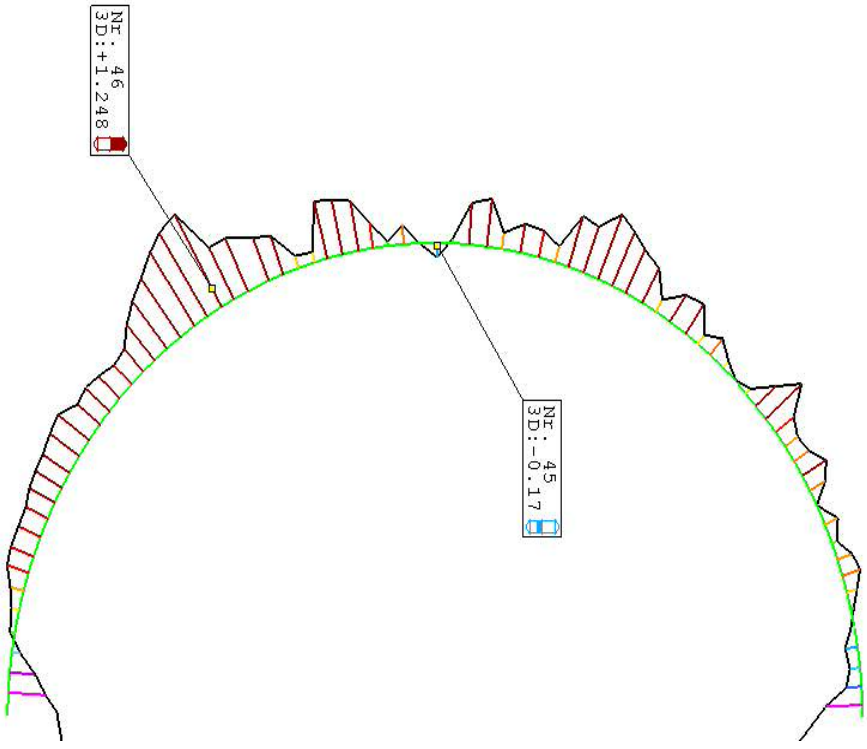

Figure 5.28: Scan of acetabulum 56mm Ream Y-Y

After reaming and cup insertion, the impacted cup was then tested for clutching, as previously described. All implants passed successfully with no femoral clutching.

Results of the impaction test scans can be found in Table 5.6. The results presented shows a considerable reduction in deformation and expansion. Figures 5.29 and 5.30 show the shell being implanted into the cadaveric specimens.

Table 5.6: Impaction results for third cadaveric experiment

Hip Side	Cup Size [mm]	Head Articulated	Dome Contact	Laser scan results [mm]	
				Deformation	Expansion
L	52/46	YES	YES	-0.101 -0.032	+0.271 +0.352
R	52/46	YES	YES	-0.118 0.079	+0.294
L	52/46	YES	YES	-0.135 0.032	+0.216 +0.24
L	54/48	YES	YES	-0.075	+0.185 +0.225
R	54/48	YES	YES	-0.271	+0.179
R	56/50	YES	YES	-0.139 0.148	+0.457 +0.298
L	56/50	YES	YES	-0.328	+0.182

Figure 5.29: CFR PEEK Monobloc impaction

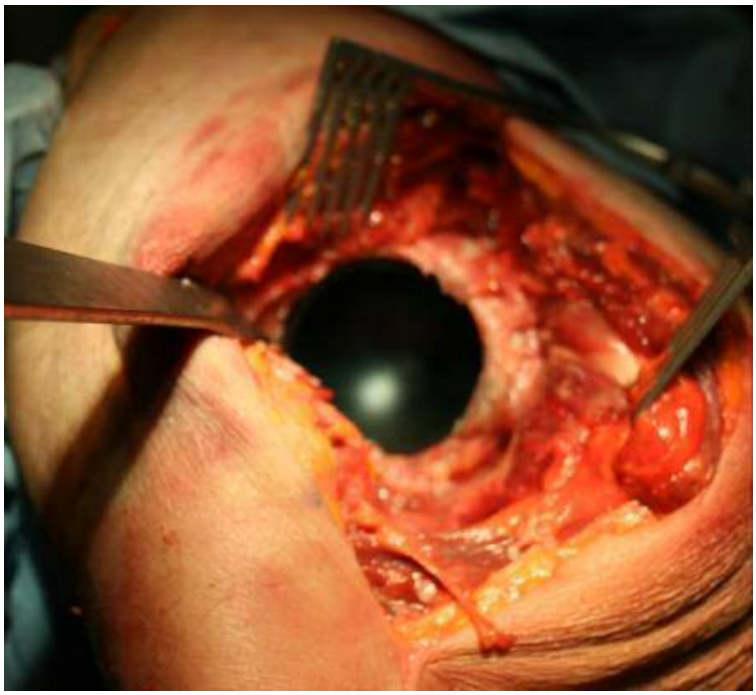

Figure 5.30: Prototype three after impaction into acetabulum

Surgeons from the previous experiments commented that traditional metallic acetabulum components, when impacted into the acetabulum, the surgeon is able to feel and hear the impaction sound differ when the shell is correctly seated. This indication allows the surgeon to feel more confident with a responsive implant. In this cadaveric study fluoroscopy was used to investigate how well the cups fitted to the reamed acetabulum (Figure 5.31). The highlighted parts are (1) the thick black line, which is the porous plasma spray (2) the 3mm internal offset designed into the implant and (3) the circumferential grooves.

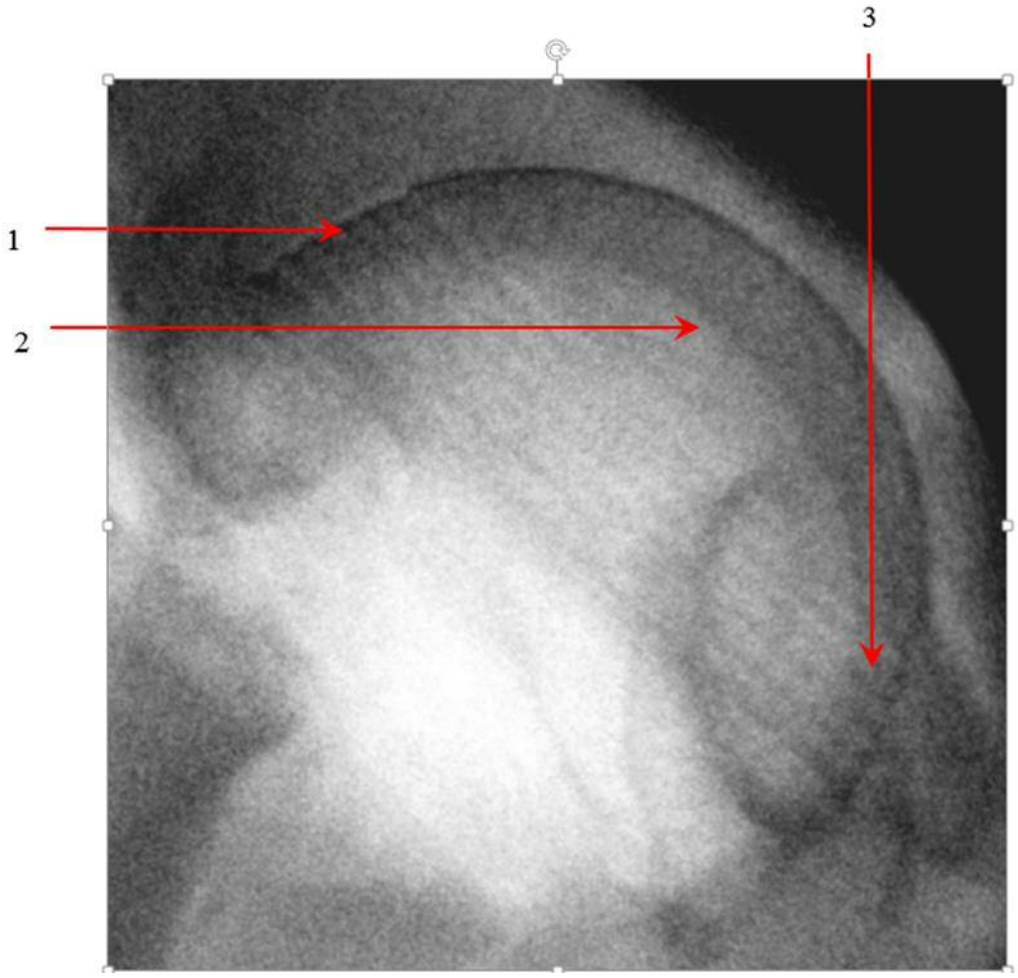

Figure 5.31: Fluoroscopy CFR PEEK Monobloc

Figures 5.32 to 5.45 show that results of the scans in the X-X and Y-Y planes. The majority of the cups had a maximum deformation less than that of the radial clearance of 0.230mm. However, the cups in Figures 5.42 to 5.45 show two cups that had a deformation greater than radial clearance, but still less than the diametric clearance of 0.460mm. The majority of the impacted shell profiles follow the CAD model (green line). The extreme peaks and troughs in the plots are air pockets inside the mould.

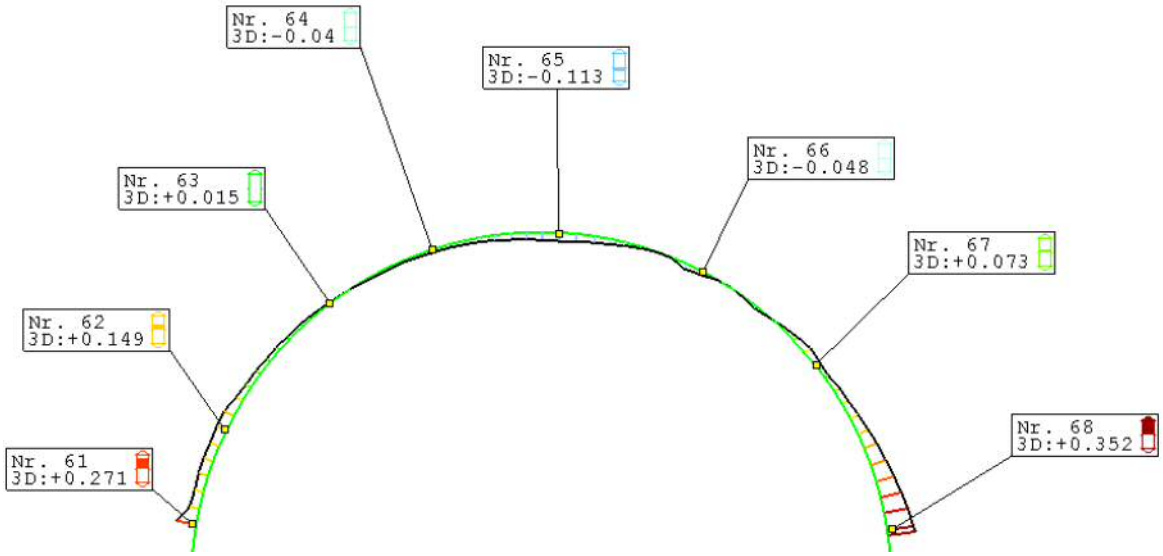

Figure 5.32: Scan of 52mm/46mm cup X-X

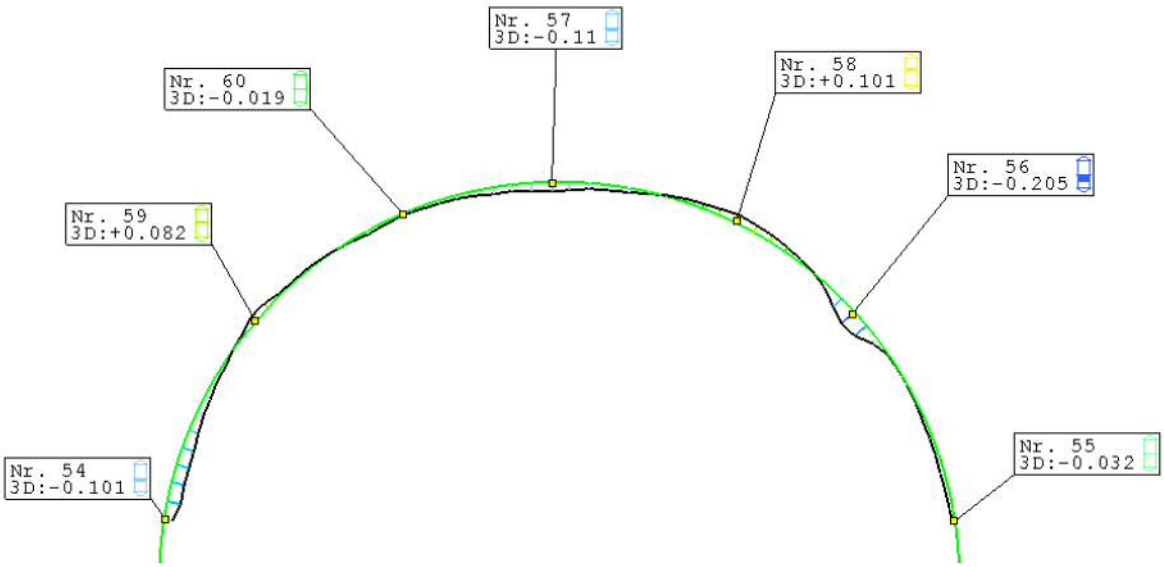

Figure 5.33: Scan of 52mm/46mm cup Y-Y

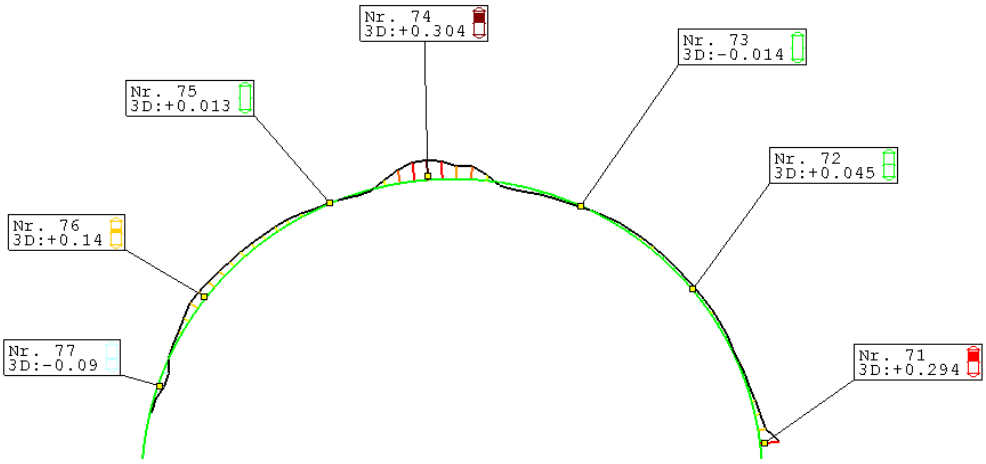

Figure 5.34: Scan of 52mm/46mm cup X-X

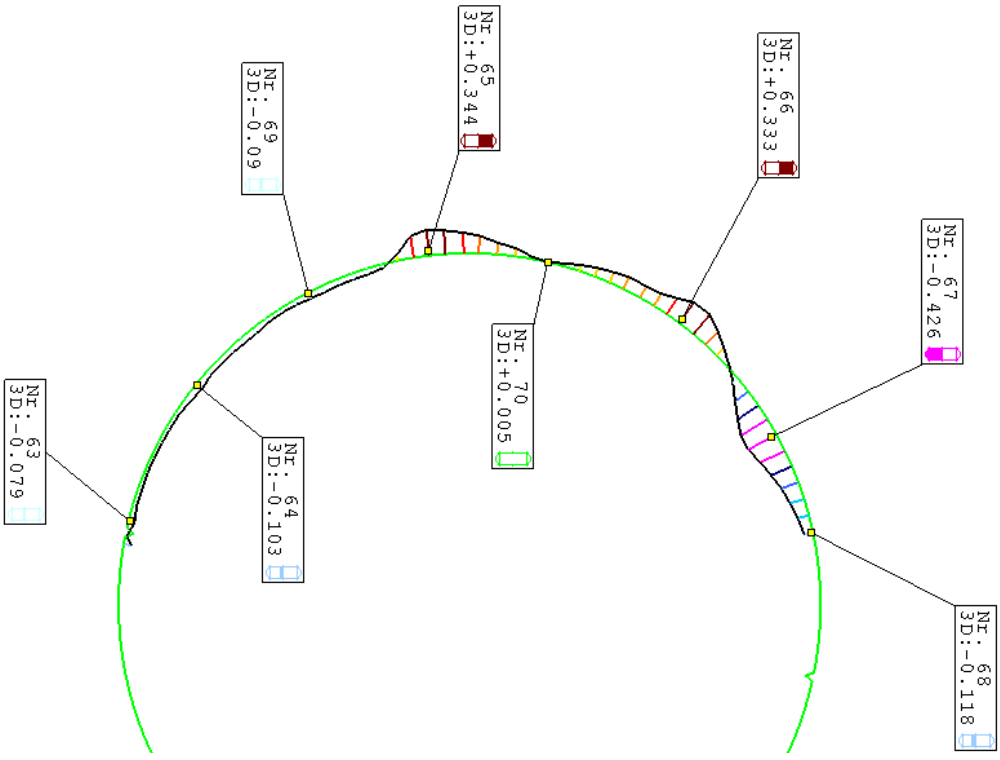

Figure 5.35: Scan of 52mm/46mm cup Y-Y

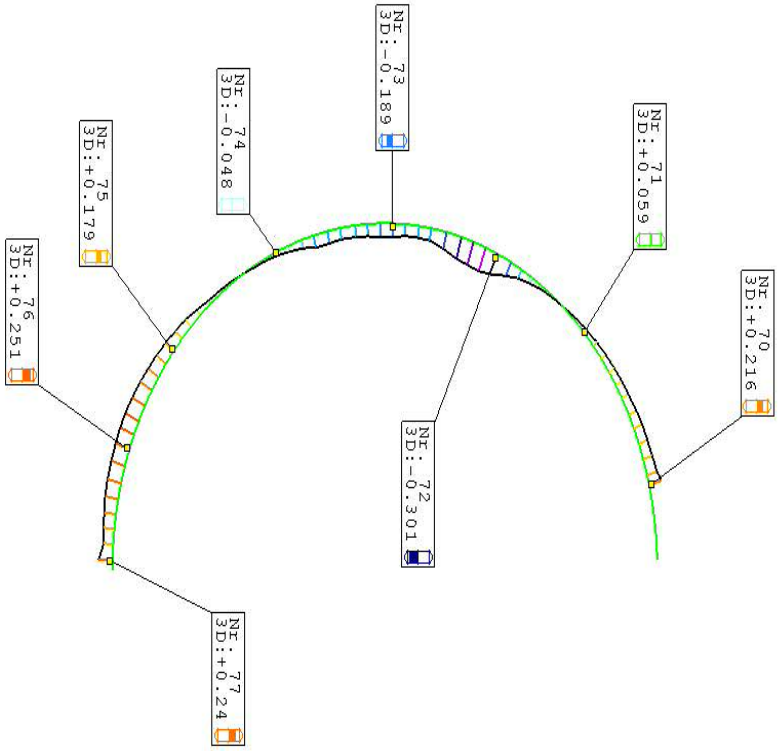

Figure 5.36: Scan of 52mm/46mm cup X-X

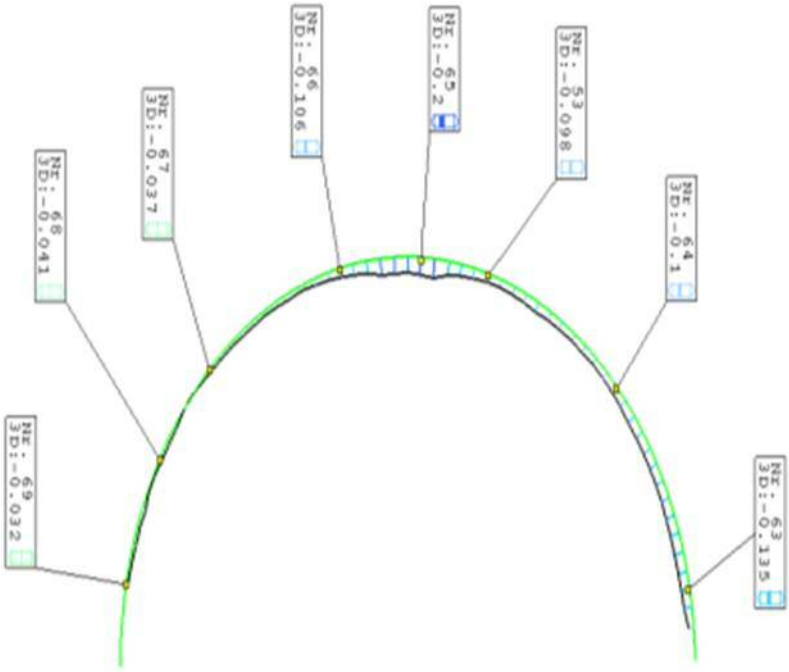

Figure 5.37: Scan of 52mm/46mm cup Y-Y

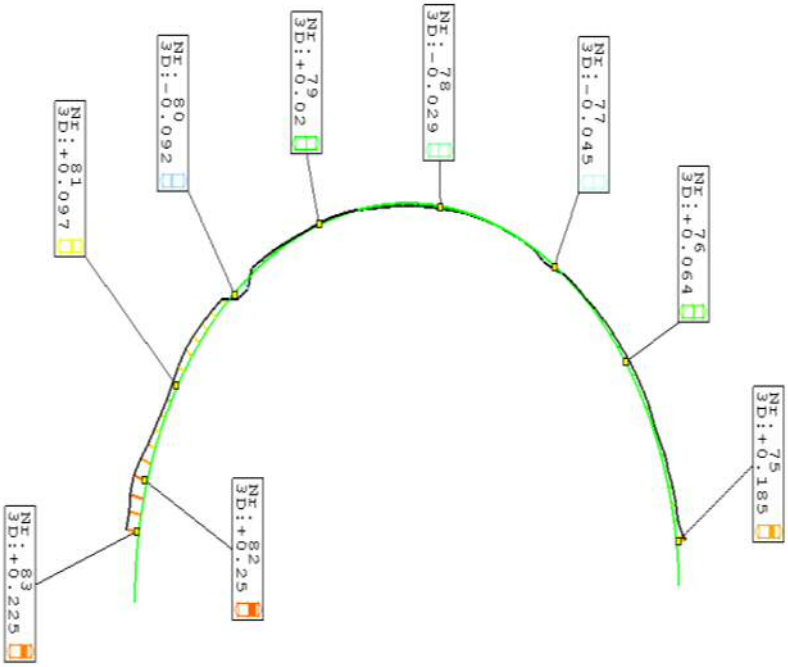

Figure 5.38: Scan of 54mm/48mm cup X-X

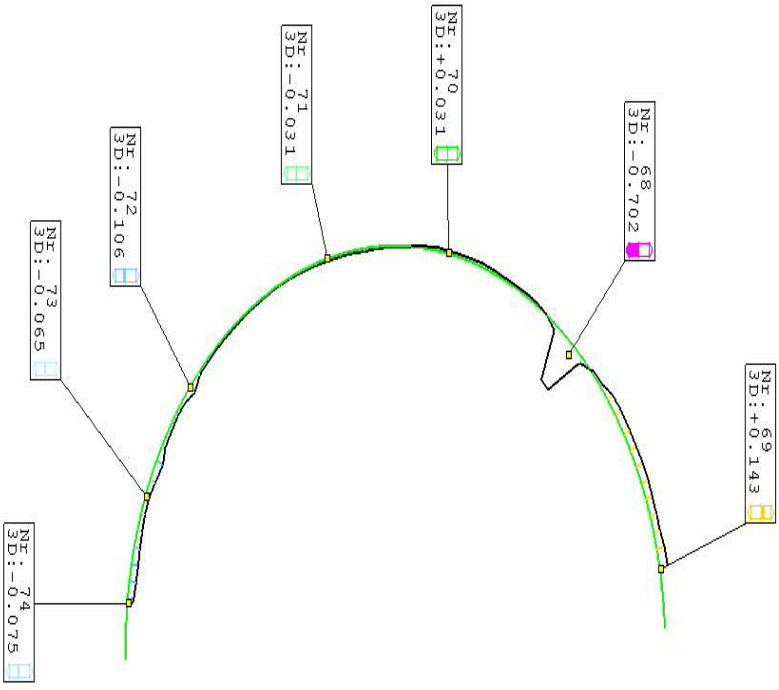

Figure 5.39: Scan of 54mm/48mm cup Y-Y

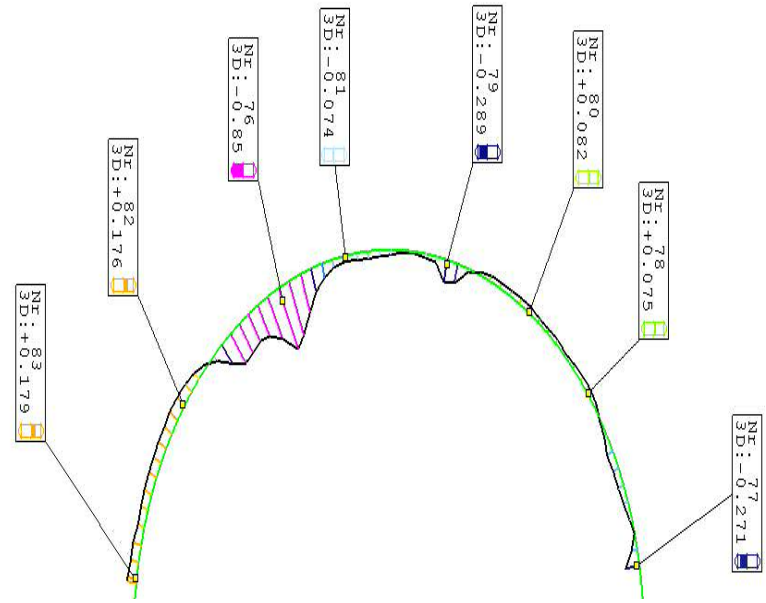

Figure 5.40: Scan of 54mm/48mm cup X-X

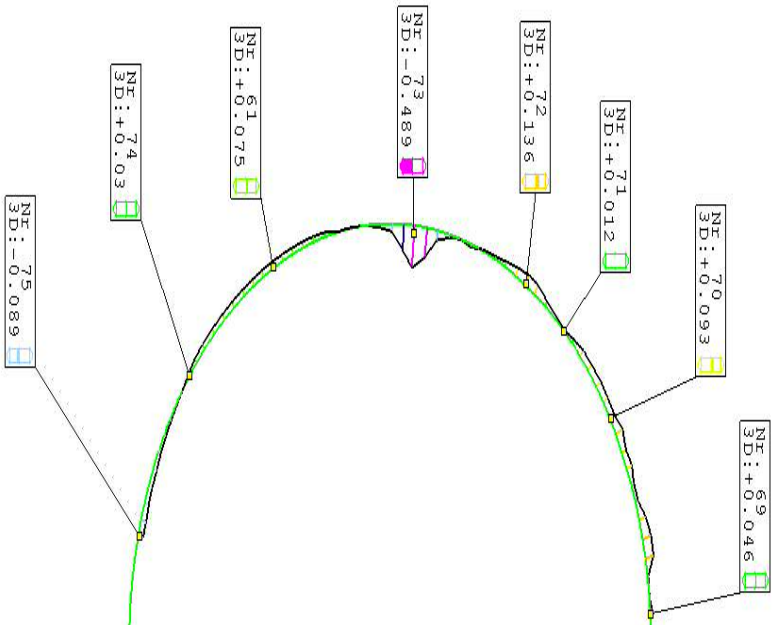

Figure 5.41: Scan of 54mm/48mm cup Y-Y

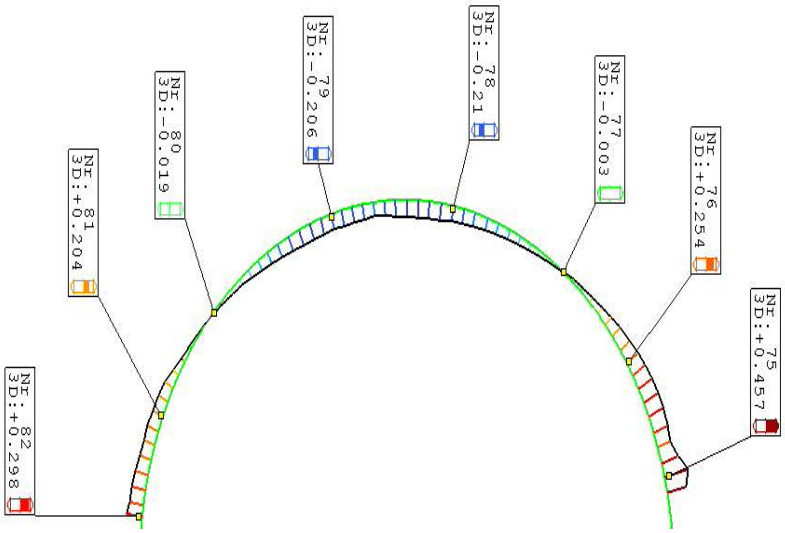

Figure 5.42: Scan of 56mm/50mm cup X-X

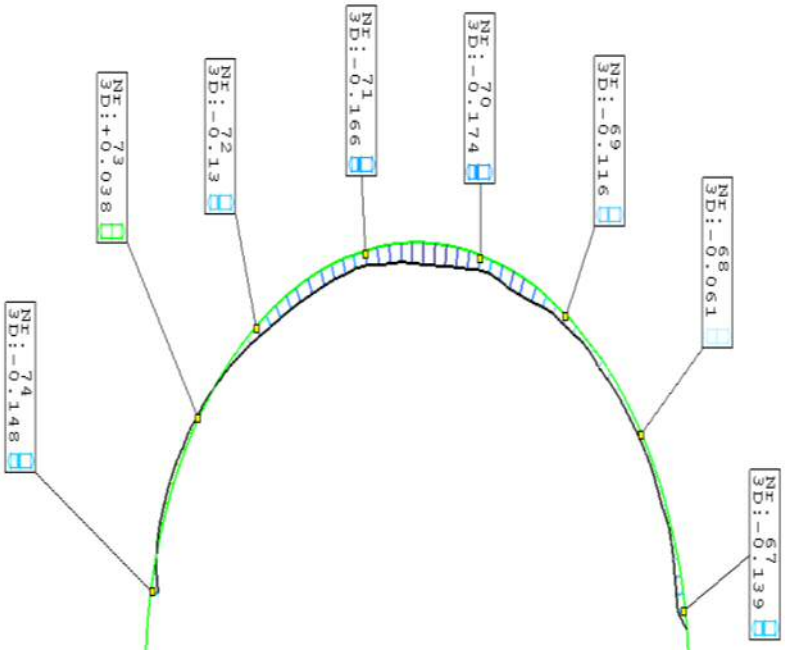

Figure 5.43: Scan of 56mm/50mm cup Y-Y

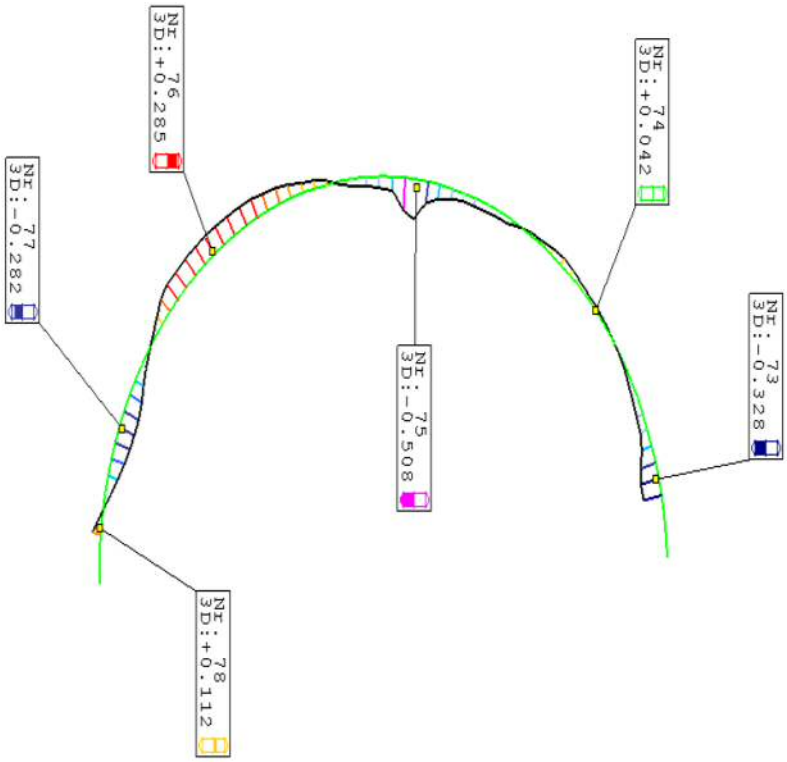

Figure 5.44: Scan of 56mm/50mm cup X-X

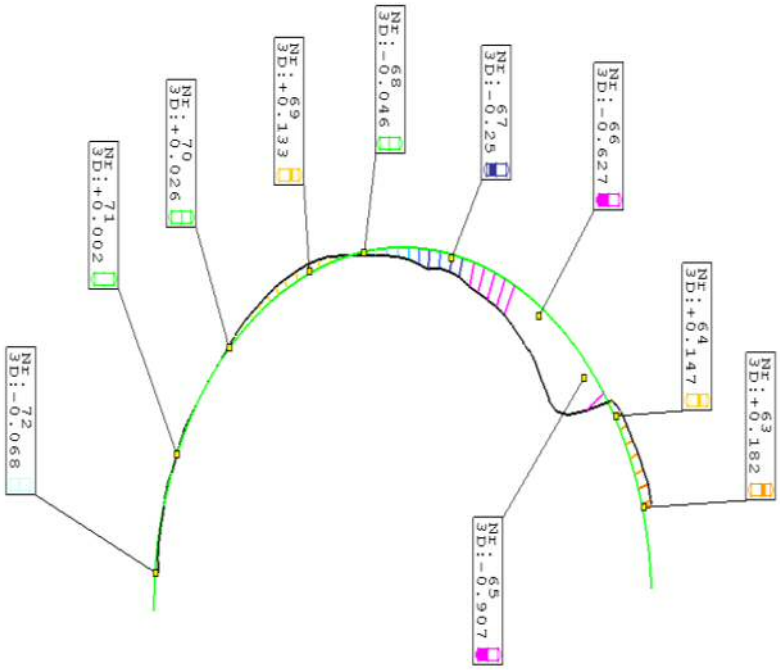

Figure 5.45: Scan of 56mm/50mm cup Y-Y

The surgeon commented that all the cups showed excellent stability in the acetabulum even when a shell was impacted into a dysplastic acetabulum (Figure 5.46). Engineer's

blue was again used to assess for clutching. The results for all implants was that pole contact was achieved demonstrating that no femoral clutching occurred.

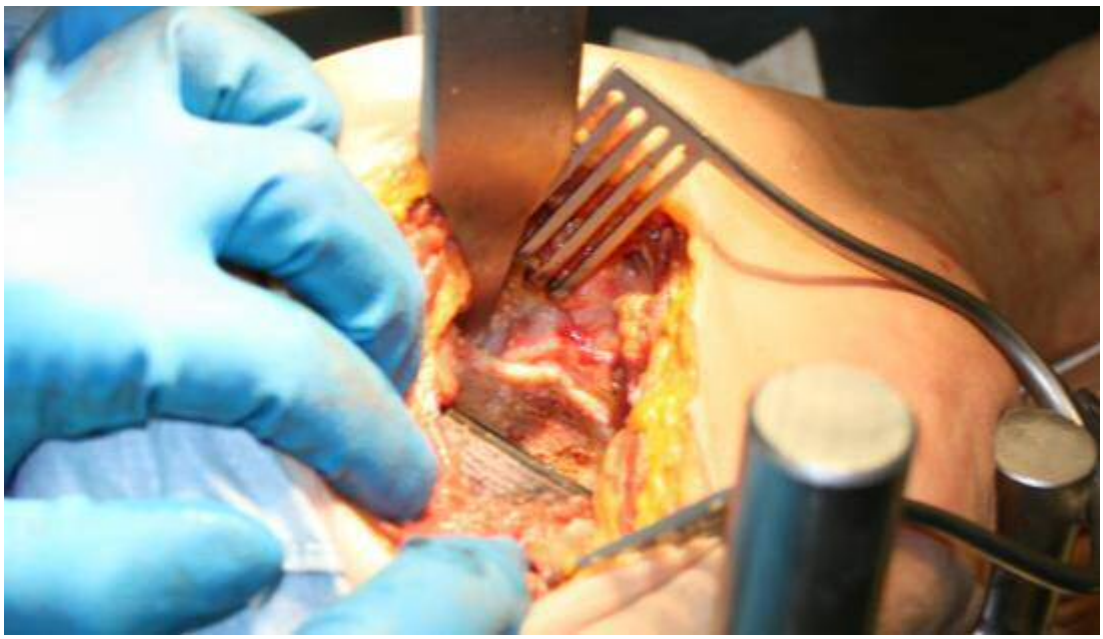

Figure 5.46: Acetabular dysplasia

5.4.3 Conclusion

The new design showed a distinct improvement with less deformation and no fractures. Furthermore, there was an excellent press fit achieved in all of the implants even with the dysplastic hip. The implants impacted easily without any concerns of fracturing the acetabulum. The smallest amount of deformation was recorded in this experiment and is comparable to what has been observed with previous implants (Jin, 2006, Squire et al., 2006b, Fritsche et al., 2008, Grimes, 2010, Markel et al., 2011). The circumferential grooves still could still be a site of fatigue crack initiation, however as the press fit was deemed excellent by the surgeon this feature was no longer required.

5.5 Cadaveric Testing Experiment Four

5.5.1 Experimental Procedure

In this investigation, the CFR PEEK cup had the circumferential grooves removed. The cup was PPS titanium coated. Based on the previous investigation Biomet decided that the cup would be available with anatomic articulation diameters of 36mm – 56mm (4mm increments) and will be used against CeramTEC's Biolox Delta heads. The cup is fourth generation with an elliptical profile and utilises the same clearance as the third generation cup (Figures 5.47 and 5.48).

Figure 5.47: CFR PEEK Monobloc prototype four

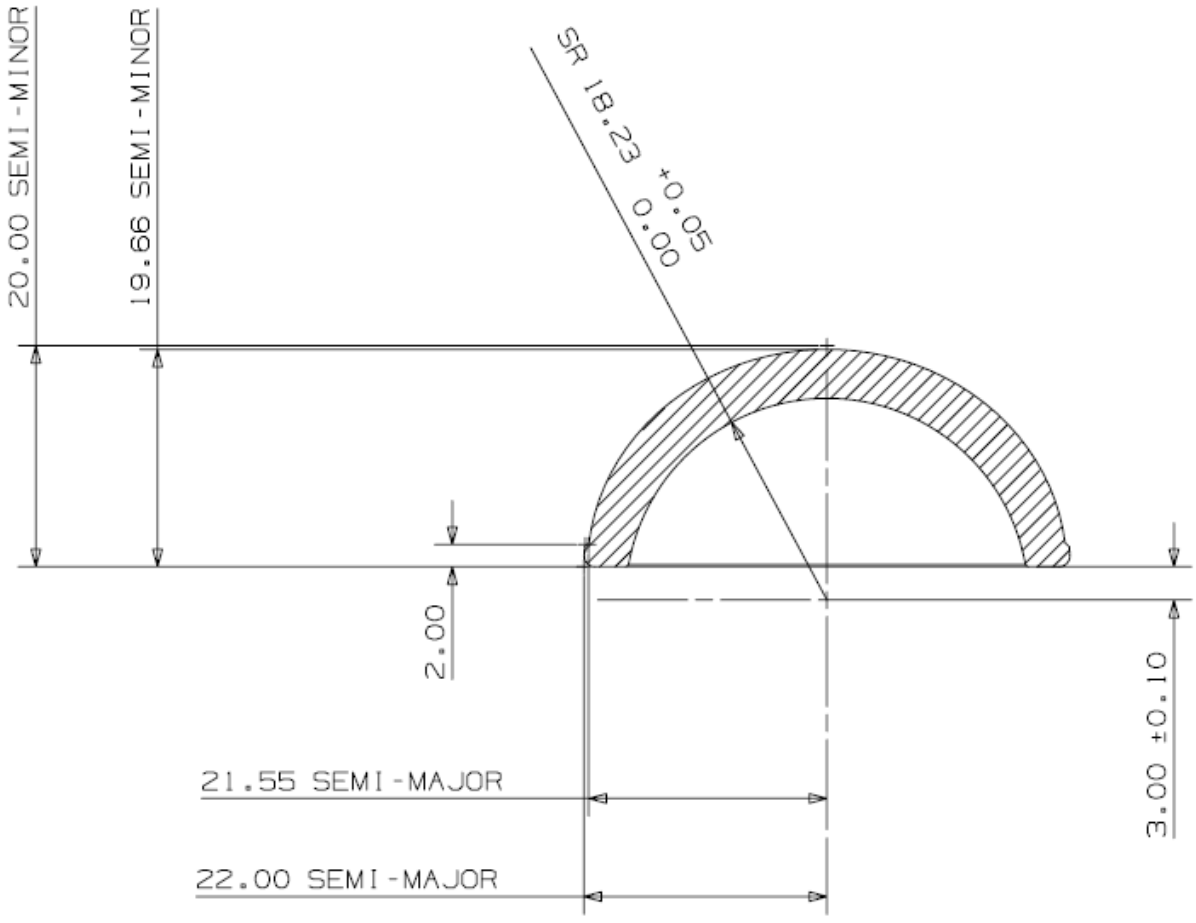

Figure 5.48: Schematic of CFR PEEK Implant version four (all dimensions in MM)

On the 23rd June, 2011 a cadaveric session was held in the Surgical Training Centre at Newcastle to investigate the deformation of CFR PEEK Monobloc shells of the proposed final design. Dr Pace completed the implanting into the cadaveric specimens. Due to availability of equipment dental putty moulds had to be used to capture deformations of the acetabulum and implant.

5.5.2 Results and Discussion

The specimens used in this experiment are not typically used for this setup, but were all that was available. There was difficulty in dislocating the joint. Traditionally this is achieved by using the leg as a lever arm to dislocate the femoral head from the acetabulum. As the specimens were only the pelvis section dislocating the joint caused a small delay as the lever arm is much smaller as shown in Figure 5.49. The specimens were prepared in the same way that Dr Pace would perform in surgery (Figure 5.50).

Figure 5.49: Cadaveric pelvis

Figure 5.50: Prepared acetabulum

Dental putty moulds were taken of the prepared acetabulum. In this investigation all specimens were at room temperature which aided in the curing process of the dental putty. The aim was to ensure that the putty had cured significantly so that the mould could be removed without the risk of damage (Figure 5.51).

Figure 5.51: Cured dental putty mould

Figure 5.52 shows a scan of dental putty from the reaming. It is the most accurate example (matching reamer profile) of reaming observed throughout all the cadaver experiments. The results for this investigation were also the most consistent of all investigations. The reamers used in this investigation were unused and therefore not

worn. It is evident that less force is required to ream the socket, which results in a more accurately prepared acetabulum.

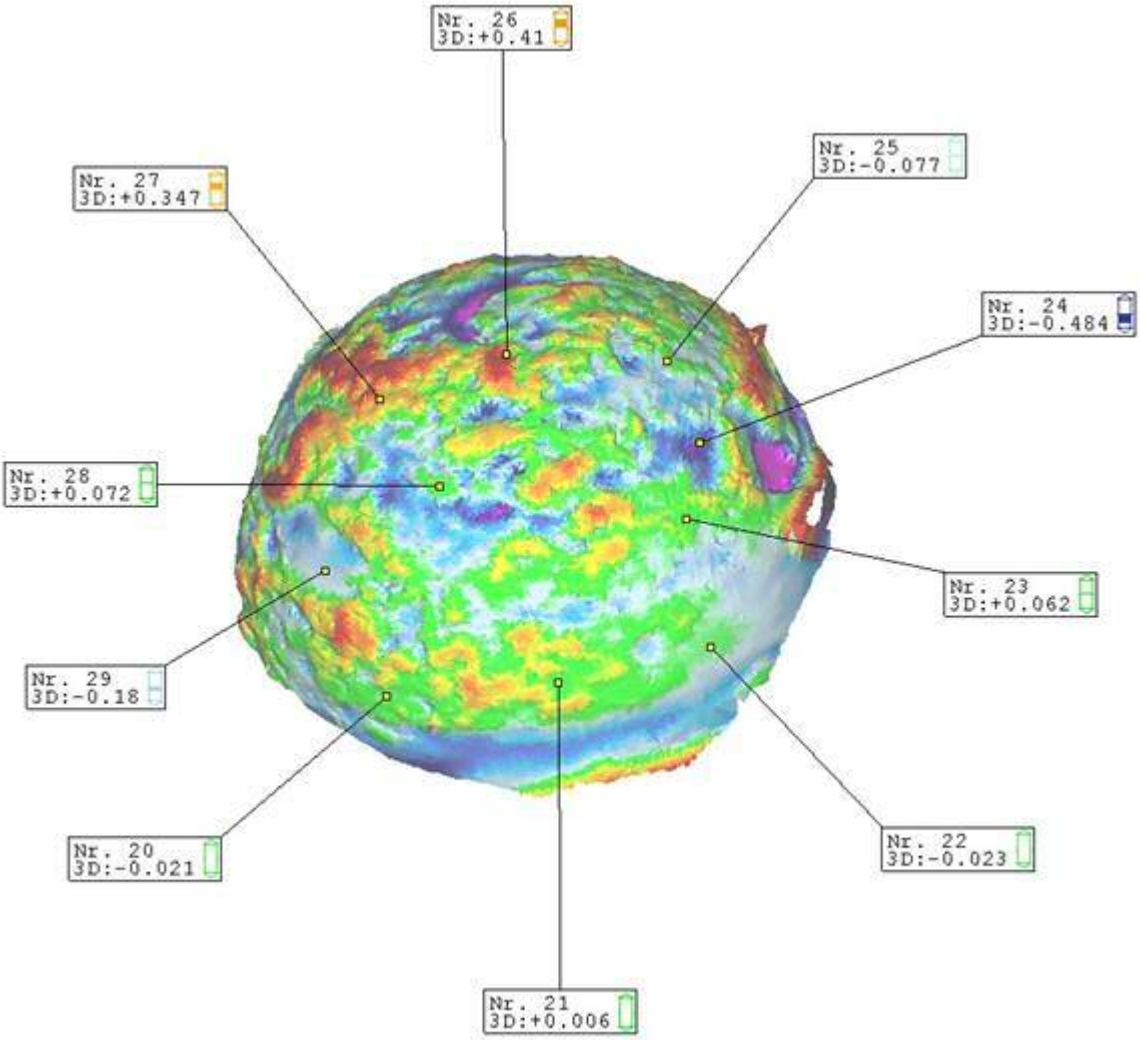

Figure 5.52: 3D image of scanned actebulum

Figure 5.53 shows an example scan for the reamed acetabulum. The green arc shows the acetabular reamer profile with the deviations highlighted with the black line. The major peaks and troughs as mentioned below are air pockets in the dental putty due to the mixing process and the need to dome the material prior to insertion. All scans showed a similar pattern but as previously stated the reaming in this laboratory matched very closely to the actual reaming tool.

The results for the measured deformation of CFR PEEK implant are presented in Table 5.7. The results show the smallest amount of deformation and are similar to previous research on MOM monobloc implants (Jin, 2006) and metal implants (Squire et al., 2006b). The much larger diametric clearance, however, does lead to the risk of the

implant deforming above the clearance and causing femoral clutching. Like all previous cadaveric experiments, engineer's blue was used on the matching femoral head and demonstrated freedom of movement.

Table 5.7: Deformation and expansion results for fourth cadaveric experiment

Cup Size [mm]	Head Articulated	Dome Contact	Laser Scan Results [mm]	
			Max Deformation	Max Expansion
***46/40**	YES	YES	-0.066	+0.067 +0.057
46/40	YES	YES	-0.01 -0.002	+0.269 +0.17
***54/48**	YES	YES	-0.13	+0.213
***50/44**	YES	YES	-0.017	+0.058 +0.119
50/44	YES	YES	-0.456 -0.353	+0.162 +0.102
54/48	YES	YES	-0.124 -0.062	+0.1 +0.095
54/48	YES	YES	-0.026 & -0.046	+0.001

*under reamed based on bone quality

This implant design is a press fit concept meaning the true size of the implant is different from the label. i.e. for 46mm outside diameter x 40mm inside diameter, the outside diameter measures 48mm at its widest point (Table 5.17). It is envisaged that depending on bone quality the surgeon would ream to 46mm and implant a 46mm shell, and the oversizing of the implant will provide the initial stability; in harder sclerotic bone the reaming parameter may change to accommodate the patient. This can be shown in specimen one, three and four where Dr Pace under reamed to 1mm instead of the standard 2mm. Figure 5.53 shows the implant fully seated accurately in the acetabulum. The surgeon commented that in all instances stability was excellent and that there was a definitive noise change during impaction and a responsive feel when the implant was seated correctly. This was verified by manually pushing the rim of the implant to check for any movement. Figure 5.54 shows a three dimensional representation of the fourth generation implant showing very little deformation has occurred.

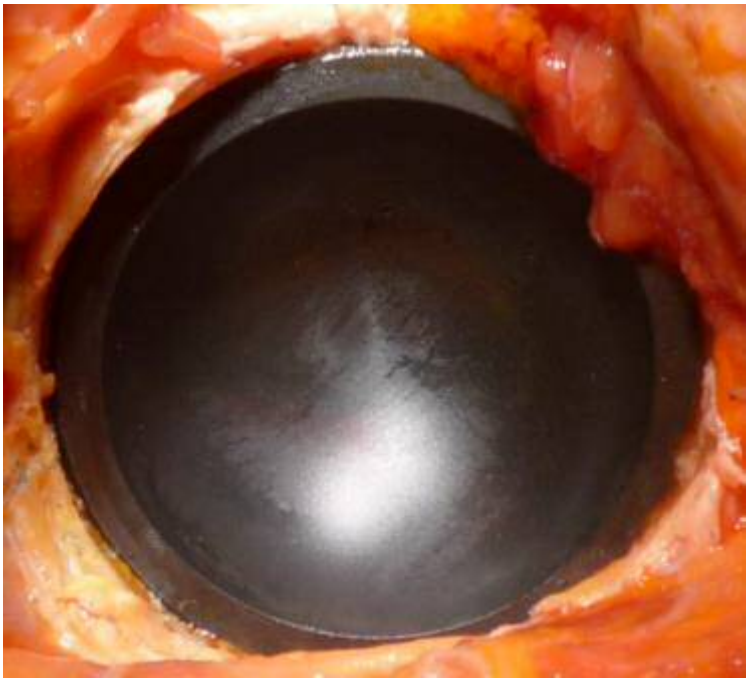

Figure 5.53: Fourth generation CFR PEEK monobloc implanted

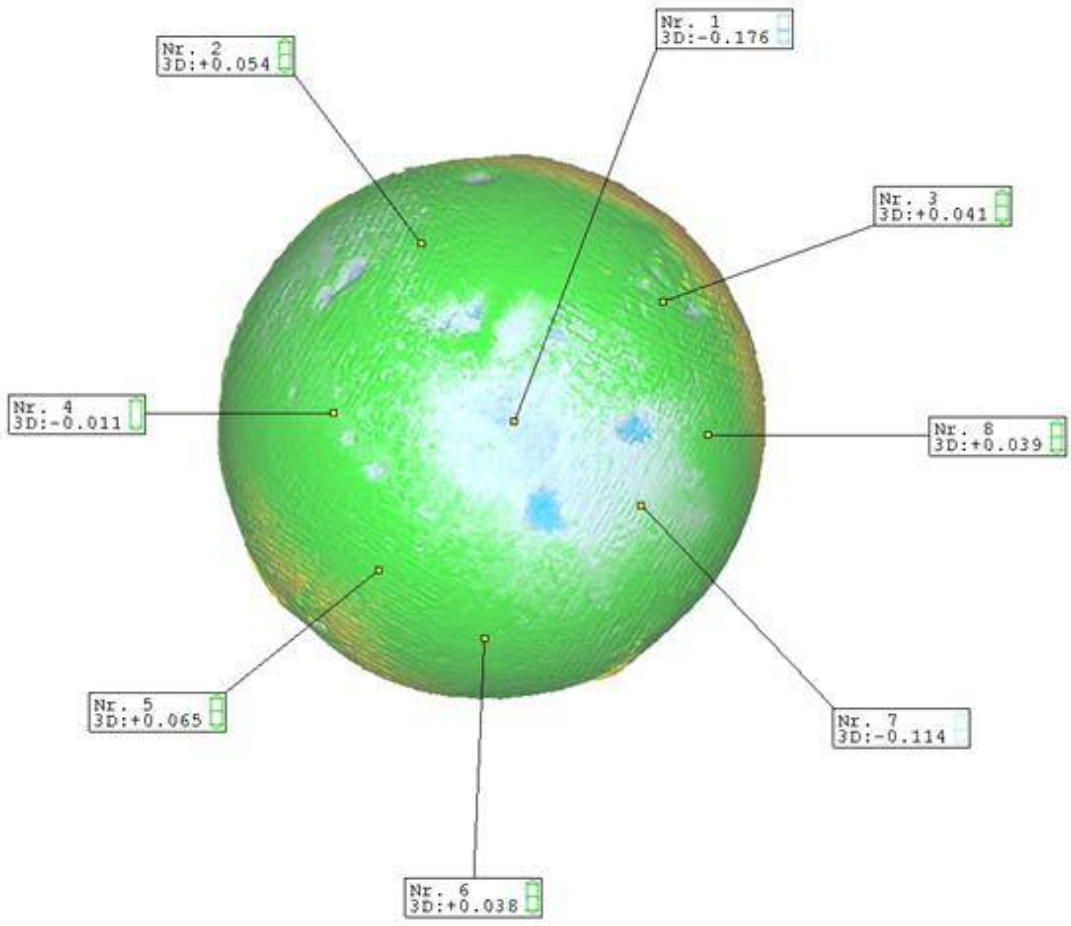

Figure 5.54: 3D scan of fourth generation CFR PEEK monobloc

5.5.3 Conclusion

Based on surgeon feedback and the results from this cadaveric experiment this is the optimal implant design to take forward to fatigue testing and further development. This design showed the lowest amount of deformation with excellent press fit and initial stability. While dental putty has been proven to be a successful moulding material, a liquid silicone may prove to be more reliable as this can fill all voids in the acetabulum and just as importantly not create air pockets which can create ambiguity in the results.

5.6 Chapter Conclusions

This chapter has presented the findings of four cadaveric experiments to investigate the evolving design of the CFR PEEK monobloc. Evolutions occurred due to the results of tribological and finite element analysis. The initial experiment focused on a hemispherical profile. Although the implants could be impacted into a prepared acetabulum large deformations occurred which would lead to problems in vivo. The second evolution did not undergo enough deformation to cause femoral clutching but fracture did occur making the implant unsuitable for real applications. A third evolution was created that reduced sharp corners to prevent fracture and introduced circumferential grooves. This design showed a reduction in deformation and importantly, no fractures. An excellent press fit was achieved in all implants without any concerns of fracturing the acetabulum or cup. The results of the press fit deemed the circumferential grooves redundant. The final evolution, with no grooves, demonstrated excellent results. There was the lowest amount of deformation, no fractures or femoral clutching and excellent press fit. This design was taken forward for further investigations.

6 Finite Element Analysis of the CFR PEEK Monobloc Cup

6.1 Introduction

It has been well documented that monobloc cups are susceptible to edge loading which occurs when the head–cup contact patch extends over the cup rim. Edge loading can lead to a loss of entrainment of synovial fluid resulting in a breakdown of the lubricating film and a large local increase in contact pressure. These can both directly lead to an increase in wear (Underwood et al., 2012, Langton et al., 2010).

A schematic showing the contact patch surrounding the Joint Reaction Force (JRF) vector is presented in Figure 6.1. The Contact Patch Edge to Rim (CPER) is described as the arc length between the edge of the contact patch and the true rim of the liner. A negative CPER Length implies the contact patch has passed over the true rim of the liner and that edge loading has occurred (Figure 6.1).

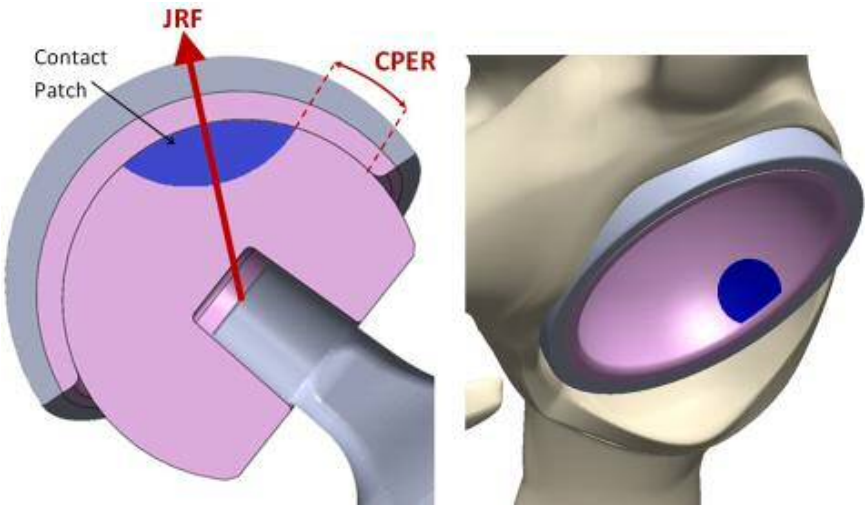

Figure 6.1: Contact patch edge to rim (CPER) (Jim W. Pierrepont et al., 2014)

The failure rates and mechanics behind this have been documented by Morlock et al. (2008). It has been shown that mal positioning of the implant results in revisions due to the failure of the implant and patients with implant-bone impingement, soft tissue impingement or painful local tissue reactions to high rate of wear (De Haan, Campbell et al. 2008). This issue does not arise solely in MoM implants but is also seen in CoC with direct correlation to cup inclination and edge loading (Walter et al., 2004, Sariali et

al., 2010). The outcome of this and the failure rates have made it one of the most active research areas in hip arthroplasty.

The aim of this study was to analyse a monobloc acetabular cup in a virtual implant simulation, where implant material, design parameters, position and orientation in a patient specific pelvic bone could be altered. In addition, an aim was to analyse the distribution of stresses, strains and strain energy density (SED) in both implant and defined regions of the pelvic bone. The implant model and Finite Element Analysis (FEA) parameters were created and submitted to Continuum Blue Ltd to complete the investigation. This Chapter presents an analysis of those FEA results.

6.2 Experimental Procedure

Prior to an FEA analysis being completed a model implant was created using Unigraphics NX 7 (Figure 6.2). This model was then inserted into an established pelvic model (Figure 6.3). Specified material properties, boundary conditions and geometry were supplied to Continuum Blue Ltd to perform the FEA. A 74 year old male was selected for the model (Table 6.1).

Figure 6.2: CFR PEEK Monobloc Ø56 x 62mm

Figure 6.3: 3D model assembly

Table 6.1: Selected characteristics for model parameters

Age	Gender	Weight	Height	Ethnicity
74	Male	75.74Kg	1.68m	Caucasian

Two finite element models for this analysis were completed, a preoperative intact model and a postoperative implanted model. The preoperative intact model investigated the implanted bone Strain Energy Density (SED) values and assessed bone remodelling for the parameters specified. The largest, thinnest implant was selected; Ø56 x 62mm as a base line. The implant was assembled to the pelvis in the optimum implant position that would be expected *in vivo.* This was at 45º inclination and 20º antiversion (Grammatopoulos et al., 2010). A stair climbing load case was applied to both the intact and implanted models (Heller et al., 2005, Bergmann et al., 2001). One intact case and fifty virtually implanted design scenarios were assessed. Specified parameters were:

- External cup radius, or major radius (32mm – 33mm)
- Internal cup radius (28.08mm – 28.275mm)
- Inclination angle (30º – 60º)
- Anteversion angle (0º – 25º)
- Cup Material (CFR PEEK, UHMWPE, CoCrMo, Biolox® Delta)

- Ultra High Molecular Weight Poly Ethylene
- Cobalt chromium molybdenum alloy
- Biolox® Delta ceramic is the brand name for Zirconia Platelet Toughened Alumina and is a fourth generation ceramic supplied by CeramTec

The material properties are presented in Table 6.2. These are required to create an accurate model and examine the way the implant will perform. Table 6.3 shows the parameters that include changes to the internal diameter, the outside diameter, the material, cup inclination and cup anteversion. Incorrect cup inclination in large MoM joints has been shown to increase wear and cause early failures thus leading to revision (De Haan et al., 2008, Shimmin et al., 2008, Williams et al., 2008, Langton et al., 2010, Underwood et al., 2012, Mellon et al., 2015). It is well document that an increased inclination can lead to edge loading; the purpose of adding these parameters is to see if cup inclination and anteversion affect the implant.

Table 6.2: Material Properties

Material	Young's Modulus [GPa]	Poisson's Ratio	Yield Stress [MPa]	UTS [MPa]
CFR PEEK	12	0.41	98	98
UHMWPE	1.29	0.38	23.9	46.8
Biolox® Delta	350	0.22	4700	-
CoCrMo	241	0.30	450	655

6.3 Results and Discussion

It has been demonstrated that von Mises stress, strain and SED in bone can be used as a useful indicator to predict bone remodelling (Van Rietbergen et al., 1993, Kerner et al., 1999, Bitsakos et al., 2005). Four regions of interest, around the acetabulum, as shown in Figure 6.4 were selected for analysis.

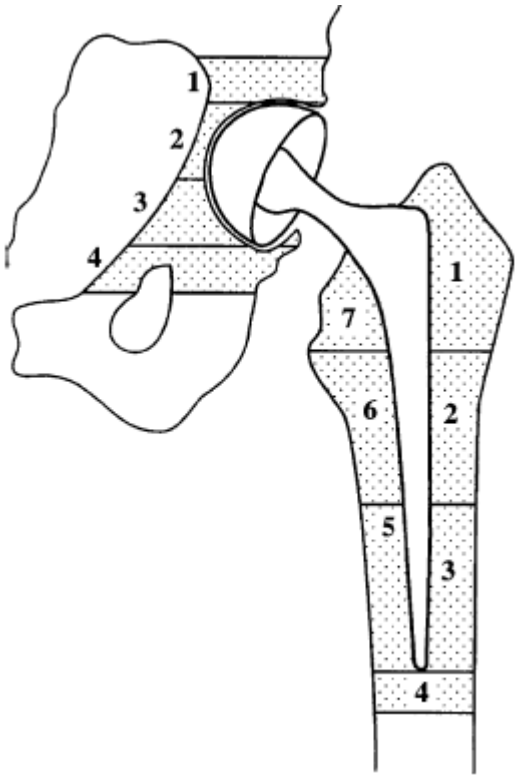

Figure 6.4: Line drawing showing placement of seven femoral and four pelvic bone mineral density (BMD) analysis regions of interest (ROI) (Wilkinson et al., 2003).

Table 6.3: Model scenarios and parameters

Scenario	Major Radius [mm]	Internal Radius [mm]	Alpha [°]	Beta [°]	Material
1	32	28.275	60	25	CFR PEEK
2	32	28.275	60	15	CFR PEEK
3	32	28.275	60	0	CFR PEEK
4	32	28.275	50	25	CFR PEEK
5	32	28.275	50	15	CFR PEEK
6	32	28.275	50	0	CFR PEEK
7	32	28.275	45	25	CFR PEEK
8	32	28.275	45	15	CFR PEEK
9	32	28.275	45	0	CFR PEEK
10	32	28.275	30	25	CFR PEEK
11	32	28.275	30	15	CFR PEEK
12	32	28.275	30	0	CFR PEEK
13	32	28.275	60	25	CFR PEEK
14	32	28.275	60	15	CFR PEEK
15	32	28.275	60	0	CFR PEEK
16	32	28.275	50	25	CFR PEEK
17	32	28.275	50	15	CFR PEEK
18	32	28.275	50	0	CFR PEEK
19	32	28.275	45	25	CFR PEEK
20	32	28.275	45	15	CFR PEEK
21	32	28.275	45	0	CFR PEEK
22	32	28.275	30	25	CFR PEEK
23	32	28.275	30	15	CFR PEEK
24	32	28.275	30	0	CFR PEEK
25	32	28.275	60	25	CoCrMo
26	33	28.275	60	25	UHMWPE
27	33	28.275	60	15	CoCrMo
28	33	28.275	60	15	UHMWPE
29	33	28.275	60	0	CoCrMo
30	33	28.275	60	0	UHMWPE
31	33	28.275	45	25	CoCrMo
32	33	28.275	45	25	UHMWPE
33	33	28.275	45	15	CoCrMo
34	33	28.275	45	15	UHMWPE
35	33	28.275	45	0	CoCrMo
36	33	28.275	45	0	UHMWPE
37	33	28.275	30	25	CoCrMo
38	33	28.275	30	25	UHMWPE
39	33	28.275	30	15	CoCrMo
40	33	28.275	30	15	UHMWPE
41	33	28.275	30	0	CoCrMo
42	33	28.275	30	0	UHMWPE
43	33	28.275	60	25	Biolox Delta
44	33	28.275	30	0	Biolox Delta
45	33	28.275	45	25	Biolox Delta
46	33	28.275	60	0	Biolox Delta
47	33	28.08	60	25	Biolox Delta
48	33	28.08	30	0	Biolox Delta
49	33	28.08	45	25	Biolox Delta
50	33	28.08	60	0	Biolox Delta

Both intact and virtual implant FEA models have had a stair climbing load case applied to them based on Heller et al. (2001). Intact and virtual implant models have been used in other studies in the same manner (Oonishi et al., 1983, Phillips et al., 2007, Kluess et al., 2009). The intact model was used as a benchmark for comparison with the implanted bone SED; this was used to evaluate the virtual bone remodelling stimulus which was then used to predict bone resorption or deposition (Huiskes et al., 1992, Anderson et al., 2010). Bone resorption effectively is bone loss through several factors, but in this study caused by stress shielding, while bone deposition is bone growth due to increased stress. In each of the parameter analyses the displacement, strain, von Mises stress and maximum principal stress were also assessed as shown in Figure 6.5.

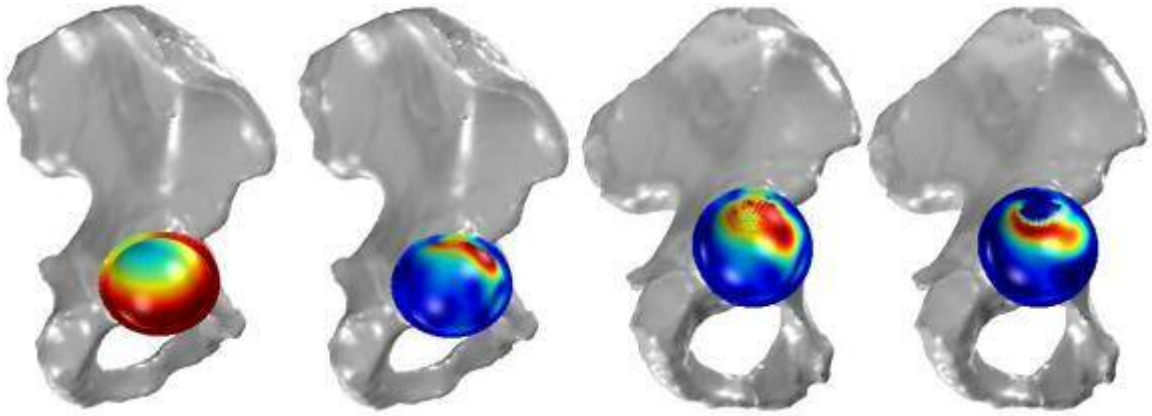

Figure 6.5: Examples of displacement, strain, von Mises stress and first principal stress.

From the virtual implant design scenarios assessed, the following observations were made:

- Increasing cup thickness reduced cup average von Mises stress, as expected.
- Increasing cup inclination angle increased cup average von Mises stress which would imply that some edge loading occurred.
- Increasing cup anteversion angle decreased cup average von Mises stress, the author has spoken to several surgeons who use CoC, whereby they modify their inclination and anteversion to prevent squeaking, reducing inclination to 30° and anteversion to 15° (Walter et al., 2007).
- Cup material properties played a major role in determining bone strain energy density (SED) response, where for the bone regions of interest assessed:
    - Low modulus materials, such UHMWPE & CFR PEEK better matched the pre-operative intact model bone stress-strain distributions.

- High modulus materials such as CoCrMo and Biolox gave typically lower SED magnitudes, increasing the likelihood of bone resorption.

- The max von Mises stress was on average over 40 times lower than the cup's material yield strength, where the lowest safety factors of maximum von Mises stress to material yield strength observed were found to be 2.26 for UHMWPE and 3.93 for CFR PEEK cup design.

Figure 6.6 represents the maximum deformation and expansion between the ischial and ilium column based on the FEA model for scenario 1 in Table 6.3. The blue dotted line represents the original cup shape and the solid line the deformation from that shape.

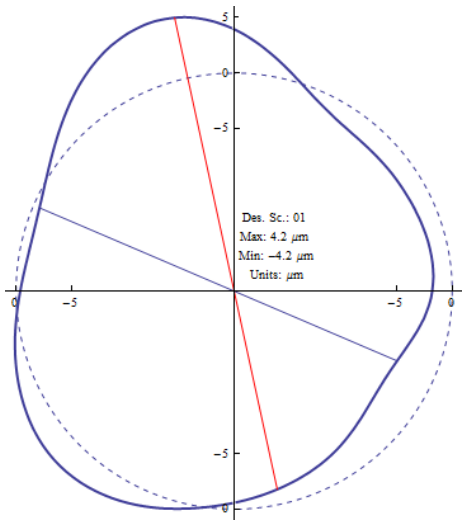

Figure 6.6: Deformation plot for Scenario 1

Using the deformation plots (Figure 6.6) for each scenario (Table 6.2) a graph of maximum deformation and expansion could be created (Figure 6.7). The y-axis represents the maximum observed deflection and expansion whilst the x-axis is linked to a specific set up parameters (scenario) from Table 6.2. All plots in this section follow this approach. For CFR PEEK scenario 22 presented the largest deformation and expansion -8.1μm and 9.6μm respectively, with scenario 15 presenting the least amount of deformation and expansion, -3.1 μm and 5.0 μm respectively. Interestingly the lowest amount of deformation came from the cup being implanted at a much greater angle than is acceptable (60º). This angle has been shown to cause edge loading on MoM implants (Underwood et al., 2012). The optimum implant placement is an inclination of 40º to 45º and anteversion of 15º to 20º. Scenarios 7, 8, 19 and 20 show consistent measurements and suggest optimum implant placement. All of the deformations fell

within the limits described in literature (Squire et al., 2006a, Fritsche et al., 2008, Jin, 2006, Markel et al., 2011).

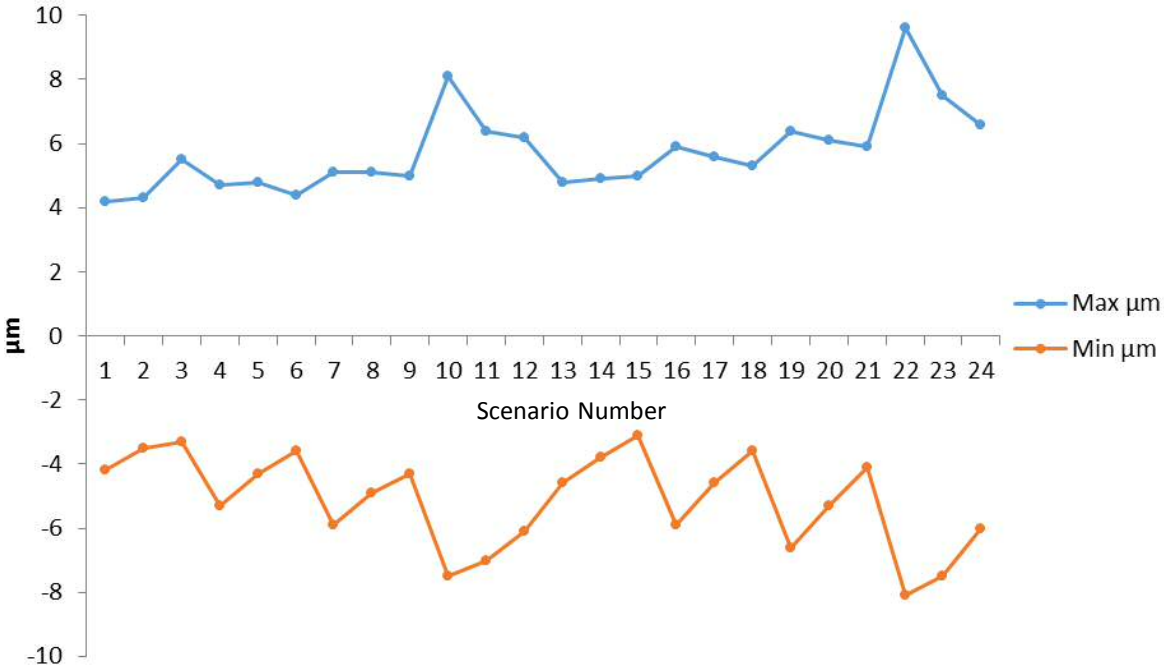

Figure 6.7: Maximum deformation and expansion for scenarios CFR PEEK

Figure 6.8 represents the maximum deformation and expansion between the ischial and ilium column based on the FEA model for the UHMWPE material scenarios (Table 6.3).

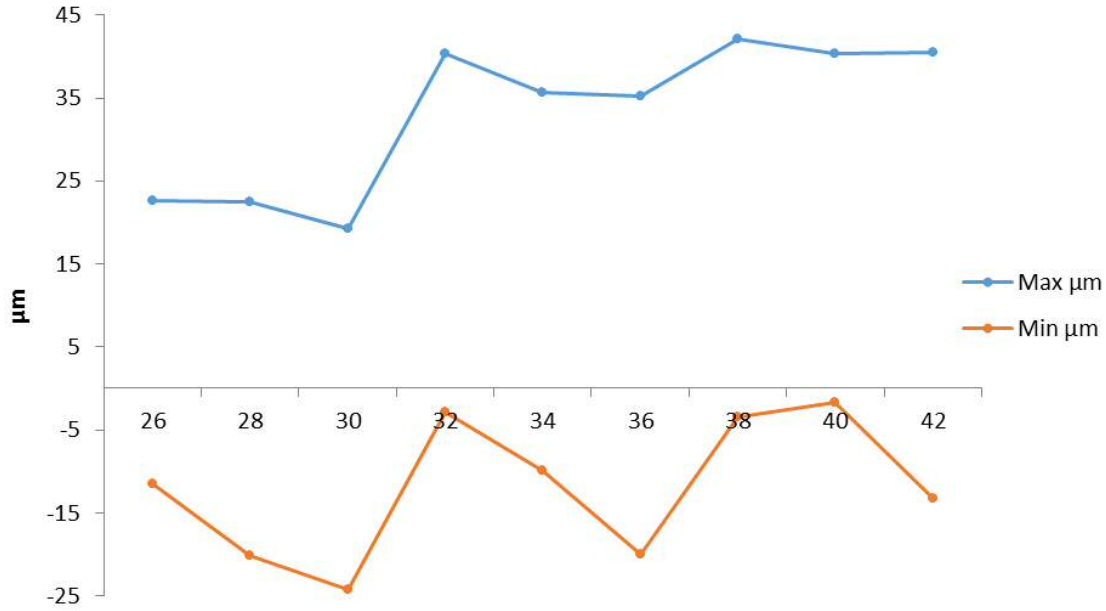

Figure 6.8: Maximum deformation and expansion for UHMWPE material for scenarios 26 to 42.

The UHMWPE cup was shown to exhibit the greatest amount of deformation and expansion of the four materials. CoCrMo and Biolox Delta ceramic implants are referred to as hard bearings and UHMWPE is referred to as a soft bearing so it would be expected that this material would exhibit the highest amount of deformation. UHMWPE monobloc constructs are used clinically, with great success, however they tend to have smaller head sizes to accommodate more material to support the construct under deformation and creep (Wyss et al., 2013, Lafon et al., 2014). UHMWPE was selected to compare soft and hard bearings and to assess bone resorption and deposition. The results suggest that UHMWPE, in this design, in vivo would lead to early failure due to the thin wall thickness of the implant.

Figure 6.9 represents the maximum deformation and expansion between the ischial and ilium column based on the FEA model. Table 6.3 shows the parameters selected for analysis.

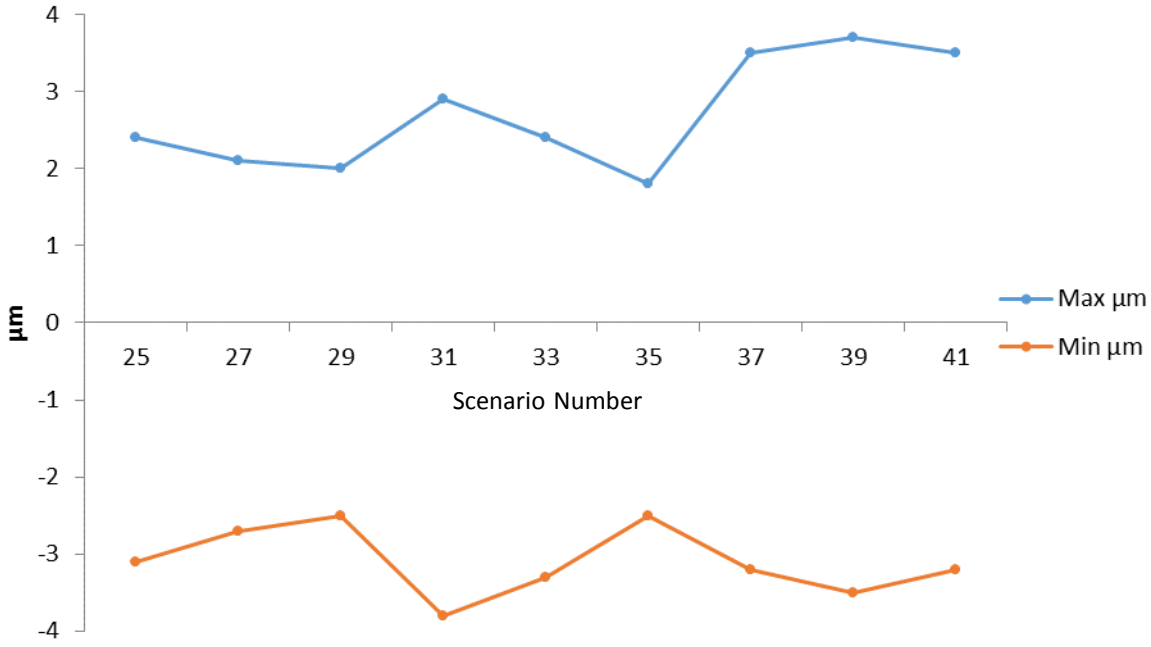

Figure 6.9: Maximum deformation and expansion for CoCrMo material

As expected the CoCrMo exhibited very low deformation and expansion measurements, when compared with other materials. Scenario 39 (Table 6.3) shows that the implant was most affected at cup inclination and anteversion of 30º and 15º with deformation of -3.5µm and expansion 3.7µm respectively.

Figure 6.10 represent the maximum deformation and expansion between the ischial and ilium column based on the FEA model. Table 6.3 presents the parameters selected to investigate for shows the Biolox Delta material.

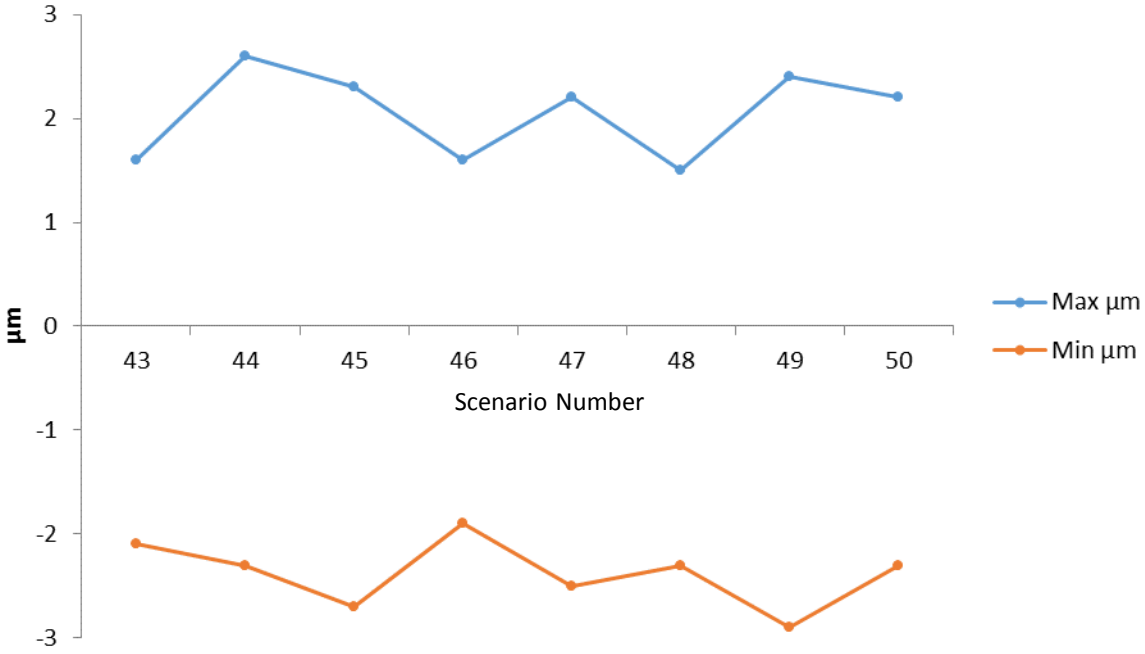

Figure 6.10: Maximum deformation and expansion for Biolox Delta material

6.4 Conclusion

The aim of this chapter was to predict how the CFR PEEK Monobloc would perform under advised implant positions within the acetabulum and also implant positions which have been documented to cause early implant failure. This allowed an understanding of the effect this had on the implant and how it performed under specific worst case gait analysis. The additions of three clinically validated materials were assessed in the parameters to compare material properties. The results of the analysis of the differing materials appear in line with literature and this provides confidence in the results (Kroeber, Ries et al. 2002, Squire, Griffin et al. 2006, Tarigopula, Hopperstad et al. 2007, Fritsche, Bialek et al. 2008, Hothan, Huber et al. 2011, Meding, Small et al. 2013). This study also provides strong confidence that the selected material CFR PEEK will not have excessive deformation, if installed at correct angles. It also suggested that the stress levels are sufficiently low that early fracture would not occur. The results demonstrated in the FEA analysis are consistent with the findings from the cadaveric experiments. The author's findings from the cadaveric experiments have validated the FEA analysis.

7 Dynamic Fatigue Testing

7.1 Introduction

Dynamic fatigue testing was undertaken to evaluate the effect of loading on the CFR PEEK Monobloc in an in-vivo simulated environment. In THA the acetabular system receives the same load as the femoral component but in the opposing direction. Based on the FEA conducted in Chapter 6 the largest and thinnest CFR PEEK Monobloc cups represented the worst case scenario as the stresses were higher in the Ø56 x 62 mm shells.

7.2 Experimental Procedure

Prototype Monobloc cups were machined on a mill/turn CNC machine from CFR PEEK NNS. The cups were then coated with Biomet's proprietary porous plasma sprayed titanium coating as shown in Figure 7.1. These cups introduced a completely novel feature, locking screws for improved fixation.

Figure 7.1: CFR PEEK Monobloc with screw holes

The screw-hole threads are a custom design which minimises the use of sharp corners that are seen on traditional and standard ISO threads. The screw holes include a taper geometry to prevent them becoming loose under load, as shown in Figure 7.2. In addition a frangible element has been included to provide versatility to the surgeon.

Figure 7.2: Screw holes with tapered geometry and frangible elements

Biomet's 56mm magnum heads were used in this investigation. Metal heads were used as opposed to ceramic heads which will be used to articulate against the CFR PEEK Monobloc. At the completion of testing ceramic heads were not available. The metal heads had the correct geometry and a similar stiffness to the ceramic cups so were expected to generate similar stresses in the cup. Table 7.1 summarises the materials used in the fatigue investigation.

Table 7.1: Materials required for testing

Description	Material	Quantity
62mm x 56mm Monobloc cup	CFR PEEK	3
56mm Magnum head	CoCr	3
Type 1 taper spigot	Ti-6Al-4V	3

As no standard currently exists for the examination of CFR PEEK the dynamic fatigue testing is derived from ASTM F2068-09; standard specification for femoral prostheses – metallic implants and BS ISO 7206-4; determination of endurance properties and performance of stemmed femoral components.

The Monobloc shell was mounted at a 60º loading angle. This is the most severe loading regime as the load is applied close to the edge of the cup, the thinnest part of the implant and the angle means the load is directly applied to the screw holes. The implants were secured in a potting fixture using Devcon aluminium liquid as shown in Figure 7.3. The potting fixtures were left to cure at room temperature for 24 hours. This ensured that the CFR PEEK Monobloc did not migrate during testing. The cups were also positioned with the screw holes at the lower side, corresponding to the anatomical superior

position, to ensure head contact is achieved. For in vivo use the screw holes would be superiorly for screw fixation into the ilium, for additional fixation, and the test replicates this since it is carried out in an inverted position.

Figure 7.3: CFR PEEK Monobloc in Fatigue Fixture

Three specimens were loaded into the tank as shown in Figure 7.4. The fatigue fixture was screwed to the tank base for stability and safety (Figure 7.4). The heads were then assembled to the titanium spigots; fine adjustment was need to ensure that all three heads were now in contact with each shell as shown in Figure 7.5. A 25kN Losenhausen fatigue machine with an MTS FlexTest controller was used for loading the three cups. The fatigue fixture was clamped to the bed of the machine using toolmaker's clamps and the head was loaded on to the fixture (Figure 7.6).

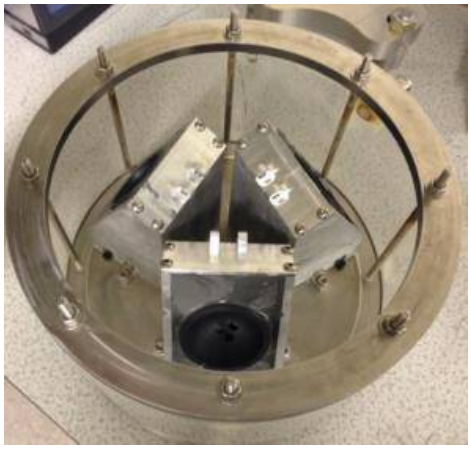

Figure 7.4: Three components loaded into fatigue fixture

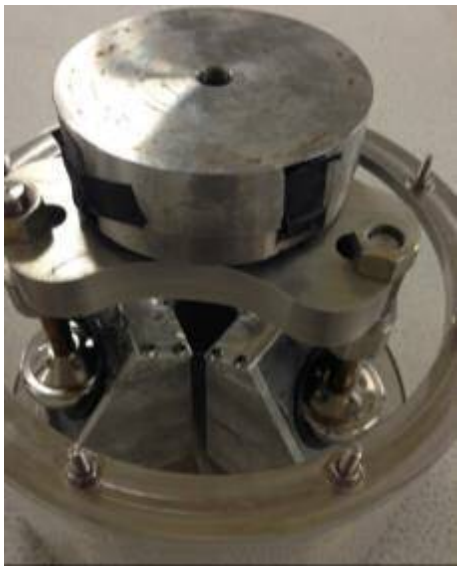

Figure 7.5: Completed fatigue fixture setup

Figure 7.6: Finished fatigue test set-up

The fatigue fixture was filled with deionized water and saline solution (9 grams per litre) which was maintained at 37ºC± 2ºC to simulate physiological condition. A water heater was used to maintain temperature in conjunction with a pump (Figure 7.7) to recirculate the water. The fluid level was maintained during the test to ensure the implants were fully submerged.

Figure 7.7: Water bath and recirculating pump

Load was applied sinusoidally at a frequency of 5Hz for 20 million cycles. This represents 20 years of in vivo use of the implant. Standards (intended for metal implants) require a frequency of loading of 10Hz, however 5Hz was selected to avoid any potential heating of the polymer and incur any thermal changes to the material (Brillhart and Botsis, 1992, Brillhart et al., 1991). It is noted in the literature that CFR PEEK & PEEK display excellent thermomechanical properties (Kurtz and Devine, 2007, Sınmazçelik and Yılmaz, 2007) meaning the frequency should not be an issue but as this was not a certification test 5Hz was used.

7.3 Results and Discussion

After 20 million cycles the dynamic fatigue was completed, if at any point one or more of the cups had failed a limit trip based on deformation would have halted the loading. All CFR PEEK Monobloc cups passed the test with no fractures or damage to the implant or the femoral head as shown in Figure 7.8.

Figure 7.8: CFR PEEK Monobloc post dynamic fatigue

Dynamic fatigue testing has been used for many years to assess the fatigue properties of materials and acetabular components. Studies have shown since the early 1990's that CFR PEEK is a suitable material for bearing surfaces (Kurtz and Devine, 2007). However, to the author's knowledge, there has only been one published document on dynamic fatigue testing of CFR PEEK monobloc cups (Latif et al., 2008a). The test performed by Latif et al. was completed at 25Hz for 10 million cycles with no failure or damage to the implant.

Notch sensitivity, within this thesis (Chapter 5) and the literature (Williams et al., 1987, Nisitani et al., 1992, Teoh, 2000) has been shown to be problematic in CFR PEEK. The design of the implant with threads deliberately included no chamfers or sharp corners, reducing the risk of fatigue failure through notch sensitivity. Visual analysis of the tested components confirmed no cracks present in the thread regions.

It was noted during the visual inspection that wear was present on the surface of the femoral heads. The black radial impressions (Figure 7.9) on the femoral head are due to the machining process during manufacture. These impressions were only noticed when the bond between the femoral head and the cup was broken, post-test. The impressions occur when there is a high contact pressure and adhesive wear occurs, as has been shown in previous tests (Langohr et al., 2011, Wang et al., 2012). This will have been more prevalent in these samples as the surface finish was achieved using conventional turning methods. The final implant will have a highly polished injection moulded surface with the fibres following the cup geometry meaning this adhesive wear would not occur.

Figure 7.9: Adhesive wear pattern

7.4 Conclusion

The aim of this chapter was to assess the fatigue properties of a large bearing monobloc with screw holes manufactured from CFR PEEK. The specimens all passed the testing with no damage or fracture to the implants, however adhesive wear was noted. This has been a novel test with little evidence of previously completed investigations of this duration. Further testing needs to be undertaken on injection moulded parts with fibre orientation playing an important part in the performance.

8 Discussion

This newly designed CFR PEEK Monobloc offers the ability to use anatomically sized femoral heads which helps with joint stability and reduces the risk of subluxation and dislocation which has been a concern in other constructs as they are unable to provide optimum head to cup ratio.

The highly polished bearing surface, which will be injection moulded, has shown a reduction of approximately 60% in friction factor when compared with an unpolished surface. The unpolished surface had similar surface roughness to that of the Mitch and ABG II implants. The polished surface will improve frictional torque, which will prevent implant loosening and hence prematurely failure. It has also been demonstrated through FEA that due to the material, design and clearance, the implant is not adversely affected by edge loading which has been shown to occur in MoM implants when the inclination has not been correctly achieved by the surgeon. Unlike traditional monobloc constructs, this prosthesis has the ability to utilise screws directly into the bearing surface for secondary fixation which is novel.

Tribology investigations showed that the final design achieved the optimum clearance for bearing performance and longevity with friction factors comparable to those of existing bearing materials. However, this material allows direct injection moulding improving manufacturing time, reduced costs and improved accuracy in final tolerances. In addition, thinner constructs can be created which allows less bone stock to be removed from the patient. Finally the opportunity to include screw fixation directly into the bearing surface is now an option.

Previous constructs were manufactured from materials such as CoCrMo which by the nature of the material created stiff constructs which were difficult to implant and seat correctly into the acetabulum. This also has an impact on the bone remodelling which leads to bone resorption which can affect the longevity of the implant. Using the developed construct, with its more flexible material, allows for a thinner walled construct which can make it easier to implant. In addition, FEA has demonstrated that bone remodelling could take place which may improve the longevity of the patient's prosthesis. Edge loading is fundamental to the longevity of implants. Incorrect

inclination and anteversion insertion leads to increased wear which will ultimately cause premature failure. The completed FEA demonstrated that there are limited stresses in the acetabulum and in the new prosthesis when implanted through a range of inclinations and anteversion.

In addition to FEA results, cadaveric studies demonstrated that the outside profile and radial clearance showed very small amounts of displacement on impaction. Displacement greater than the radial clearance can cause clutching of the femoral head which can cause several problems which include the interruption of the fluid lubrication regime which increases friction and increased wear which leads to early failure, it can also lead to high torque which can rip the implant from the acetabulum.

One of the major constraints in monobloc designs is that there is no option for secondary fixation such as screws. The material selected along with the design allows the surgeon the option to asses' bone quality and implant stability during surgery and utilise the novel design of introducing locking screws for additional stability.

In summary the research in this thesis has addressed a large number of critical issues associated with the functionality, longevity and adaptability of hip prosthesis for total hip replacements. On completion of this thesis Zimmer Biomet have invested over £100k to manufacture injection moulding tools and further validation work is underway.

9 Conclusions and Future Work

9.1 Conclusions

Providing an orthopaedic prosthesis that can be implanted into a patient and meet the daily demands, whilst lasting for tens of years requires several key developments to ensure that it can improve the patient's life and restore natural hip mobility.

The main findings of this extensive study are as follows:

- A new cup was developed using CFR PEEK
- Tribological testing demonstrated that the CFR PEEK cup with a ceramic head produced consistent results with low friction and a large envelope for the radial clearance.
- Polishing the surface reduced the friction factor by up to 63% whilst producing friction factor results similar to those for proven materials such as polyethylene.
- Cadaveric experiments helped to determine the outside and inside geometry of the final implant by means of analysing deformation and implant impaction and seating, deformation and fracture were minimised.
- Finite element analysis further supported the deformation results and demonstrated that the CFR PEEK is less susceptible to damage due to edge loading unlike hard bearings such as CoC and MoM.
- Dynamic fatigue testing of the prosthesis demonstrated no adverse effects or fatigue failures after loading representing 20 years in vivo use.

9.2 Further work

Whilst a large amount of work has been undertaken, and significant advancements have been made to bring the prosthesis to where it is now, further work needs to be completed. Due to the cost of injection moulding tools all work has been completed on machined cups. All the completed practical investigations need to be repeated using an injection moulded cup. Further work should focus on tribology testing to validate the surface finish and also wear testing is needed to assess the wear properties of an injection moulded component. Whilst the ABG II and Mitch prosthesis were injection moulded the bearing surface was machined afterwards. To the author's knowledge this

will be the first prosthesis to be fully injection moulded without any machining of the bearing surface. Although the screws have been designed, they need to be validated through physical testing. In addition, fatigue testing with the screws in place needs to be completed. Based on these results, the screw hole positioning and the number of screw holes should be explored, especially screw hole positioning into the periphery of the implant as this could further benefit the patient in severe revision cases.

10 References

*MANLEY, M. T. O., K L; **#KURTZ, S M; ***RUSHTON, N, ##FIELD, R E 2007. • BIOMECHANICS OF A PEEK HORSESHOE-SHAPED CUP : COMPARISONS WITH A PREDICATE 53rd Annual Meeting of the Orthopaedic Research Society Poster No : 1717. Society, 1717-1717.

AAOS. 2012. Current Concerns with Metal-on-Metal Hip Arthroplasty [Online]. American Academy of Orthopaedic Surgeons. Available: http://www6.aaos.org/news/PDFopen/PDFopen.cfm?page_url=http://www.aaos.org/about/papers/advistmt/1035.asp [Accessed 11th April 2015 2015].

AL-HAJJAR, M., LESLIE, I. J., TIPPER, J., WILLIAMS, S., FISHER, J. & JENNINGS, L. M. 2010. Effect of cup inclination angle during microseparation and rim loading on the wear of BIOLOX(R) delta ceramic-on-ceramic total hip replacement. J Biomed Mater Res B Appl Biomater, 95, 263-8.

ALEXANDER, J. W., KAMARIC, E. & NOBLE, P. C. The accuracy of acetabular reaming in total hip replacement. 45th annual meeting of the orthopaedic research society, 1999 Anaheim, CA. 906.

ANDERSON, A. E., ELLIS, B. J., MAAS, S. A. & WEISS, J. A. 2010. Effects of idealized joint geometry on finite element predictions of cartilage contact stresses in the hip. J Biomech, 43, 1351-7.

ANDERSON, A. E., PETERS, C. L., TUTTLE, B. D. & WEISS, J. A. 2005. Subject-specific finite element model of the pelvis: development, validation and sensitivity studies. J Biomech Eng, 127, 364-73.

AUGER, D. D., DOWSON, D., FISHER, J. & JIN, Z. M. 1993. Friction and lubrication in cushion form bearings for artificial hip joints. Proc Inst Mech Eng H, 207, 25-33.

AVANZINI, A., DONZELLA, G., GALLINA, D., PANDINI, S. & PETROGALLI, C. 2013. Fatigue behavior and cyclic damage of peek short fiber reinforced composites. Composites Part B: Engineering, 45, 397-406.

BARINK, M., VAN KAMPEN, A., DE WAAL MALEFIJT, M. & VERDONSCHOT, N. 2005. A three-dimensional dynamic finite element model of the prosthetic knee joint: simulation of joint laxity and kinematics. Proc Inst Mech Eng H, 219, 415-24.

BEAVER, R., MCCORMICK, C. & KOP, A. 2002. 2.3 Fractures in Misaligned Ceramic Acetabular Liners: A Laboratory Study. Bioceramics in Joint Arthroplasty: Proceedings, 65.

BERGMANN, G., DEURETZBACHER, G., HELLER, M., GRAICHEN, F., ROHLMANN, A., STRAUSS, J. & DUDA, G. N. 2001. Hip contact forces and gait patterns from routine activities. J Biomech, 34, 859-71.

BEVILL, S. L., BEVILL, G. R., PENMETSA, J. R., PETRELLA, A. J. & RULLKOETTER, P. J. 2005. Finite element simulation of early creep and wear in total hip arthroplasty. J Biomech, 38, 2365-74.

BICHARA, D. A., MALCHAU, E., SILLESEN, N. H., CAKMAK, S., NIELSEN, G. P. & MURATOGLU, O. K. 2014. Vitamin E-diffused highly cross-linked UHMWPE

particles induce less osteolysis compared to highly cross-linked virgin UHMWPE particles in vivo. J Arthroplasty, 29, 232-7.

BIOMET. 2014. G7 Bispherical Acetabular System Brochure.

BIOMET 2015. G7 Bispherical surgical Technique.

BIRKINSHAW, C., JONES, E. & FLANAGAN, S. 2010. In vitro friction and lubrication of large bearing hip prostheses. Proceedings of the Institution of Mechanical Engineers, Part H: Journal of Engineering in Medicine, 224, 853-864.

BITSAKOS, C., KERNER, J., FISHER, I. & AMIS, A. A. 2005. The effect of muscle loading on the simulation of bone remodelling in the proximal femur. J Biomech, 38, 133-9.

BORRUTO, A. 2010. A new material for hip prosthesis without considerable debris release. Med Eng Phys, 32, 908-13.

BREKELMANS, W., POORT, H. & SLOOFF, T. 1972. A new method to analyse the mechanical behaviour of skeletal parts. Acta Orthop Scand, 43, 301-317.

BRILLHART, M. & BOTSIS, J. 1992. Fatigue fracture behaviour of PEEK: 2. Effects of thickness and temperature. Polymer, 33, 5225-5232.

BRILLHART, M., GREGORY, B. L. & BOTSIS, J. 1991. Fatigue fracture behaviour of PEEK: 1. Effects of load level. Polymer, 32, 1605-1611.

BROCKETT, C., WILLIAMS, S., JIN, Z., ISAAC, G. & FISHER, J. 2007. Friction of total hip replacements with different bearings and loading conditions. J Biomed Mater Res B Appl Biomater, 81, 508-15.

BROCKETT, C. L., HARPER, P., WILLIAMS, S., ISAAC, G. H., DWYER-JOYCE, R. S., JIN, Z. & FISHER, J. 2008. The influence of clearance on friction, lubrication and squeaking in large diameter metal-on-metal hip replacements. J Mater Sci Mater Med, 19, 1575-9.

BROOKS, R. A., JONES, E., STORER, A. & RUSHTON, N. 2004. Biological evaluation of carbon-fibre-reinforced polybutyleneterephthalate (CFRPBT) employed in a novel acetabular cup. Biomaterials, 25, 3429-3438.

BURROUGHS, B. R., HALLSTROM, B., GOLLADAY, G. J., HOEFFEL, D. & HARRIS, W. H. 2005. Range of Motion and Stability in Total Hip Arthroplasty With 28-, 32-, 38-, and 44-mm Femoral Head Sizes: An In Vitro Study. The Journal of Arthroplasty, 20, 11-19.

CAPERAY. 2013. I Guarantee this Device Won't Fail! [Online]. Available: http://www.caperay.com/blog/index.php/2013/i-guarantee-this-device-wont-fail/ [Accessed].

CATELAS, I., WIMMER, M. & UTZSCHNEIDER, S. 2011. Polyethylene and metal wear particles: characteristics and biological effects. Seminars in Immunopathology, 33, 257-271.

CERAMTEC 2015. Biolox delta Scientfic Information and Performance Data.

CHEN, F., OU, H., LU, B. & LONG, H. 2016. A constitutive model of polyether-ether-ketone (PEEK). J Mech Behav Biomed Mater, 53, 427-33.

CHENG, H. 1984. Micro-elastohydrodynamic lubrication.

CHEVALIER, J. 2006. What future for zirconia as a biomaterial? Biomaterials, 27, 535-543.

CHEVALIER, J. & GREMILLARD, L. 2009. Ceramics for medical applications: A picture for the next 20 years. Journal of the European Ceramic Society, 29, 1245-1255.

CILINGIR, A. C., UCAR, V. & KAZAN, R. 2007. Three-Dimensional Anatomic Finite Element Modelling of Hemi-Arthroplasty of Human Hip Joint. 63-72.

COOKE, A. F., DOWSON, D. & WRIGHT, V. 1978. The rheology of synovial fluid and some potential synthetic lubricants for degenerate synovial joints. Eng. Med, 7, 66–72.

COX, M. A., DRIESSEN, N. J., BOERBOOM, R. A., BOUTEN, C. V. & BAAIJENS, F. P. 2008. Mechanical characterization of anisotropic planar biological soft tissues using finite indentation: experimental feasibility. J Biomech, 41, 422-9.

D'ANTONIO, J. A. & SUTTON, K. 2009. Ceramic materials as bearing surfaces for total hip arthroplasty. Journal of the American Academy of Orthopaedic Surgeons, 17, 63-68.

DALSTRA, M., HUISKES, R. & VAN ERNING, L. 1995. Development and validation of a three-dimensional finite element model of the pelvic bone. J Biomech Eng, 117, 272-8.

DANIEL, J., PYNSENT, P. B. & MCMINN, D. J. 2004. Metal-on-metal resurfacing of the hip in patients under the age of 55 years with osteoarthritis. J Bone Joint Surg Br, 86, 177-84.

DAVIM, J. P. & MARQUES, N. 2001. Evaluation of tribological behaviour of polymeric materials for hip prostheses application. Tribology Letters, 11, 91-94.

DE HAAN, R., CAMPBELL, P. A., SU, E. P. & DE SMET, K. A. 2008. Revision of metal-on-metal resurfacing arthroplasty of the hip: the influence of malpositioning of the components. J Bone Joint Surg Br, 90, 1158-63.

DELAUNAY, C., PETIT, I., LEARMONTH, I. D., OGER, P. & VENDITTOLI, P. A. 2010. Metal-on-metal bearings total hip arthroplasty: the cobalt and chromium ions release concern. Orthop Traumatol Surg Res, 96, 894-904.

DOWSON, D. & JIN, Z. M. 2006. Metal-on-metal hip joint tribology. Proc Inst Mech Eng H, 220, 107-18.

ESSNER, A., SUTTON, K. & WANG, A. 2005. Hip simulator wear comparison of metal-on-metal, ceramic-on-ceramic and crosslinked UHMWPE bearings. Wear, 259, 992-995.

EVERITT, H. 2011. Deformation on Impaction of a Large Diameter Carbon Fibre Reinforced Poly-Ether-Ether-Ketone Acetabular Cup and its Effects on the Tribology of the Bearing. Cardiff University.

FAM, H., BRYANT, J. T. & KONTOPOULOU, M. 2007. Rheological properties of synovial fluids. Biorheology, 44, 59-74.

FANG, H. W., YANG, C. B., CHANG, C. H., HUANG, C. H., LIU, H. L. & FANG, S. B. 2006. The potential role of phagocytic capacity in the osteolytic process induced by polyethylene wear particles. J Int Med Res, 34, 655-64.

FDA. 2008. Medical Devices - Recalls Specfic to Metal-on-Metal Hip Implants [Online]. FDA U.S Food and Drug Administration. Available: http://www.fda.gov/MedicalDevices/ProductsandMedicalProcedures/ImplantsandProsthetics/MetalonMetalHipImplants/ucm241770.htm [Accessed 11th April 2015].

FERGUSON, S. J., VISSER, J. M. & POLIKEIT, A. 2006. The long-term mechanical integrity of non-reinforced PEEK-OPTIMA polymer for demanding spinal applications: experimental and finite-element analysis. Eur Spine J, 15, 149-56.

FIELD, R. E., CRONIN, M. D., SINGH, P. J., BURTENSHAW, C. & RUSHTON, N. 2006. Bone remodeling around the Cambridge cup: a DEXA study of 50 hips over 2 years. Acta orthopaedica, 77, 726-732.

FIELD, R. E. & RUSHTON, N. 2005. Five-year clinical, radiological and postmortem results of the Cambridge Cup in patients with displaced fractures of the neck of the femur. J Bone Joint Surg Br, 87, 1344-51.

FISHER, J., ISAAC, G., JIN, Z. M., WILLIAMS, S. & BROCKETT, C. L. 2007. A comparison of friction in 28 mm conventional and 55 mm resurfacing metal-on-metal hip replacements. Proceedings of the Institution of Mechanical Engineers, Part J: Journal of Engineering Tribology, 221, 391-398.

FRITSCHE, A., BIALEK, K., MITTELMEIER, W., SIMNACHER, M., FETHKE, K., WREE, A. & BADER, R. 2008. Experimental investigations of the insertion and deformation behavior of press-fit and threaded acetabular cups for total hip replacement. J Orthop Sci, 13, 240-7.

GARLE, C. 2003. Use of a novel carbon fibre composite material for the femoral stem component of a THR system: in vitro biological assessment. Biomaterials, 24, 4871-4879.

GIANNIKAS, K. A., DIN, R., SADIQ, S. & DUNNINGHAM, T. H. 2002. Medium-term results of the ABG total hip arthroplasty in young patients. J Arthroplasty, 17, 184-8.

GOLDSMITH, A. A. J., DOWSON, D. & SMITH, S. L. 2001. The lubrication of metal-on-metal total hip joints: a slide down the Stribeck curve. Proceedings of the Institution of Mechanical Engineers, Part J: Journal of Engineering Tribology, 215, 483-493.

GOMEZ, P. F. & MORCUENDE, J. A. 2005. Early attempts at hip arthroplasty--1700s to 1950s. Iowa Orthop J, 25, 25-9.

GONZALEZ DELLA VALLE, A., SU, E., ZOPPI, A., SCULCO, T. P. & SALVATI, E. A. 2004. Wear and periprosthetic osteolysis in a match-paired study of modular and nonmodular uncemented acetabular cups. J Arthroplasty, 19, 972-7.

GRAMMATOPOULOS, G., PANDIT, H., GLYN-JONES, S., MCLARDY-SMITH, P., GUNDLE, R., WHITWELL, D., GILL, H. S. & MURRAY, D. W. 2010. Optimal acetabular orientation for hip resurfacing. J Bone Joint Surg Br, 92, 1072-8.

GREEN, S. 2011. Compounds and composite materials. PEEK Biomaterials Handbook, 23.

GRIMES, J. B. 2010. Does Deformation of Metal-On-Metal Acetabular Components Contribute to Early Failure? The Journal of Arthroplasty, 25, e21.

HAMILTON, W. G., MCAULEY, J. P., BLUMENFELD, T. J., LESKO, J. P., HIMDEN, S. E. & DENNIS, D. A. 2015. Midterm Results of Delta Ceramic-on-Ceramic Total Hip Arthroplasty. J Arthroplasty, 30, 110-5.

HAMROCK, B. J. & DOWSON, D. 1981. Ball bearing lubrication : the elastohydrodynamics of elliptical contacts, New York, Wiley.

HEATON-ADEGBILE, P., ZANT, N. P. & TONG, J. 2006. In vitro fatigue behaviour of a cemented acetabular reconstruction. J Biomech, 39, 2882-6.

HELLER, M. O., BERGMANN, G., DEURETZBACHER, G., DÜRSELEN, L., POHL, M., CLAES, L., HAAS, N. P. & DUDA, G. N. 2001. Musculo-skeletal loading conditions at the hip during walking and stair climbing. Journal of Biomechanics, 34, 883-893.

HELLER, M. O., BERGMANN, G., KASSI, J. P., CLAES, L., HAAS, N. P. & DUDA, G. N. 2005. Determination of muscle loading at the hip joint for use in pre-clinical testing. J Biomech, 38, 1155-63.

HENDRICH, C., ENGELMAIER, F., MEHLING, I., SAUER, U., KIRSCHNER, S. & MARTELL, J. M. 2007. Cementless acetabular reconstruction and structural bone-grafting in dysplastic hips. Surgical technique. J Bone Joint Surg Am, 89 Suppl 2 Pt.1, 54-67.

HOLZWARTH, U. & COTOGNO, G. 2012. Total Hip Arthroplasty State of the Art, Challenges and Prospects. JRC Scientific and Policy Reports, European Commission.

HOTHAN, A., HUBER, G., WEISS, C., HOFFMANN, N. & MORLOCK, M. 2011. Deformation characteristics and eigenfrequencies of press-fit acetabular cups. Clin Biomech (Bristol, Avon), 26, 46-51.

HOWLING, G. I., SAKODA, H., ANTONARULRAJAH, A., MARRS, H., STEWART, T. D., APPLEYARD, S., RAND, B., FISHER, J. & INGHAM, E. 2003. Biological response to wear debris generated in carbon based composites as potential bearing surfaces for artificial hip joints. J Biomed Mater Res B Appl Biomater, 67, 758-64.

HUISKES, R. & CHAO, E. Y. S. 1983. A survey of finite element analysis in orthopedic biomechanics: The first decade. Journal of Biomechanics, 16, 385-409.

HUISKES, R., WEINANS, H. & RIETBERGEN, B. V. 1992. The Relationship Between Stress Shielding and Bone Resorption Around Total Hip Stems and the Effects of Flexible Materials. Clinical Orthopaedics and Related Research, 274, 124-134.

HUNTER, A., ARCHER, C. W., WALKER, P. S. & BLUNN, G. W. 1995. Attachment and proliferation of osteoblasts and fibroblasts on biomaterials for orthopaedic use. Biomaterials, 16, 287-95.

IMAGES, C. 2002. Surgeon Mr Charnley Holds an artificial hip joint made from stainless steel and plastic. [Online]. Available: http://www.corbisimages.com/stock-photo/rights-managed/HU020087/mr-charnley-and-artificial-hip-joint [Accessed].

INGHAM, E. & FISHER, J. 2000. Biological reactions to wear debris in total joint replacement. Proc Inst Mech Eng H, 214, 21-37.

INSTITUTE, J. R. 2014. Hip Resurfacing/Replacment [Online]. Available: http://www.jri-docs.com/hip-resurfacing-replacement/ [Accessed 26th Spetember 2015 2015].

INVIBIO (2009) CFR PEEK Product brouchure

JIM W. PIERREPONT, M., ANDREW J. SHIMMIN, MBBS, FRACS2, JONATHAN V. BARÉ, MBBS, FRACS2, HANS FEYEN2, BRAD P. MILES,, PHD3., 1UNIVERSITY OF SYDNEY, S., AUSTRALIA, 2MELBOURNE ORTHOPAEDIC GROUP, MELBOURNE, AUSTRALIA, 3OPTIMIZED ORTHO, SYDNEY, & AUSTRALIA. 2014. An Investigation into the Dynamic Loading of Ceramic-on-Ceramic Total Hip Replacements and its Relevance to Squeaking. ORS 2014 Annual Meeting Poster No: 0868.

JIN, Z. M. 2006. Deformation of press-fitted metallic resurfacing cups. Part 1: experimental simulation. Proceedings of the Institution of Mechanical Engineers, Part H: Journal of Engineering in Medicine, 220, 299-309.

JIN, Z. M., STONE, M., INGHAM, E. & FISHER, J. 2006. (v) Biotribology. Current Orthopaedics, 20, 32-40.

JONES, D. P., LEACH, D. C. & MOORE, D. R. 1985. Speciality Polymers 84Mechanical properties of poly(ether-ether-ketone) for engineering applications. Polymer, 26, 1385-1393.

KATZER, A., MARQUARDT, H., WESTENDORF, J., WENING, J. V. & VON FOERSTER, G. 2002. Polyetheretherketone—cytotoxicity and mutagenicity in vitro. Biomaterials, 23, 1749-1759.

KERNER, J., HUISKES, R., VAN LENTHE, G. H., WEINANS, H., VAN RIETBERGEN, B., ENGH, C. A. & AMIS, A. A. 1999. Correlation between pre-operative periprosthetic bone density and post-operative bone loss in THA can be explained by strain-adaptive remodelling. Journal of Biomechanics, 32, 695-703.

KIM, Y. S., BROWN, T. D., PEDERSEN, D. R. & CALLAGHAN, J. J. 1995. Reamed surface topography and component seating in press-fit cementless acetabular fixation. J Arthroplasty, 10 Suppl, S14-21.

KLUESS, D., SOUFFRANT, R., MITTELMEIER, W., WREE, A., SCHMITZ, K. P. & BADER, R. 2009. A convenient approach for finite-element-analyses of orthopaedic implants in bone contact: modeling and experimental validation. Comput Methods Programs Biomed, 95, 23-30.

KONDO, Y., KOYAMA, T. & SASAKI, S. 2013. Tribological Properties of Ionic Liquids.

KROEBER, M., RIES, M. D., SUZUKI, Y., RENOWITZKY, G., ASHFORD, F. & LOTZ, J. 2002. Impact biomechanics and pelvic deformation during insertion of press-fit acetabular cups. J Arthroplasty, 17, 349-54.

KUNTZ, M. Validation of a new high performance alumina matrix composite for use in total joint replacement. Seminars in Arthroplasty, 2006. Elsevier, 141-145.

KUNTZ, M., SHNEIDER, N. & HEROS, R. 2005. Controlled zirconia phase transformation in BIOLOX® delta—a feature of safety. Bioceramics and Alternative Bearings in Joint Arthroplasty. Springer.

KURTZ, S. M. & DEVINE, J. N. 2007. PEEK biomaterials in trauma, orthopedic, and spinal implants. Biomaterials, 28, 4845-69.

KURTZ, S. M., GAWEL, H. A. & PATEL, J. D. 2011. History and systematic review of wear and osteolysis outcomes for first-generation highly crosslinked polyethylene. Clin Orthop Relat Res, 469, 2262-77.

KURTZ, S. M. & NEVELOS, J. 2012. Chapter 16 - Arthroplasty Bearing Surfaces. In: KURTZ, S. M. (ed.) PEEK Biomaterials Handbook. Oxford: William Andrew Publishing.

LAFON, L., MOUBARAK, H., DRUON, J. & ROSSET, P. 2014. Cementless RM Pressfit Cup: a clinical and radiological study of 91 cases with at least four years follow-up. Orthop Traumatol Surg Res, 100, S225-9.

LANGDOWN, A. J., PICKARD, R. J., HOBBS, C. M., CLARKE, H. J., DALTON, D. J. & GROVER, M. L. 2007. Incomplete seating of the liner with the Trident acetabular system: a cause for concern? J Bone Joint Surg Br, 89, 291-5.

LANGOHR, G. D. G., GAWEL, H. A. & MEDLEY, J. B. 2011. Wear performance of all-polymer PEEK articulations for a cervical total level arthroplasty system. Proceedings of the Institution of Mechanical Engineers, Part J: Journal of Engineering Tribology, 225, 499-513.

LANGTON, D. J., JAMESON, S. S., JOYCE, T. J., HALLAB, N. J., NATU, S. & NARGOL, A. V. 2010. Early failure of metal-on-metal bearings in hip resurfacing and large-diameter total hip replacement: A consequence of excess wear. J Bone Joint Surg Br, 92, 38-46.

LATIF, A. M., MEHATS, A., ELCOCKS, M., RUSHTON, N., FIELD, R. E. & JONES, E. 2008a. Pre-clinical studies to validate the MITCH PCR Cup: a flexible and anatomically shaped acetabular component with novel bearing characteristics. J Mater Sci Mater Med, 19, 1729-36.

LATIF, A. M. H., MEHATS, A., ELCOCKS, M., RUSHTON, N., FIELD, R. E. & JONES, E. 2008b. Pre-clinical studies to validate the MITCH PCR™ Cup: a flexible and anatomically shaped acetabular component with novel bearing characteristics. Journal of Materials Science: Materials in Medicine, 19, 1729-1736.

LEE, T. C. & TAYLOR, D. 1999. Bone remodelling: Should we cry wolff? Irish Journal of Medical Science, 168, 102-105.

LIEBERMAN, J. R., KAY, R. M., HAMLET, W. P., PARK, S. H. & KABO, J. M. 1996. Wear of the polyethylene liner-metallic shell interface in modular acetabular components. An in vitro analysis. J Arthroplasty, 11, 602-8.

LINK, M. D. 2008. Evolving Uses For Implantable PEEK and PEEK Based Compounds Medical Device Link. Medical Device Technology, 39-41.

LIU, F., JIN, Z., ROBERTS, P. & GRIGORIS, P. 2006a. Importance of head diameter, clearance, and cup wall thickness in elastohydrodynamic lubrication analysis of metal-on-metal hip resurfacing prostheses. Proc Inst Mech Eng H, 220, 695-704.

LIU, Y., WANG, Q. J., WANG, W., HU, Y. & ZHU, D. 2006b. Effects of Differential Scheme and Mesh Density on EHL Film Thickness in Point Contacts. Journal of Tribology, 128, 641.

LONS, A., ARNOULD, A., POMMEPUY, T., DRUMEZ, E. & GIRARD, J. 2015. Excellent short-term results of hip resurfacing in a selected population of young patients. Orthop Traumatol Surg Res, 101, 661-5.

MADL, A. K., KOVOCHICH, M., LIONG, M., FINLEY, B. L., PAUSTENBACH, D. J. & OBERDORSTER, G. 2015. Toxicology of wear particles of cobalt-chromium alloy metal-on-metal hip implants Part II: Importance of physicochemical properties and dose in animal and in vitro studies as a basis for risk assessment. Nanomedicine, 11, 1285-98.

MAJUMDER, S., ROYCHOWDHURY, A. & PAL, S. 2007. Simulation of hip fracture in sideways fall using a 3D finite element model of pelvis-femur-soft tissue complex with simplified representation of whole body. Med Eng Phys, 29, 1167-78.

MANLEY, M. 2007. Biomechanics of a PEEK horseshoe-shaped cup: Comparisons with a predicate deformable cup. Paper C655/058. Institution of Mechanical Engineers," Engineers & Surgeons: Joined at the Hip" London, April, 19, 21.

MARKEL, D., DAY, J., SISKEY, R., LIEPINS, I., KURTZ, S. & ONG, K. 2011. Deformation of metal-backed acetabular components and the impact of liner thickness in a cadaveric model. Int Orthop, 35, 1131-7.

MATSUSHITA, A., NAKASHIMA, Y., JINGUSHI, S., YAMAMOTO, T., KURAOKA, A. & IWAMOTO, Y. 2009. Effects of the Femoral Offset and the Head Size on the Safe Range of Motion in Total Hip Arthroplasty. The Journal of Arthroplasty, 24, 646-651.

MCKEE, G. K. 1982. Total hip replacement--past, present and future. Biomaterials, 3, 130-5.

MEDING, J. B., et al. (2013). "Acetabular cup design influences deformational response in total hip arthroplasty." Clin Orthop Relat Res **471**(2): 403-409.

MEINHARD KUNTZ 2014. The effect of chromia content on hardness of zirconia platelet

toughened alumina composites.

MELLON, S. J., GRAMMATOPOULOS, G., ANDERSEN, M. S., PANDIT, H. G., GILL, H. S. & MURRAY, D. W. 2015. Optimal acetabular component orientation estimated using edge-loading and impingement risk in patients with metal-on-metal hip resurfacing arthroplasty. J Biomech, 48, 318-23.

MORLOCK, M. M., BISHOP, N., ZUSTIN, J., HAHN, M., RÜTHER, W. & AMLING, M. 2008. Modes of Implant Failure After Hip Resurfacing: Morphological and Wear Analysis of 267 Retrieval Specimens.

MORRISON, C., MACNAIR, R., MACDONALD, C., WYKMAN, A., GOLDIE, I. & GRANT, M. H. 1995. In vitro biocompatibility testing of polymers for orthopaedic implants using cultured fibroblasts and osteoblasts. Biomaterials, 16, 987-92.

MOSER, R. & LIGHTNER, J. G. 2007. Using Three-Dimensional Digital Imaging Correlation Techniques to Validate Tire Finite-Element Model. Experimental Techniques, 31, 29-36.

MYBURGH, J., SNYCKERS, C., OSCHMAN, Z. & MONNI, T. 2012. Metal-on-metal arthroplasty using the Metasul prosthesis with a minimum ten-year follow-up. SA Orthopaedic Journal, 11, 73-78.

NISITANI, H., NOGUCHI, H. & KIM, Y. H. 1992. Evaluation of fatigue strength of plain and notched specimens of short carbon-fiber reinforced polyetheretherketone in comparison with polyetheretherketone. Engineering Fracture Mechanics, 43, 685-705.

NJR 2015. 12th Annual Report 2015 National joint registry for England, Wales, Northern Ireland and the Isle of Man.

OLIVEIRA, C. A., CANDELÁRIA, I. S., OLIVEIRA, P. B., FIGUEIREDO, A. & CASEIRO-ALVES, F. 2015. Metallosis: A diagnosis not only in patients with metal-on-metal prostheses. European Journal of Radiology Open, 2, 3-6.

OONISHI, H., ISHA, H. & HASEGAWA, T. 1983. Mechanical analysis of the human pelvis and its application to the artificial hip joint--by means of the three dimensional finite element method. J Biomech, 16, 427-44.

ORTHOPAEDICS, D. 2015. Hemiarthroplasty of the Hip [Online]. Available: http://www.wheelessonline.com/ortho/hemiarthroplasty_of_the_hip [Accessed 26th Spetember 2015 2015].

PACE, N., MARINELLI, M. & SPURIO, S. 2008. Technical and histologic analysis of a retrieved carbon fiber-reinforced poly-ether-ether-ketone composite alumina-bearing liner 28 months after implantation. J Arthroplasty, 23, 151-5.

PACE, N., MARINELLI, M., SPURIO, S. & R, D. M. 2005. International Society for Technology in Arthroplasty (ISTA) 2005 P2-6 : Primary total hip arthroplasty with carbon fibre reinforced poly-ether- ether-ketone composite acetabular cup component 36-months results . P13-3 : Elemental and histological analys. Technology, 2-3.

PACE, N., SPURIO, S., PAVAN, L., RIZZUTO, G. & STREICHER, R. M. 2002. Clinical Trial of a New CF-PEEK Acetabular Insert in Hip Arthroplasty European Hip Society 2002 Domestic Meeting. Wear.

PHILLIPS, A. T., PANKAJ, P., HOWIE, C. R., USMANI, A. S. & SIMPSON, A. H. 2007. Finite element modelling of the pelvis: inclusion of muscular and ligamentous boundary conditions. Med Eng Phys, 29, 739-48.

RAE, P. J., BROWN, E. N. & ORLER, E. B. 2007. The mechanical properties of poly(ether-ether-ketone) (PEEK) with emphasis on the large compressive strain response. Polymer, 48, 598-615.

RIES, M. D., HARBAUGH, M., SHEA, J. & LAMBERT, R. 1997. Effect of cementless acetabular cup geometry on strain distribution and press-fit stability. J Arthroplasty, 12, 207-12.

RIGDON, R. H. & WARREN, J. W. 1941. Amniotic fluid (Amfetin) in its relation to inflammation: Observations in the rabbit and in man. The American Journal of Surgery, 53, 481-485.

ROBERTS, B. J., UNSWORTH, A. & MIAN, N. 1982. Modes of lubrication in human hip joints. Ann Rheum Dis, 41, 217-24.

ROBOTTI, P., VEDOVA, S., FABBRI, A., MIGLIARESI, C., FONTANARI, V. & ZAPPINI, G. 2009. PEEK and CFR-PEEK : Properties PEEK and CFR-PEEK : Applications Bone-PEEK Implant Interface. Materials Engineering, 1-12.

ROGERS, A., KULKARNI, R. & DOWNES, E. M. 2003. The ABG hydroxyapatite-coated hip prosthesis: one hundred consecutive operations with average 6-year follow-up. J Arthroplasty, 18, 619-25.

S.C. SCHOLES A, A. U. A.,) , R.M. HALL B , R. SCOTT C 2000. <The effects of material combination and lubricant on the friction of total hip prothesis.pdf>.

SARIALI, E., STEWART, T., JIN, Z. & FISHER, J. 2010. In vitro investigation of friction under edge-loading conditions for ceramic-on-ceramic total hip prosthesis. J Orthop Res, 28, 979-85.

SCHOLES, S. & UNSWORTH, A. View Staff Profile.

SCHOLES, S. & UNSWORTH, A. 2006a. The effects of proteins on the friction and lubrication of artificial joints. Proceedings of the Institution of Mechanical Engineers, Part H: Journal of Engineering in Medicine, 220, 687-693.

SCHOLES, S., UNSWORTH, A., HALL, R. & SCOTT, R. 2000a. The effects of material combination and lubricant on the friction of total hip prostheses. Wear, 241, 209-213.

SCHOLES, S. C., INMAN, I. A., UNSWORTH, A. & JONES, E. 2008. Tribological assessment of a flexible carbon-fibre-reinforced poly(ether-ether-ketone) acetabular cup articulating against an alumina femoral head. Proc Inst Mech Eng H, 222, 273-83.

SCHOLES, S. C. & UNSWORTH, A. 2000. Comparison of friction and lubrication of different hip prostheses. Proc Inst Mech Eng H, 214, 49-57.

SCHOLES, S. C. & UNSWORTH, A. 2006b. The effects of proteins on the friction and lubrication of artificial joints. Proc Inst Mech Eng H, 220, 687-93.

SCHOLES, S. C. & UNSWORTH, A. 2009a. Pitch-based carbon-fibre-reinforced poly (ether-ether-ketone) OPTIMA assessed as a bearing material in a mobile bearing unicondylar knee joint. Proc Inst Mech Eng H, 223, 13-25.

SCHOLES, S. C. & UNSWORTH, A. 2009b. Wear studies on the likely performance of CFR-PEEK/CoCrMo for use as artificial joint bearing materials. J Mater Sci Mater Med, 20, 163-70.

SCHOLES, S. C., UNSWORTH, A. & GOLDSMITH, A. A. 2000b. A frictional study of total hip joint replacements. Phys Med Biol, 45, 3721-35.

SCHOLES, S. C., UNSWORTH, A., HALL, R. M. & SCOTT, R. 2000c. The effects of material combination and lubricant on the friction of total hip prostheses. Wear, 241, 209-213.

SEMLITSCH, M. & PANIC, B. 1983. Ten years of experience with test criteria for fracture-proof anchorage stems of artificial hip joints. Engineering in medicine, 12, 185-198.

SHIM, V. B., PITTO, R. P., STREICHER, R. M., HUNTER, P. J. & ANDERSON, I. A. 2008. Development and validation of patient-specific finite element models of the hemipelvis generated from a sparse CT data set. J Biomech Eng, 130, 051010.

SHIMMIN, A., BEAULE, P. E. & CAMPBELL, P. 2008. Metal-on-metal hip resurfacing arthroplasty. J Bone Joint Surg Am, 90, 637-54.

SHULTZ, T. R., BLAHA, J. D., GRUEN, T. A. & NORMAN, T. L. 2006. Cortical bone viscoelasticity and fixation strength of press-fit femoral stems: finite element model. J Biomech Eng, 128, 7-12.

SIDDIQUI, I. A., SABAH, S. A., SATCHITHANANDA, K., LIM, A. K., HENCKEL, J., SKINNER, J. A. & HART, A. J. 2013. Cross-sectional imaging of the metal-on-metal hip prosthesis: the London ultrasound protocol. Clin Radiol, 68, e472-8.

SıNMAZÇELIK, T. & YıLMAZ, T. 2007. Thermal aging effects on mechanical and tribological performance of PEEK and short fiber reinforced PEEK composites. Materials & Design, 28, 641-648.

SMITH, N., JONES, E., UNSWORTH, A., MARSDEN, H. R., BURGESS, I. C. & SCHOLES, S. C. 2006. Compliant Layer Acetabular Cups: Friction Testing of a Range of Materials and Designs for a New Generation of Prosthesis that Mimics the Natural Joint. Proceedings of the Institution of Mechanical Engineers, Part H: Journal of Engineering in Medicine, 220, 583-596.

SOBIERAJ, M. C., MURPHY, J. E., BRINKMAN, J. G., KURTZ, S. M. & RIMNAC, C. M. 2010. Notched fatigue behavior of PEEK. Biomaterials, 31, 9156-62.

SPRINGER, B. D., HABET, N. A., GRIFFIN, W. L., NANSON, C. J. & DAVIES, M. A. 2012. Deformation of 1-Piece Metal Acetabular Components. The Journal of Arthroplasty, 27, 48-54.

SQUIRE, M., GRIFFIN, W. L., MASON, J. B., PEINDL, R. D. & ODUM, S. 2006a. Acetabular Component Deformation with Press-Fit Fixation. The Journal of Arthroplasty, 21, 72-77.

SQUIRE, M., GRIFFIN, W. L., MASON, J. B., PEINDL, R. D. & ODUM, S. 2006b. Acetabular component deformation with press-fit fixation. J Arthroplasty, 21, 72-7.

STEVEN M. KURTZ, P. D. 2012. PEEK Biomaterials Handbook.

STEVEN M. KURTZ, P. D. & AND RICHARD UNDERWOOD, P. D. 2011. Metal-on on-Metal Hips: Device Mechanics and Failure Modes [Online]. Available: http://www.fda.gov/downloads/AdvisoryCommittees/CommitteesMeetingMaterials/MedicalDevices/MedicalDevicesAdvisoryCommittee/OrthopaedicandRehabilitationDevicesPanel/UCM310240.pdf [Accessed].

STREIT, M. R., WEISS, S., ANDREAS, F., BRUCKNER, T., WALKER, T., KRETZER, J. P., EWERBECK, V. & MERLE, C. 2014. 10-year results of the uncemented Allofit press-fit cup in young patients. Acta Orthop, 85, 368-74.

STROH, D. A., ISSA, K., JOHNSON, A. J., DELANOIS, R. E. & MONT, M. A. 2013. Reduced Dislocation Rates and Excellent Functional Outcomes With Large-Diameter Femoral Heads. The Journal of Arthroplasty, 28, 1415-1420.

TAI, N. H., MA, C. C. M. & WU, S. H. 1995. Fatigue behaviour of carbon fibre/PEEK laminate composites. Composites, 26, 551-559.

TANSEY, E. M. 2006. EARLY DEVELOPMENT OF TOTAL HIP REPLACEMENT The transcript of a Witness Seminar held by the Wellcome Trust Centre. 29.

TARIGOPULA, V., ET AL. (2007). "A Study of Large Plastic Deformations in Dual Phase Steel Using Digital Image Correlation and FE Analysis." Experimental mechanics 48(2): 181-196.

TEOH, S. 2000. Fatigue of biomaterials: a review. International Journal of Fatigue, 22, 825-837.

TONI, A., TERZI, S., SUDANESE, A. & BIANCHI, G. 2000. Fracture of ceramic components in total hip arthroplasty. Hip International, 10, 49-56.

UNDERWOOD, R. J., ZOGRAFOS, A., SAYLES, R. S., HART, A. & CANN, P. 2012. Edge loading in metal-on-metal hips: low clearance is a new risk factor. Proceedings of the Institution of Mechanical Engineers, Part H: Journal of Engineering in Medicine, 226, 217-226.

UNSWORTH, A. 1978. The effects of lubrication in hip joint prostheses. Phys Med Biol, 23, 253-68.

UNSWORTH, A., ASH, H. E., BURGESS, I. C., SCHOLES, S. C. & JONES, E. 2009. Compliant layer bearings in artificial joints. Part 2: simulator and fatigue testing to assess the durability of the interface between an elastomeric layer and a rigid substrate. Proceedings of the Institution of Mechanical Engineers, Part H: Journal of Engineering in Medicine, 223, 1-13.

UNSWORTH, A. & SCHOLES, S. C. 2009. Pitch-based carbon-fibre-reinforced poly (ether–ether–ketone) OPTIMA® assessed as a bearing material in a mobile bearing unicondylar knee joint. Proceedings of the Institution of Mechanical Engineers, Part H: Journal of Engineering in Medicine, 223, 13-26.

UNSWORTH, A., SCHOLES, S. C., D ELFICK, A. P. & VASSILIOU, K. 2006. The effect of 'running-in' on the tribology and surface morphology of metal-on-metal Birmingham hip resurfacing device in simulator studies. Proceedings of the Institution of Mechanical Engineers, Part H: Journal of Engineering in Medicine, 220, 269-277.

UTZSCHNEIDER, S., BECKER, F., GRUPP, T. M., SIEVERS, B., PAULUS, A., GOTTSCHALK, O. & JANSSON, V. 2010. Inflammatory response against different carbon fiber-reinforced PEEK wear particles compared with UHMWPE in vivo. Acta Biomater, 6, 4296-304.

VAN HEUMEN, M., HEESTERBEEK, P., SWIERSTRA, B., VAN HELLEMONDT, G. & GOOSEN, J. 2014. Dual mobility acetabular component in revision total hip arthroplasty for persistent dislocation: no dislocations in 50 hips after 1–5 years. Journal of Orthopaedics and Traumatology, 16, 15-20.

VAN RIETBERGEN, B., HUISKES, R., WEINANS, H., SUMNER, D. R., TURNER, T. M. & GALANTE, J. O. 1993. ESB Research Award 1992. The mechanism of bone remodeling and resorption around press-fitted THA stems. J Biomech, 26, 369-82.

VAUGHAN, P., JOHNSTON, P. & KEENE, G. 2010. ACCURACY OF ACETABULAR REAMERS IN TOTAL HIP ARTHROPLASTY. Journal of Bone & Joint Surgery, British Volume, 92, 396-396.

VENDITTOLI, P.-A., LAVIGNE, M., GIRARD, J. & ROY, A. 2006. A randomised study comparing resection of acetabular bone at resurfacing and total hip replacement. Journal of Bone & Joint Surgery, British Volume, 88, 997-1002.

WALTER, W. L., INSLEY, G. M., WALTER, W. K. & TUKE, M. A. 2004. Edge loading in third generation alumina ceramic-on-ceramic bearings. The Journal of Arthroplasty, 19, 402-413.

WALTER, W. L., LUSTY, P. J., WATSON, A., O'TOOLE, G., TUKE, M. A., ZICAT, B. & WALTER, W. K. 2006. Stripe Wear and Squeaking in Ceramic Total Hip Bearings. Seminars in Arthroplasty, 17, 190-195.

WALTER, W. L., O'TOOLE G, C., WALTER, W. K., ELLIS, A. & ZICAT, B. A. 2007. Squeaking in ceramic-on-ceramic hips: the importance of acetabular component orientation. J Arthroplasty, 22, 496-503.

WANG, A., ESSNER, A. & KLEIN, R. 2001. Effect of contact stress on friction and wear of ultra-high molecular weight polyethylene in total hip replacement. Proc Inst Mech Eng H, 215, 133-9.

WANG, A., LIN, R., POLINENI, V. K., ESSNER, A., STARK, C. & DUMBLETON, J. H. 1998. Carbon fiber reinforced polyether ether ketone composite as a bearing surface for total hip replacement. Tribology International, 31, 661-667.

WANG, A., LIN, R., STARK, C. & DUMBLETON, J. H. 1999. Suitability and limitations of carbon F reinforced PEEK composites as bearing surfaces for total joint replacements. Wear, 225-229, 724-727.

WANG, Q. Q., WU, J. J., UNSWORTH, A., BRISCOE, A., JARMAN-SMITH, M., LOWRY, C., SIMPSON, D. & COLLINS, S. 2012. Biotribological study of large diameter ceramic-on-CFR-PEEK hip joint including fluid uptake, wear and frictional heating. J Mater Sci Mater Med, 23, 1533-42.

WILKINSON, J. M., HAMER, A. J., ROGERS, A., STOCKLEY, I. & EASTELL, R. 2003. Bone mineral density and biochemical markers of bone turnover in aseptic loosening after total hip arthroplasty. J Orthop Res, 21, 691-6.

WILLIAMS, D. F., MCNAMARA, A. & TURNER, R. M. 1987. Potential of polyetheretherketone (PEEK) and carbon-fibre-reinforced PEEK in medical applications. Journal of Materials Science Letters, 6, 188-190.

WILLIAMS, S., BUTTERFIELD, M., STEWART, T., INGHAM, E., STONE, M. & FISHER, J. 2003. Wear and deformation of ceramic-on-polyethylene total hip replacements with joint laxity and swing phase microseparation. Proc Inst Mech Eng H, 217, 147-53.

WILLIAMS, S., LESLIE, I., ISAAC, G., JIN, Z., INGHAM, E. & FISHER, J. 2008. Tribology and wear of metal-on-metal hip prostheses: influence of cup angle and head position. J Bone Joint Surg Am, 90 Suppl 3, 111-7.

WYSS, T., KAGI, P., MAYRHOFER, P., NOTZLI, H., PFLUGER, D. & KNAHR, K. 2013. Five-year results of the uncemented RM pressfit cup clinical evaluation and migration measurements by EBRA. J Arthroplasty, 28, 1291-6.

XIE, Y. & WILLIAMS, J. 1996. The prediction of friction and wear when a soft surface slides against a harder rough surface. Wear, 196, 21-34.

YAMAKO, G., CHOSA, E., TOTORIBE, K., HANADA, S., MASAHASHI, N., YAMADA, N. & ITOI, E. 2014. In-vitro biomechanical evaluation of stress shielding

and initial stability of a low-modulus hip stem made of β type Ti-33.6Nb-4Sn alloy. Medical Engineering & Physics, 36, 1665-1671.

YAN, Y., et al. (2009). "The influence of swing phase load on the electrochemical response, friction, and ion release of metal-on-metal hip prostheses in a friction simulator." Proceedings of the Institution of Mechanical Engineers, Part J: Journal of Engineering Tribology 223(3): 303-309

ZHANG, Z., BREIDT, C., CHANG, L. & FRIEDRICH, K. 2004. Wear of PEEK composites related to their mechanical performances. Tribology International, 37, 271-277.